Catalysis Science & Technology

Cyclometallated C^N Diphosphine Ruthenium Catalysts for Oppenauer-Type Oxidation / Transfer Hydrogenation Reactions and Cytotoxic Activity

Dario Alessi,[a] Pierfrancesco del Mestre,[b] Eleonora Aneggi,[a] Maurizio Ballico,[a] Antonio P. Beltrami[b], Marta Busato,[a] Daniela Cesselli,[b] Alexandra Heidecker,[c] Daniele Zuccaccia,[a] and Walter Baratta[a] *

[a] *Dipartimento di Scienze Agroalimentari, Ambientali e Animali, Università di Udine, Via Cotonificio 108, I-33100 Udine, Italy*

[b] *Dipartimento di Area Medica – Istituto di Genetica Medica, Università di Udine, Via Chiusaforte, F3, I-33100 Udine, Italy*

[c] *Inorganic Chemistry/Molecular Catalysis, Department of Chemistry & Catalysis Research Center, TUM, Lichtenbergstraße 4, 85747 Garching b. München, Germany*

Supporting Information

Table of Contents:

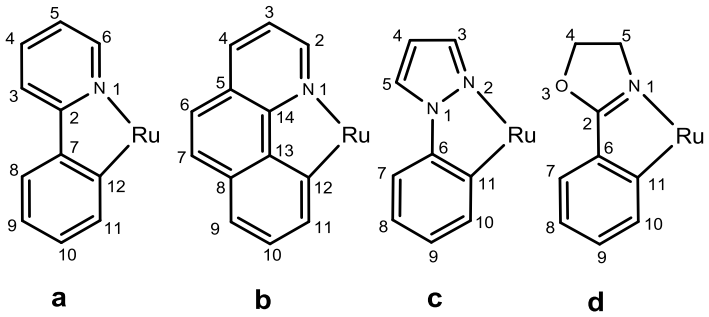

Scheme S1: C^N ligands a-d in the [Ru(C^N)(η^2-OAc)(dppb)] complexes.

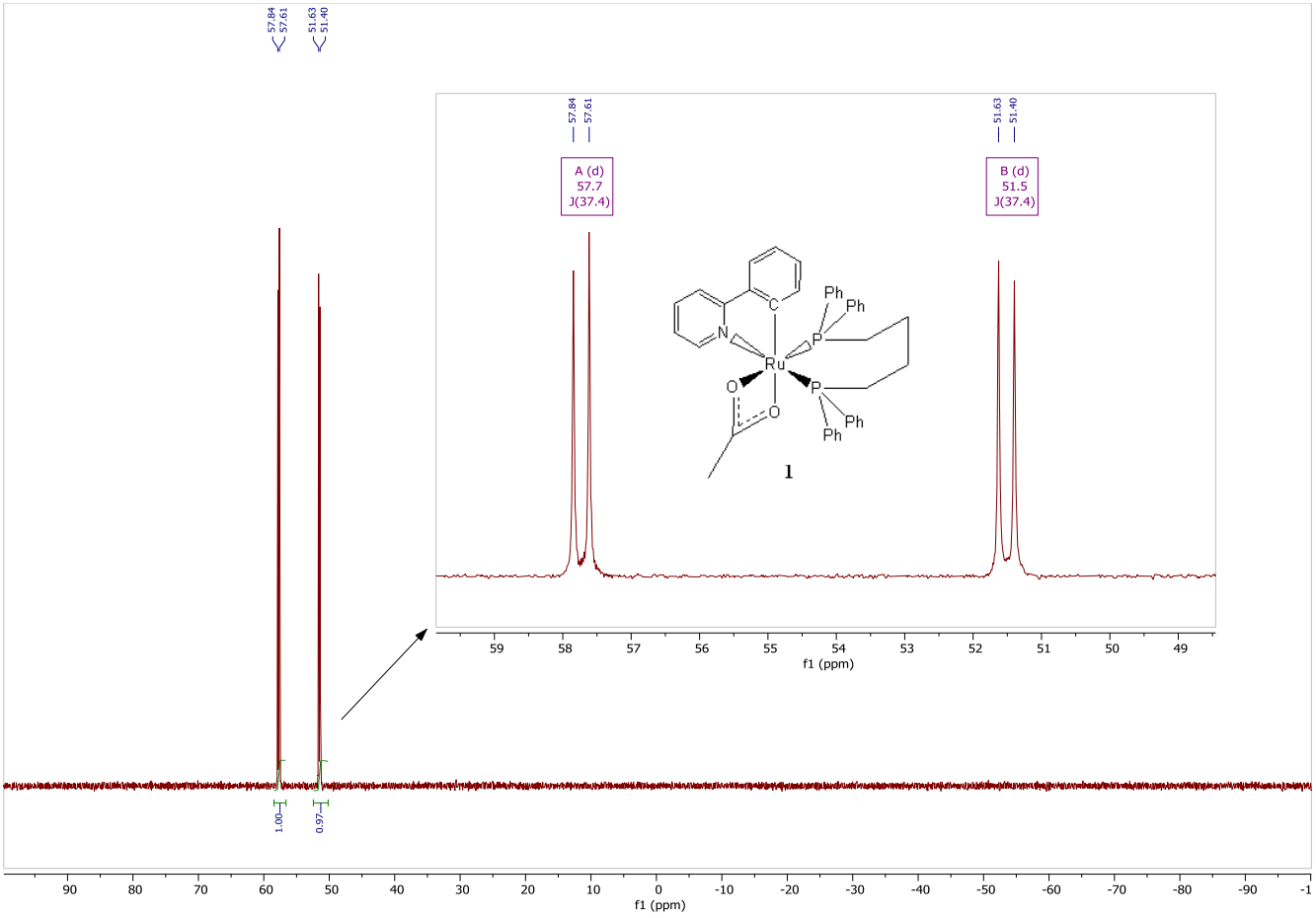

Figure S1. $^{31}P\{^1H\}$ NMR spectrum (162.0 MHz) of [Ru(**a**)(η^2-OAc)(dppb)] (**1**) in CD_2Cl_2 at 25 °C.

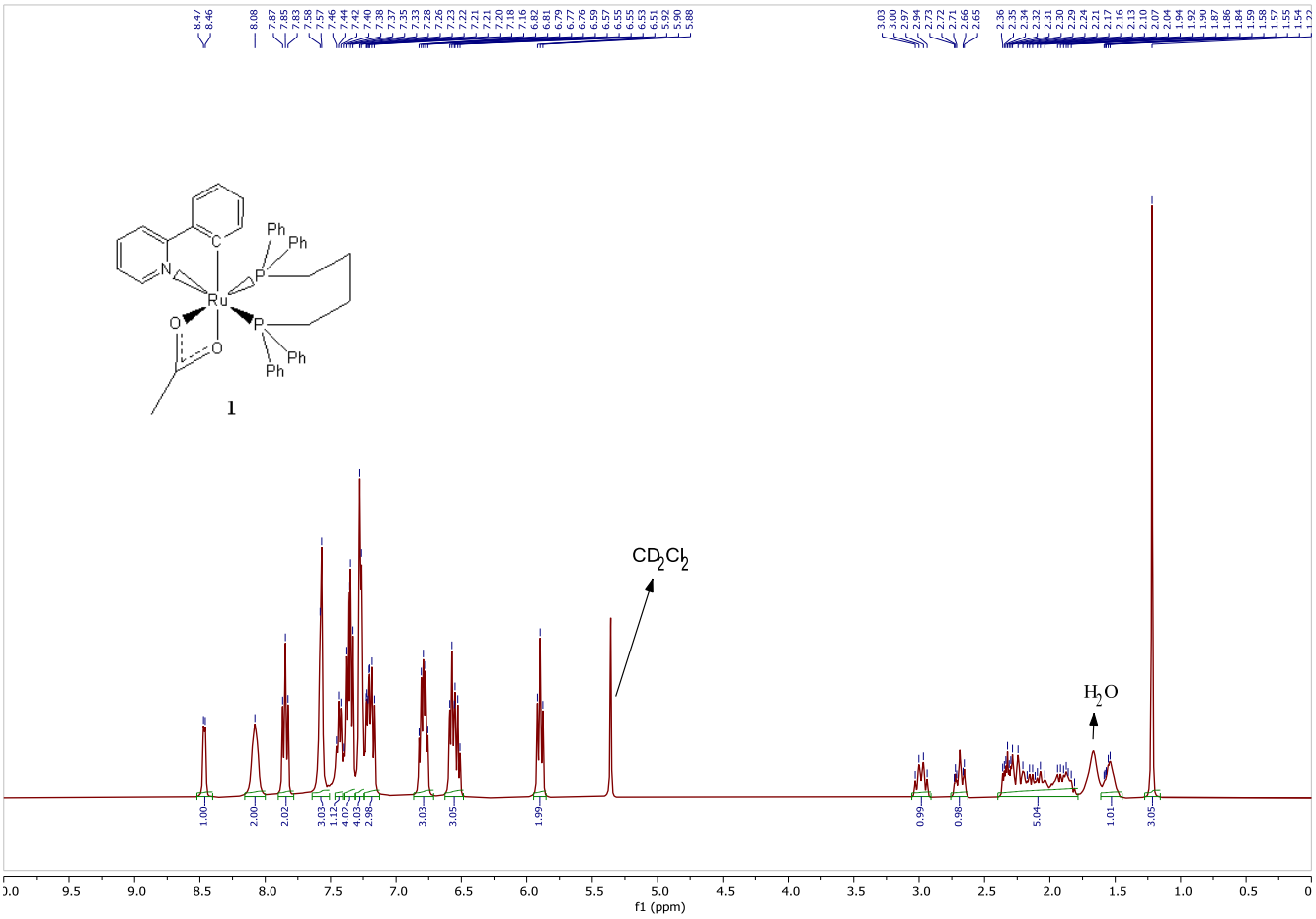

Figure S2. ^{1}H NMR spectrum (400.1 MHz) of [Ru(**a**)(η^2-OAc)(dppb)] (**1**) in CD_2Cl_2 at 25 °C.

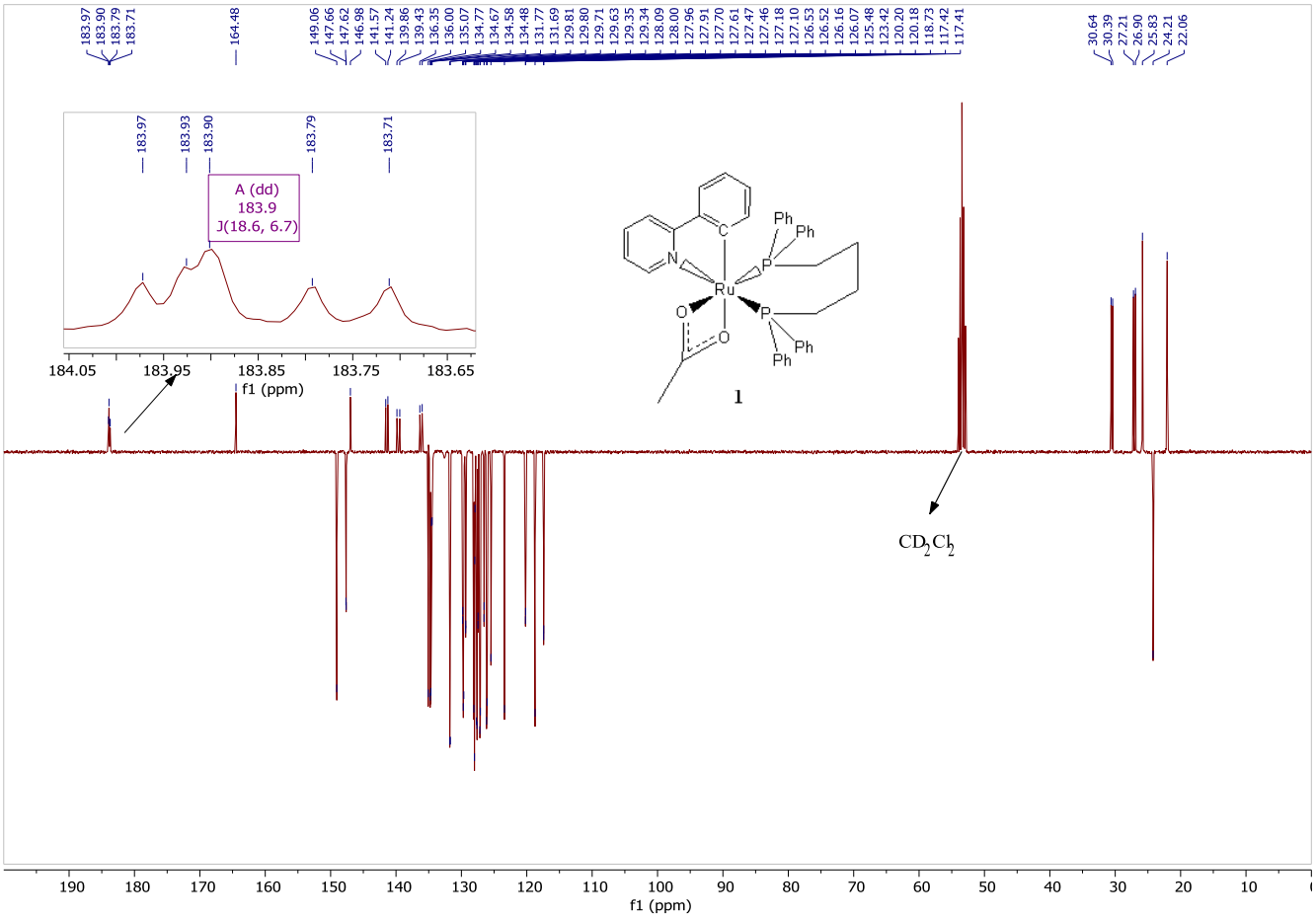

Figure S3. $^{13}C\{^{1}H\}$ DEPTQ NMR spectrum (100.6 MHz) of [Ru(**a**)(η^2-OAc)(dppb)] (**1**) in CD_2Cl_2 at 25 °C.

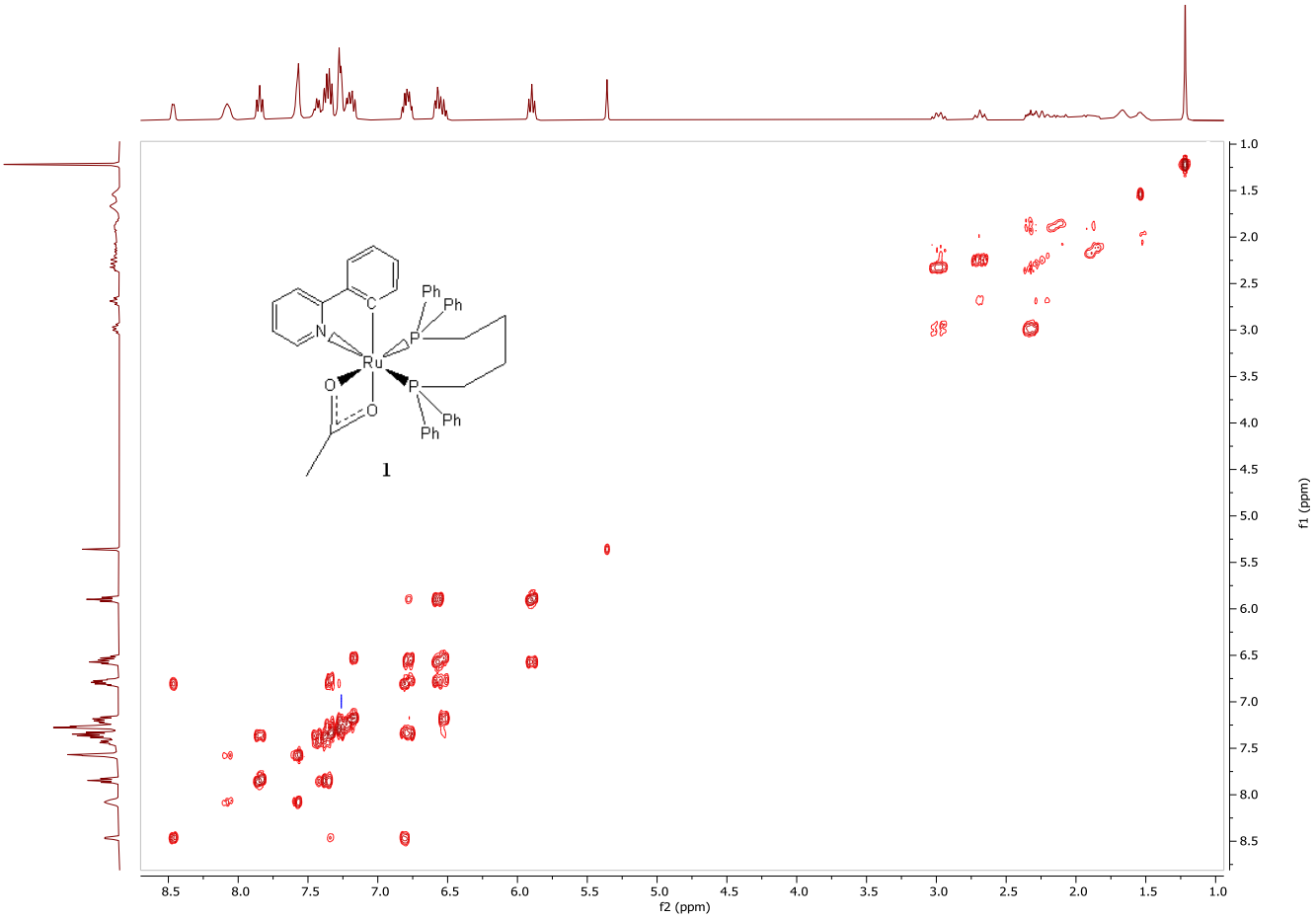

Figure S4. ^{1}H-^{1}H COSY 2D NMR spectrum of [Ru(**a**)(η^2-OAc)(dppb)] (**1**) in CD_2Cl_2 at 25 °C.

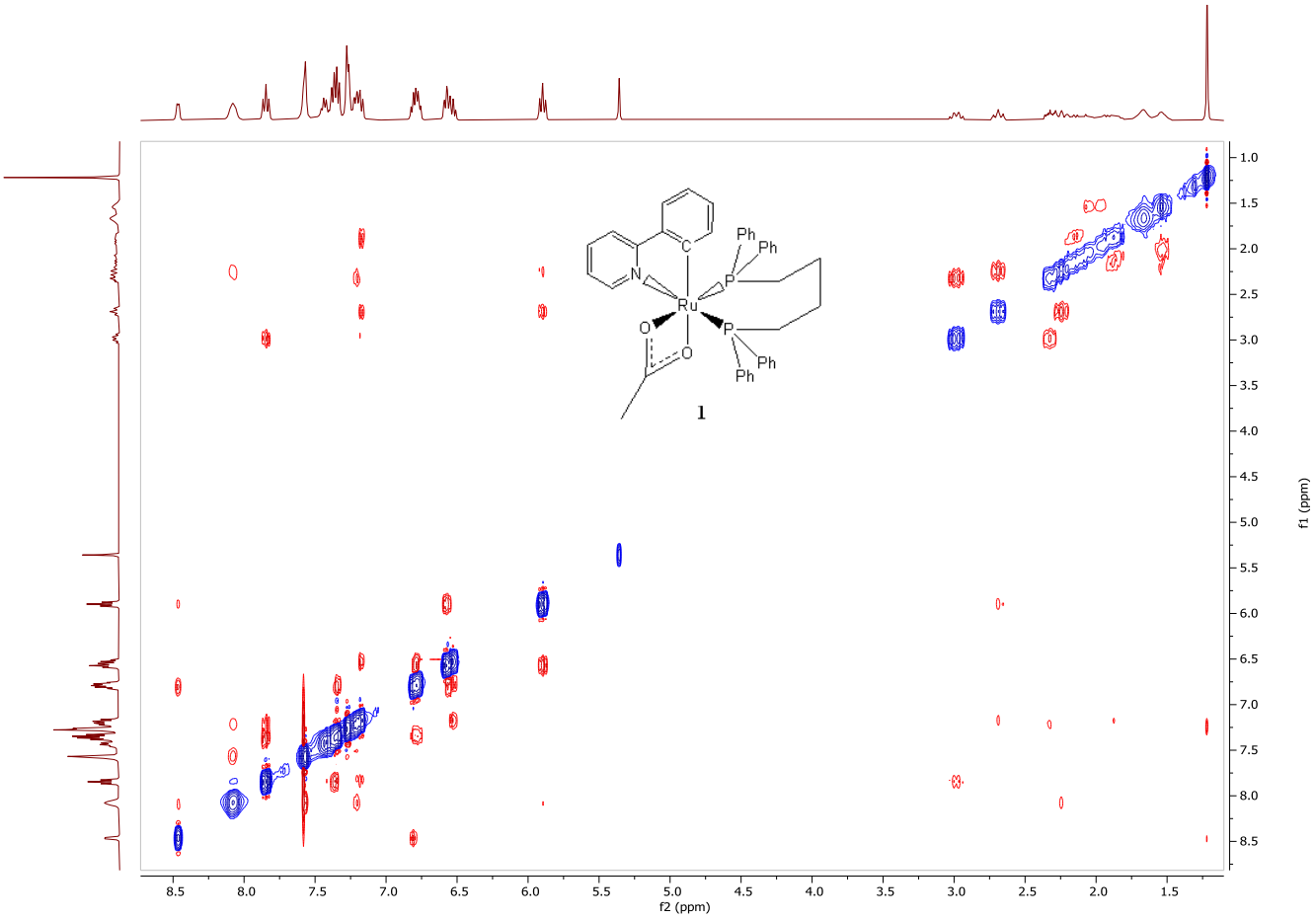

Figure S5. ^{1}H-^{1}H NOESY 2D NMR spectrum of [Ru(**a**)(η^2-OAc)(dppb)] (**1**) in CD_2Cl_2 at 25 °C.

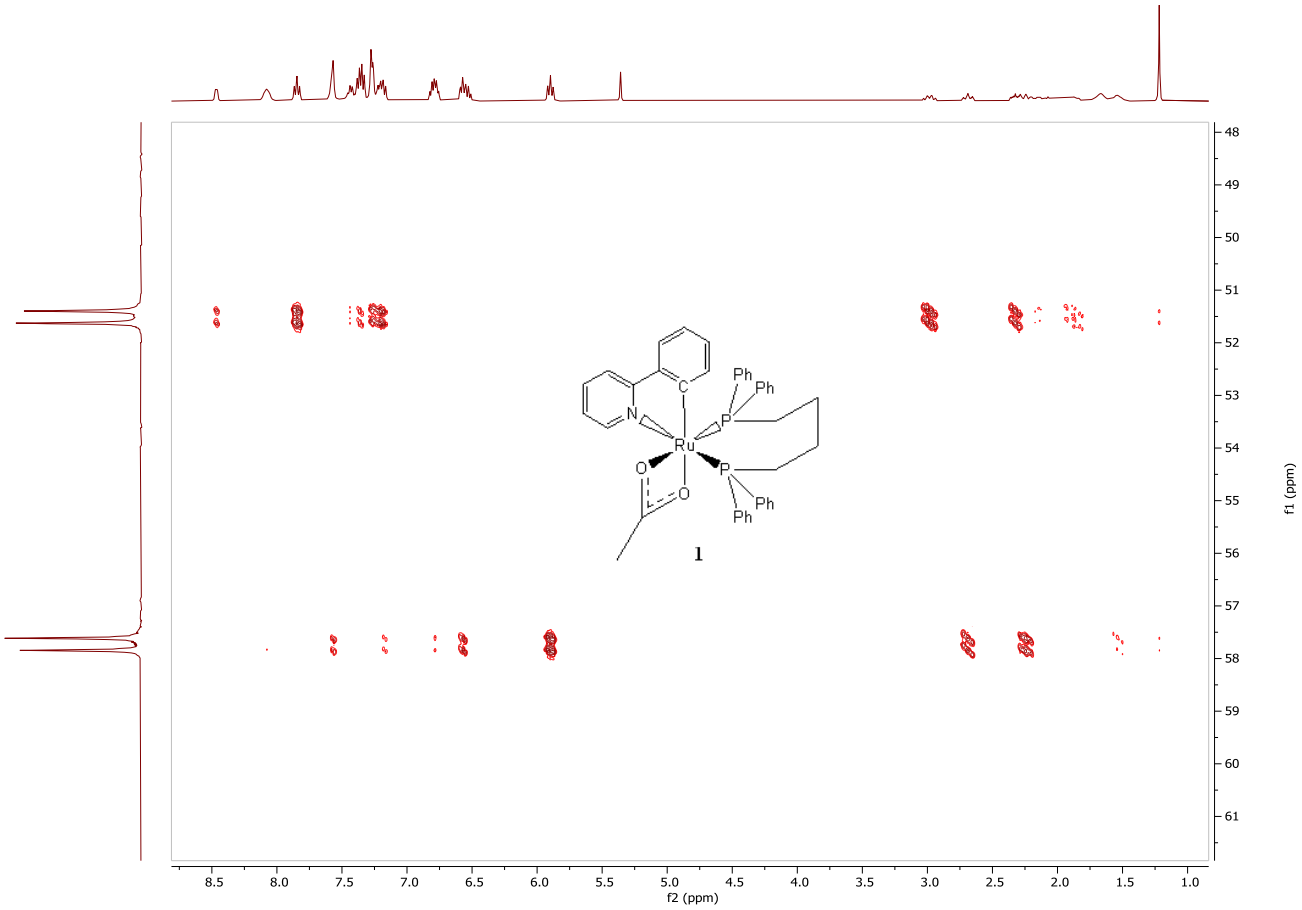

Figure S6. ^{1}H-^{31}P HMBC 2D NMR spectrum of [Ru(**a**)(η^2-OAc)(dppb)] (**1**) in CD_2Cl_2 at 25 °C.

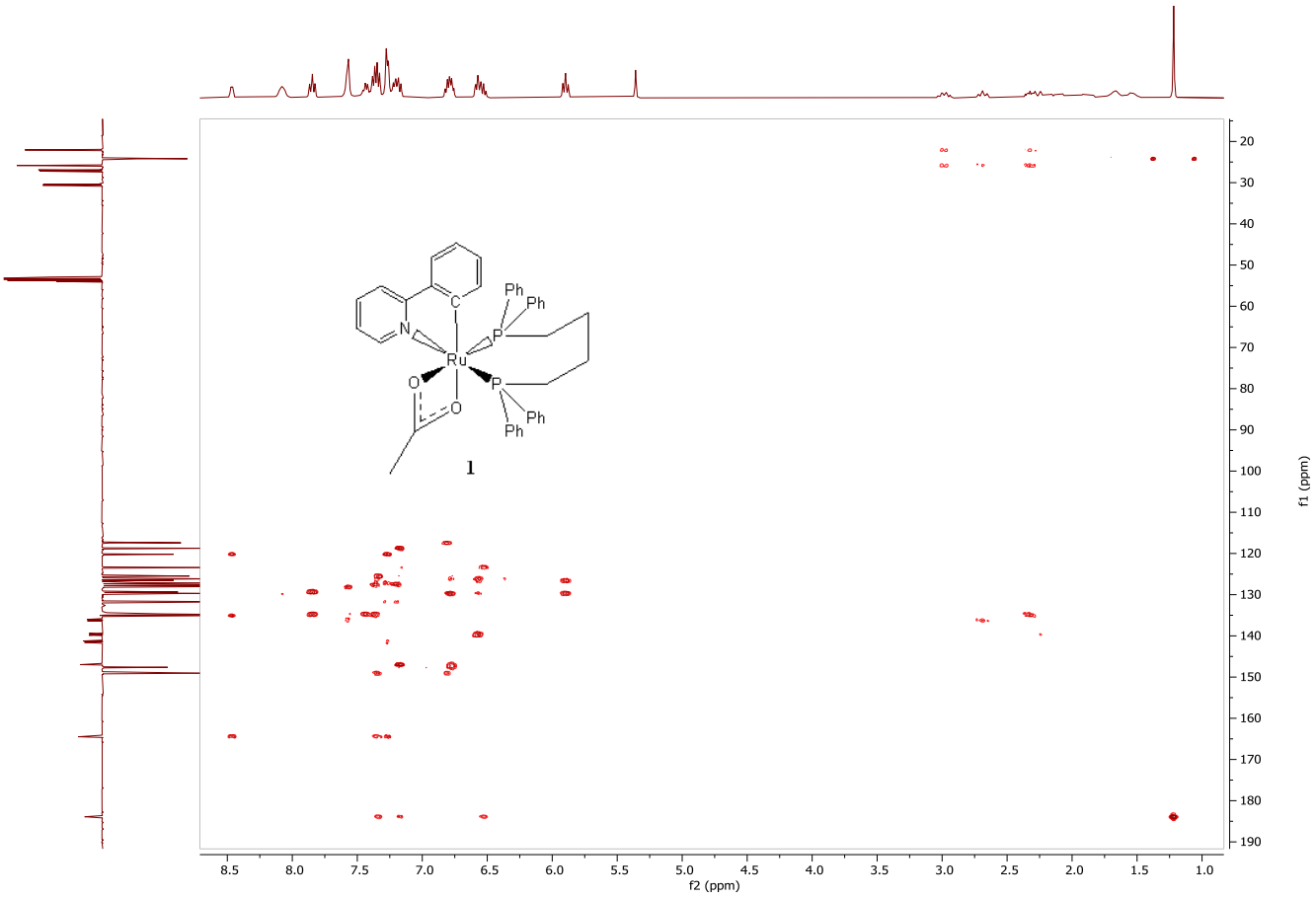

Figure S7. ^{1}H-^{13}C HMBC 2D NMR spectrum of [Ru(**a**)(η^2-OAc)(dppb)] (**1**) in CD_2Cl_2 at 25 °C.

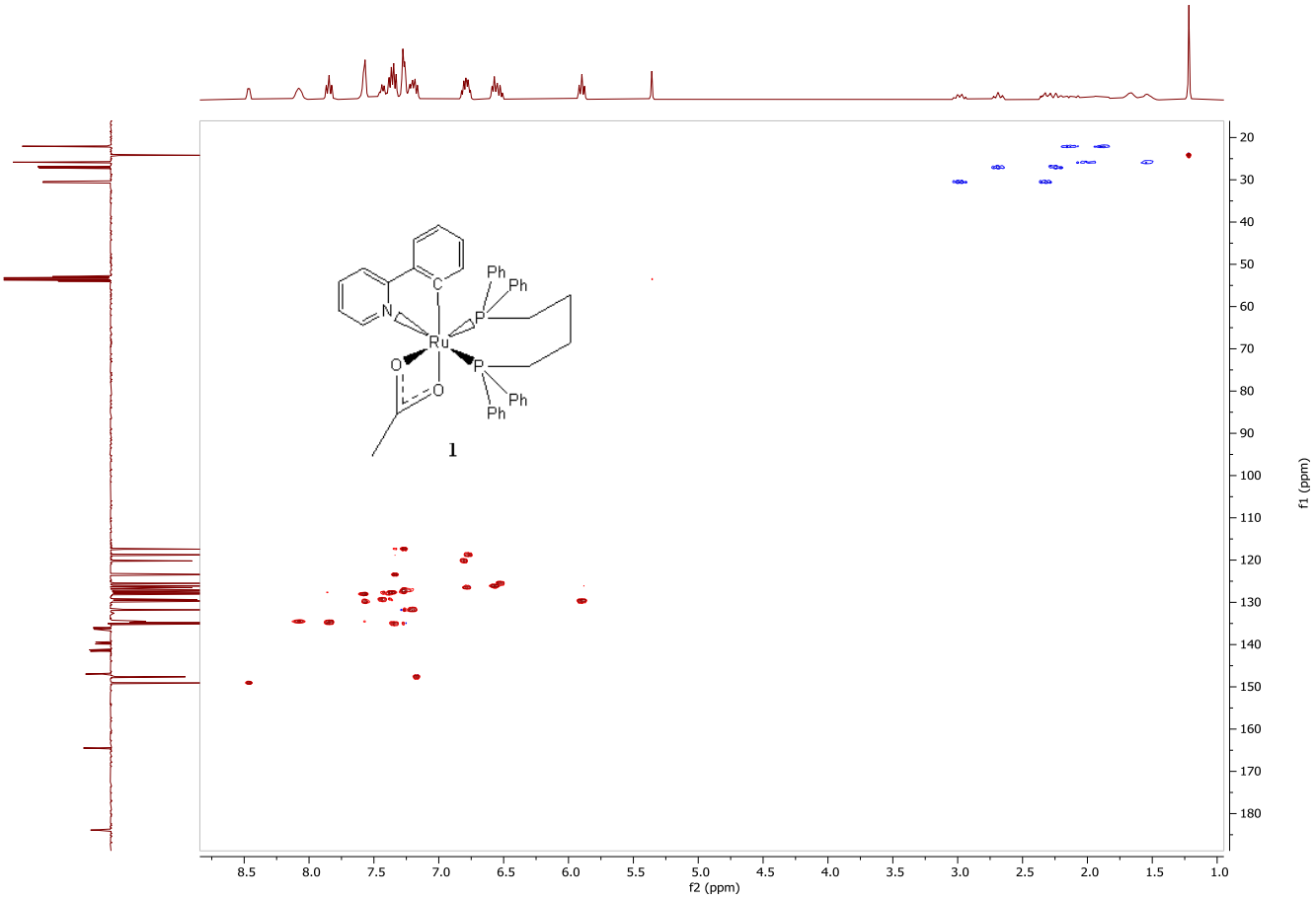

Figure S8. ^{1}H-^{13}C HSQC 2D NMR spectrum of [Ru(**a**)(η^2-OAc)(dppb)] (**1**) in CD_2Cl_2 at 25 °C.

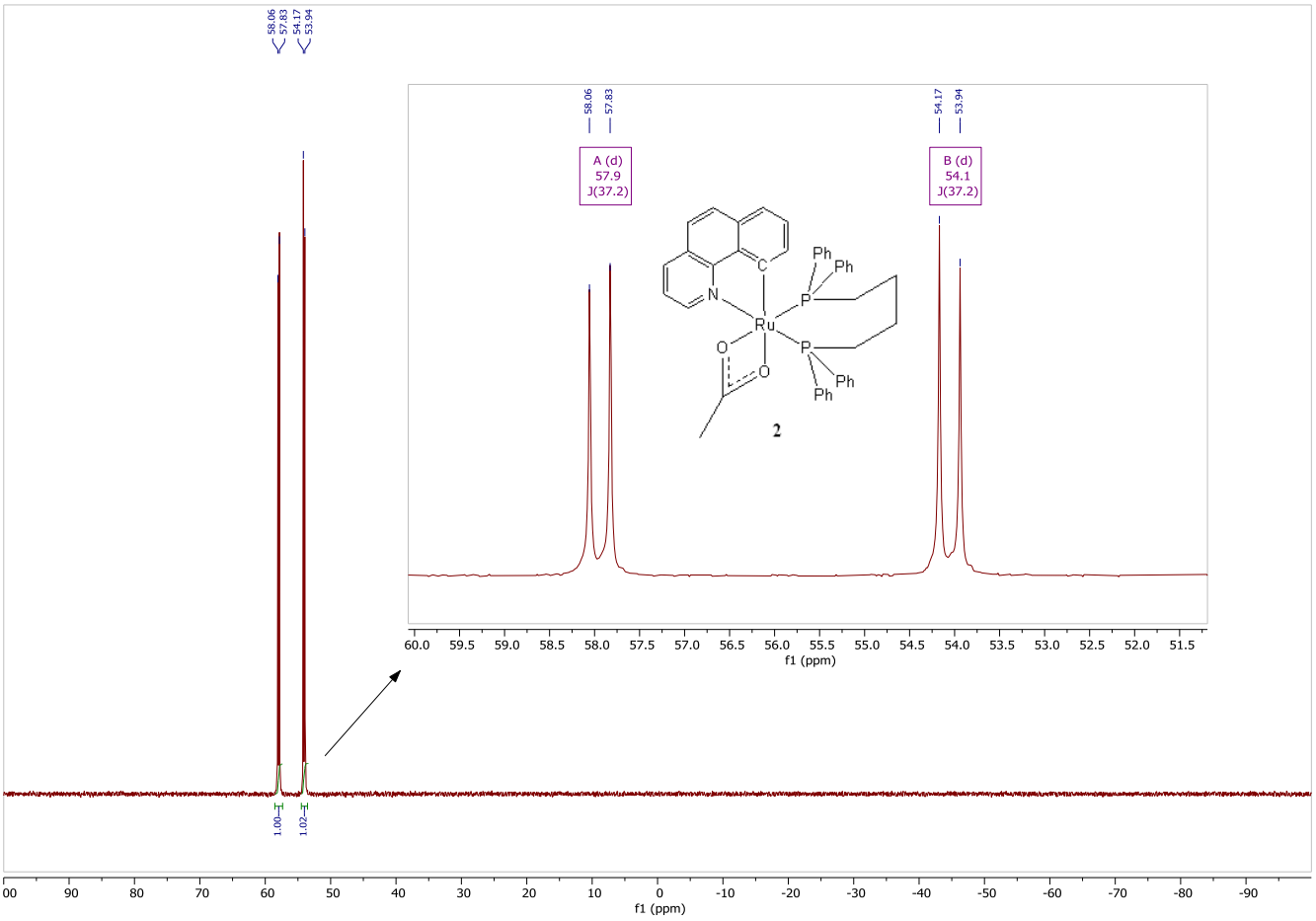

Figure S9. $^{31}P\{^{1}H\}$ NMR spectrum (162.0 MHz) of [Ru(**b**)(η^2-OAc)(dppb)] (**2**) in toluene-d^8 at 25 °C.

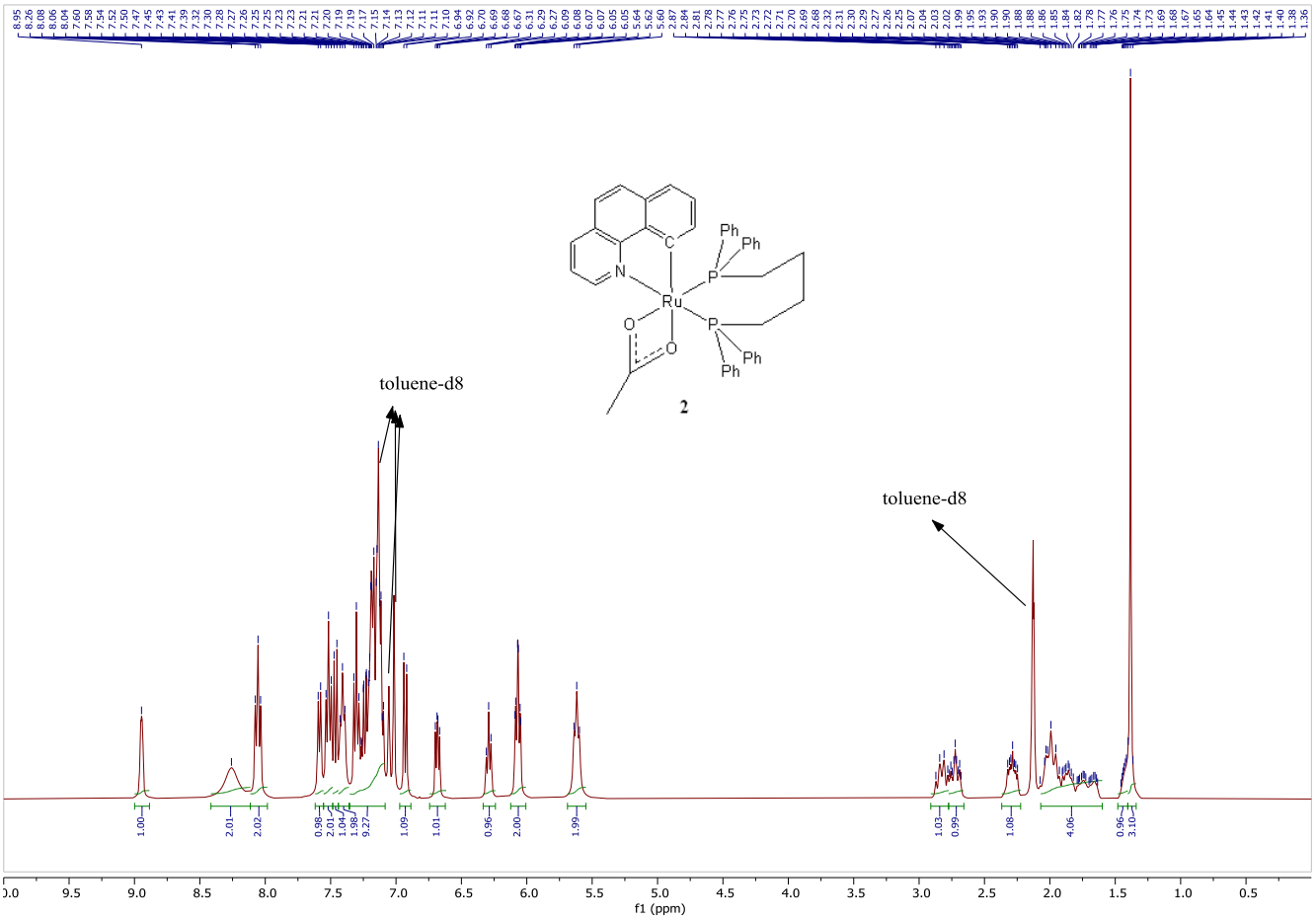

Figure S10. ^{1}H NMR spectrum (400.1 MHz) of [Ru(**b**)(η^{2}-OAc)(dppb)] (**2**) in toluene-*d*^{8} at 25 °C.

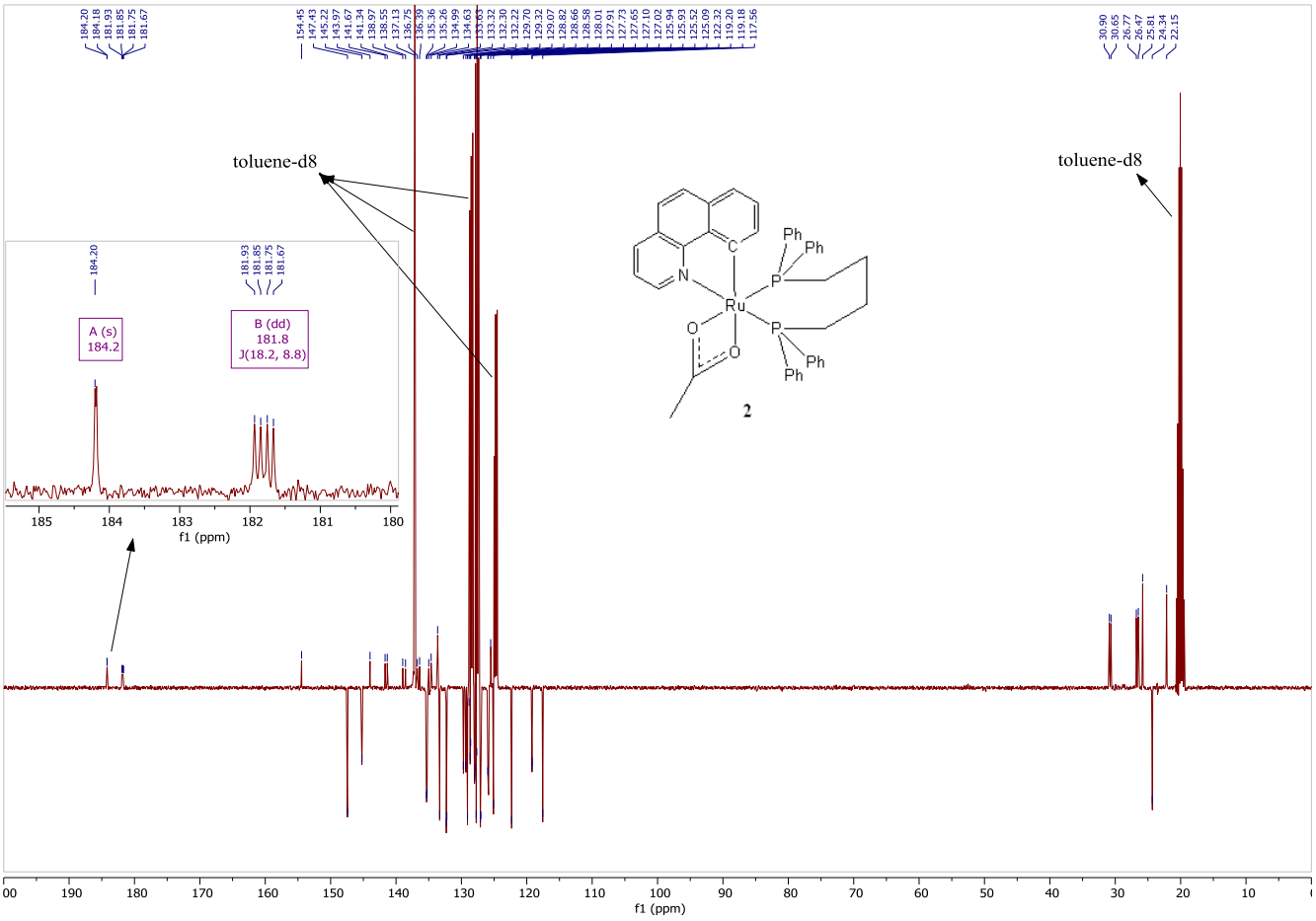

Figure S11. $^{13}C\{^{1}H\}$ DEPTQ NMR spectrum (100.6 MHz) of [Ru(**b**)(η^2-OAc)(dppb)] (**2**) in toluene-d^8 at 25 °C.

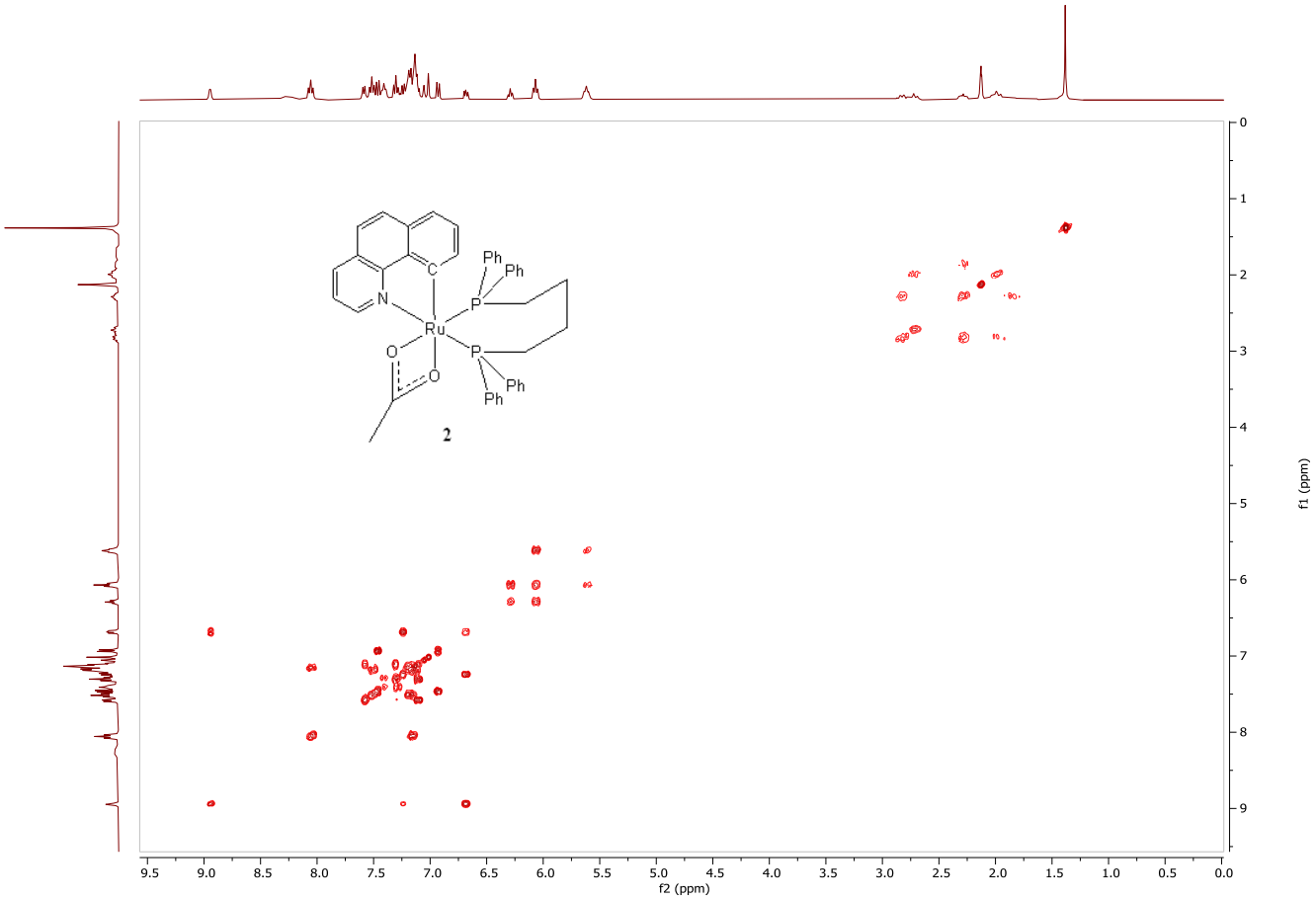

Figure S12. ^{1}H-^{1}H COSY 2D NMR spectrum of [Ru(**b**)(η^2-OAc)(dppb)] (**2**) in toluene-d^8 at 25 °C.

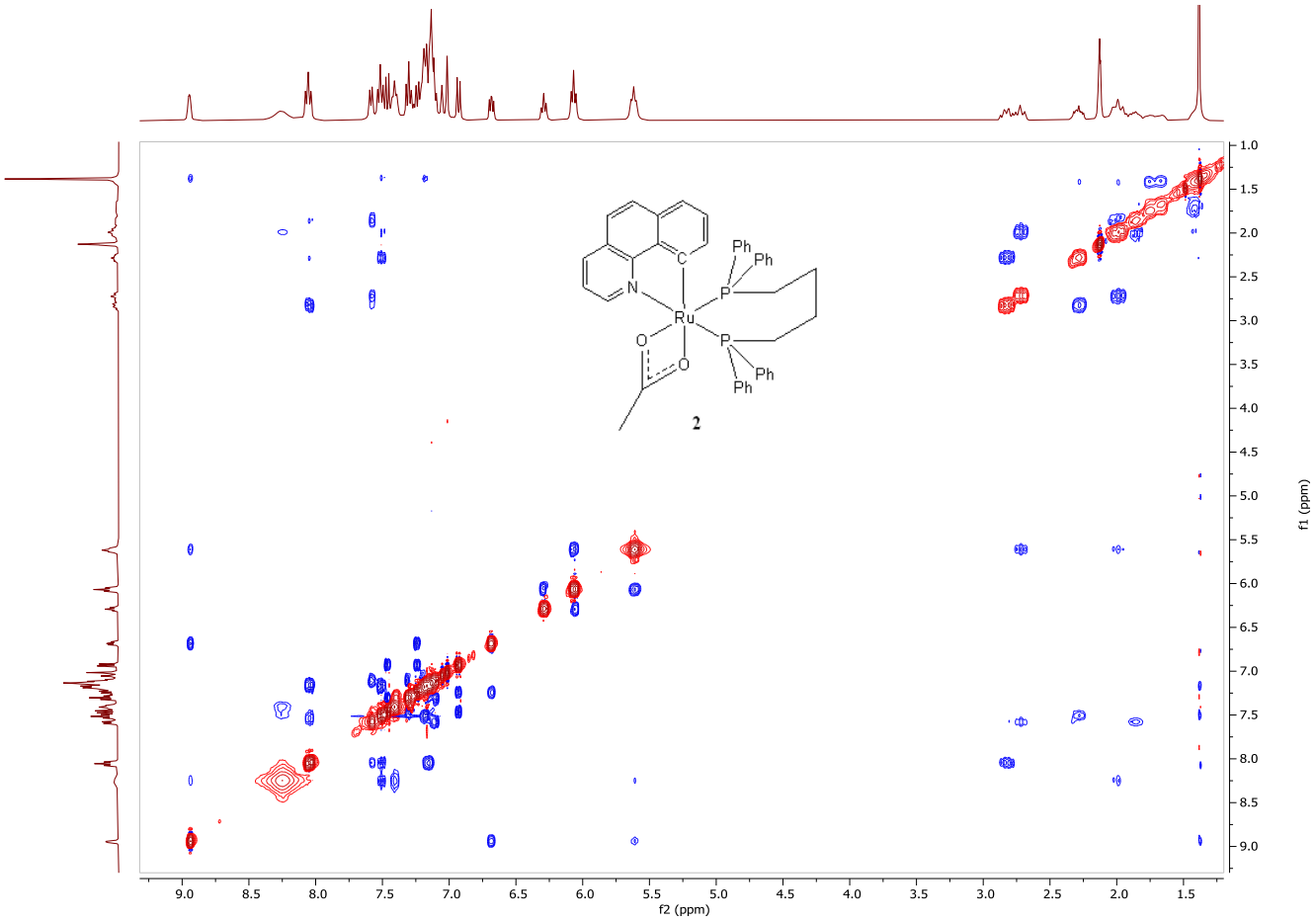

Figure S13. ^{1}H-^{1}H NOESY 2D NMR spectrum of [Ru(**b**)(η^{2}-OAc)(dppb)] (**2**) in toluene-d^{8} at 25 °C.

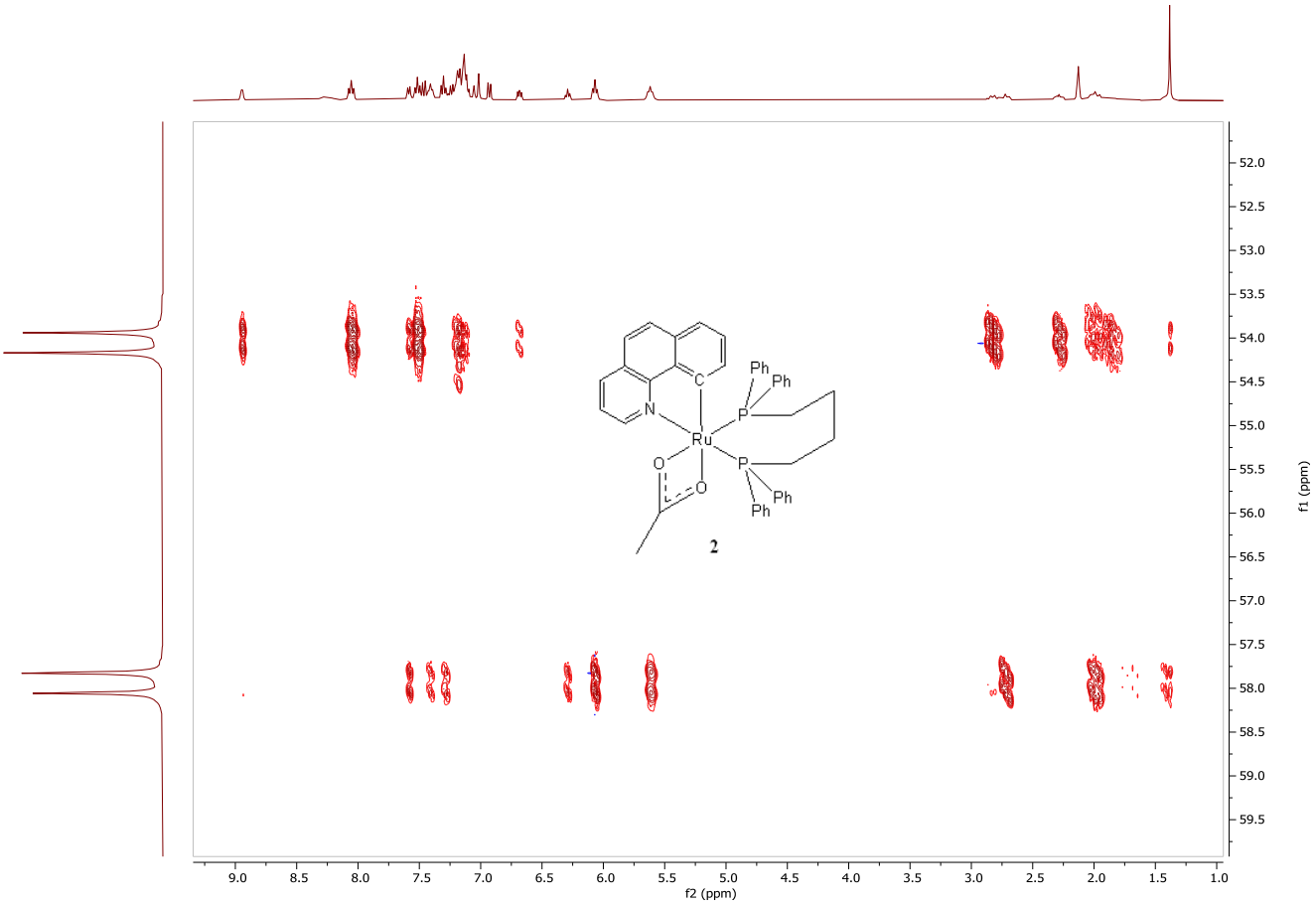

Figure S14. ^{1}H-^{31}P HMBC 2D NMR spectrum of [Ru(**b**)(η^2-OAc)(dppb)] (**2**) in CD_2Cl_2 at 25 °C.

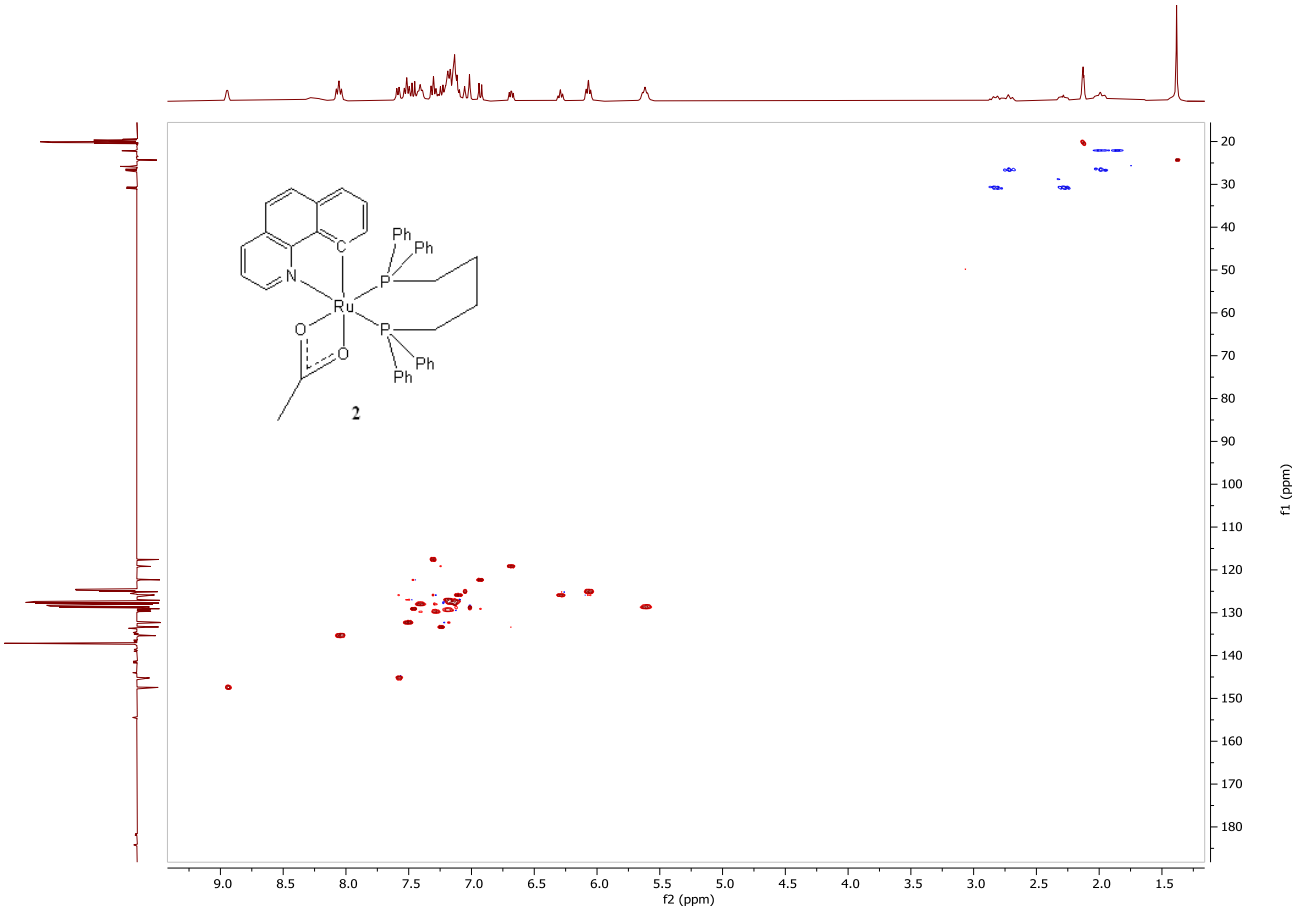

Figure S15. ^{1}H-^{13}H HSQC 2D NMR spectrum of [Ru(**b**)(η^2-OAc)(dppb)] (**2**) in CD_2Cl_2 at 25 °C.

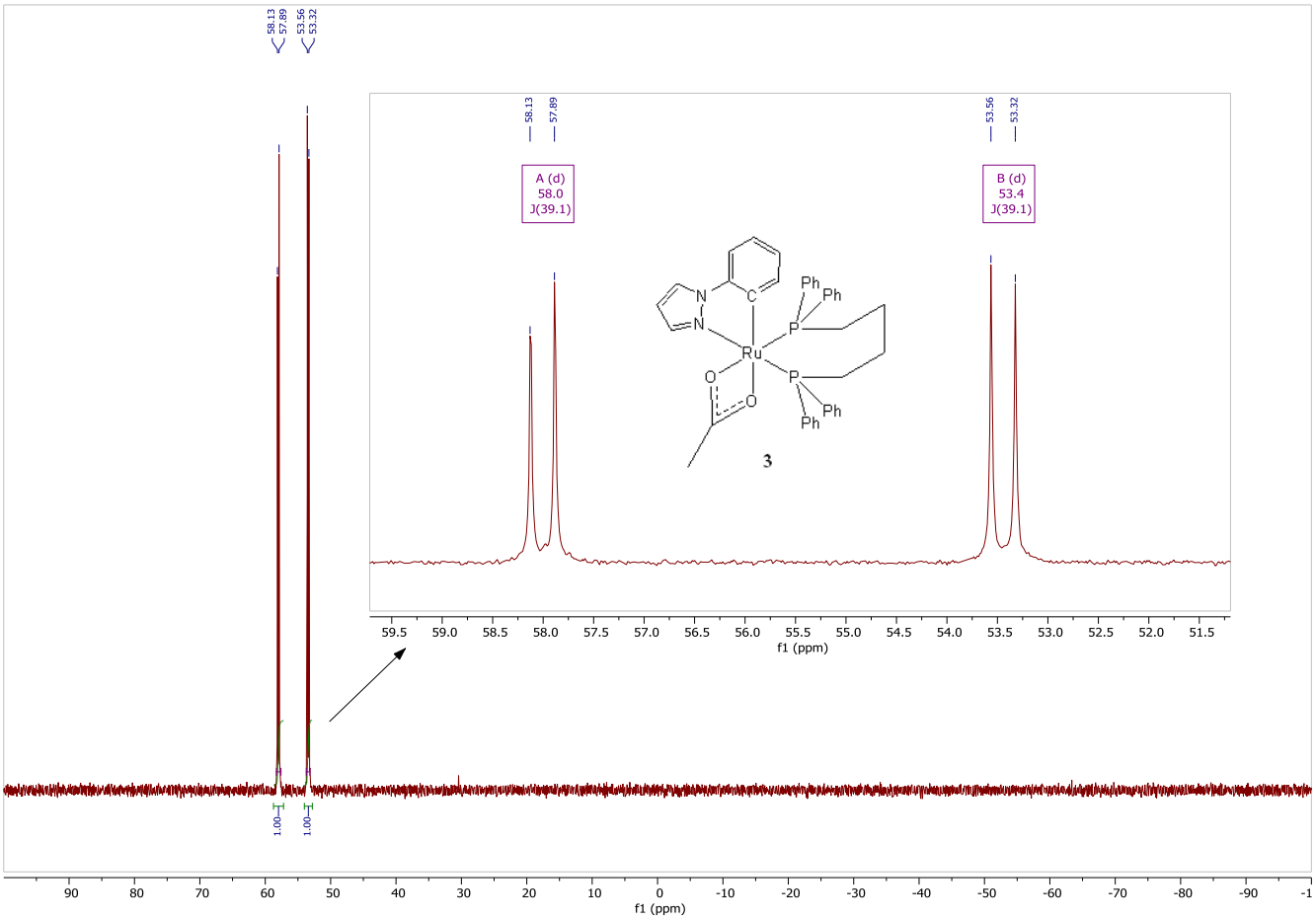

Figure S16. $^{31}P\{^{1}H\}$ NMR spectrum (162.0 MHz) of [Ru(**c**)(η^2-OAc)(dppb)] (**3**) in CD_2Cl_2 at 25 °C.

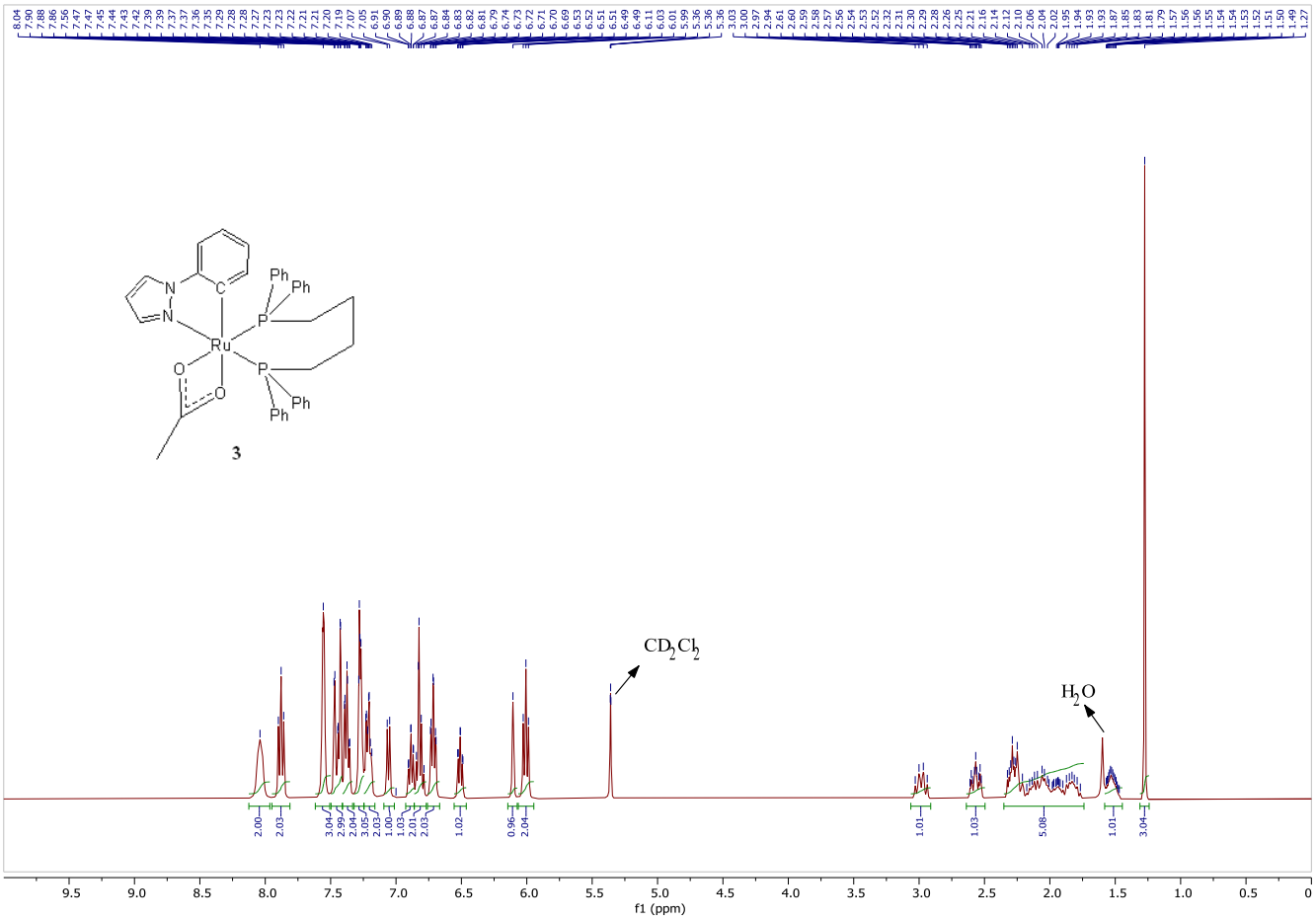

Figure S17. ^{1}H NMR spectrum (400.1 MHz) of [Ru(**c**)(η^2-OAc)(dppb)] (**3**) in CD_2Cl_2 at 25 °C.

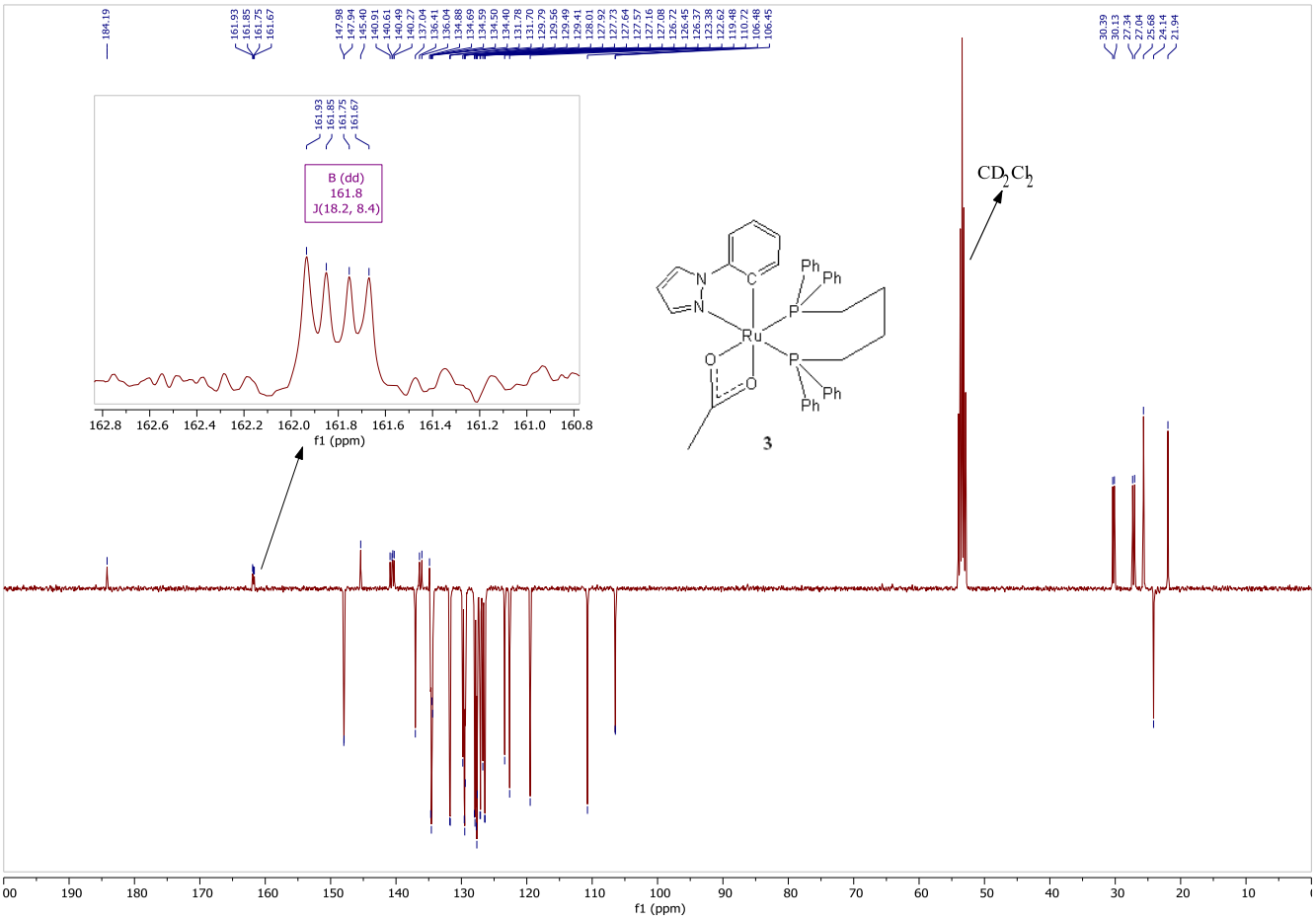

Figure S18. $^{13}C\{^{1}H\}$ DEPTQ NMR spectrum (100.6 MHz) of [Ru(**c**)(η^2-OAc)(dppb)] (**3**) in CD_2Cl_2 at 25 °C.

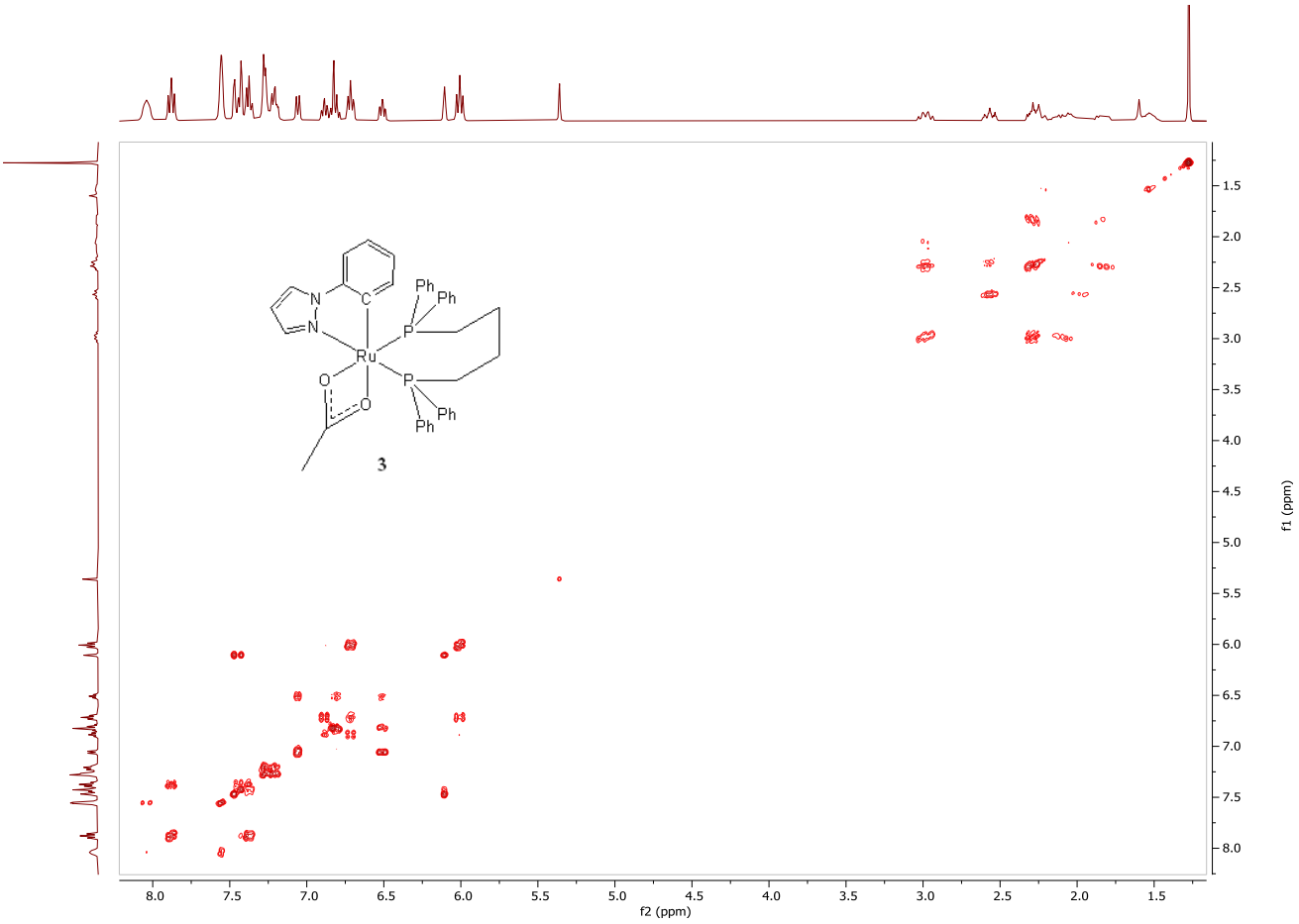

Figure S19. ^{1}H-^{1}H COSY 2D NMR spectrum of [Ru(**c**)(η^2-OAc)(dppb)] (**3**) in CD_2Cl_2 at 25 °C.

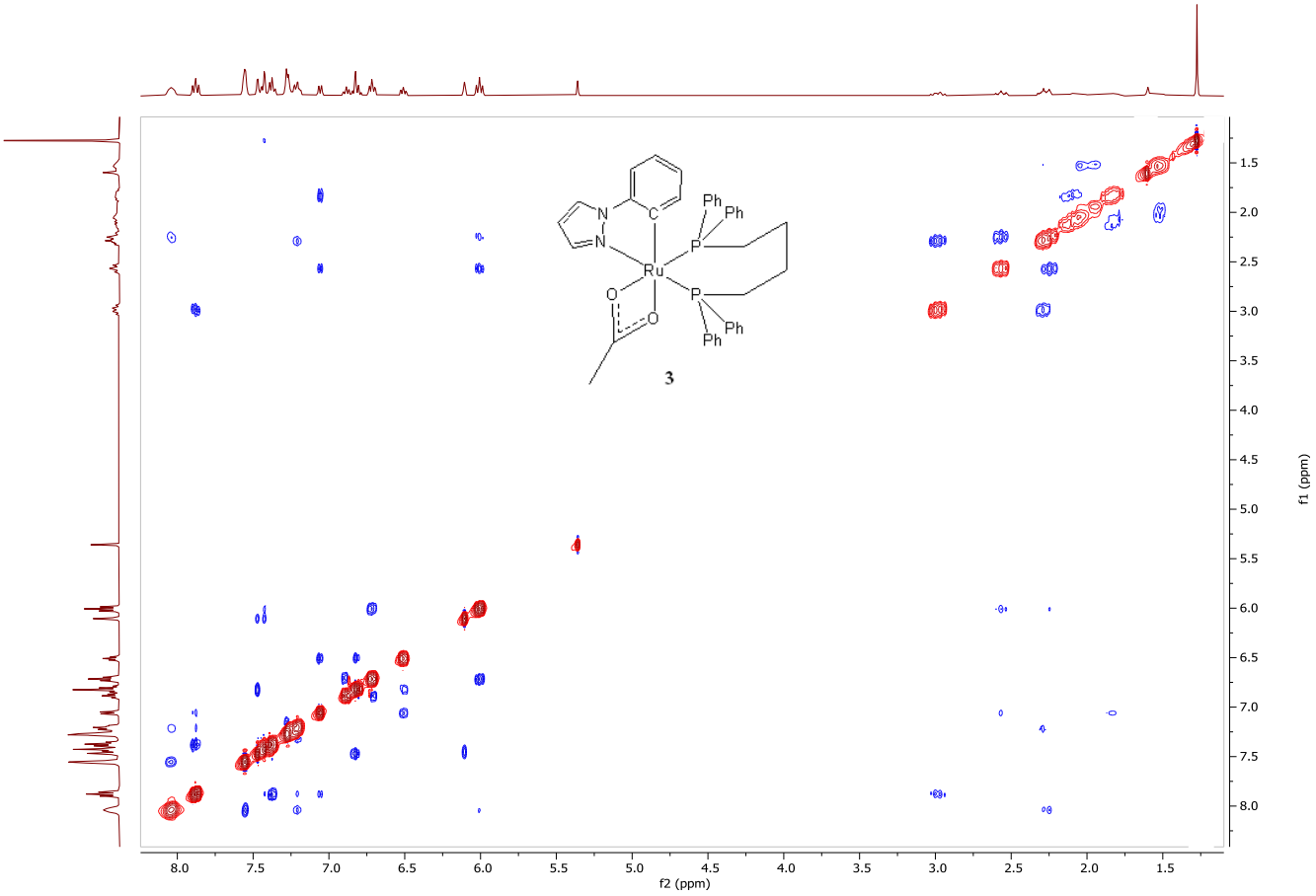

Figure S20. ^{1}H-^{1}H NOESY 2D NMR spectrum of [Ru(**c**)(η^2-OAc)(dppb)] (**3**)) in CD_2Cl_2 at 25 °C.

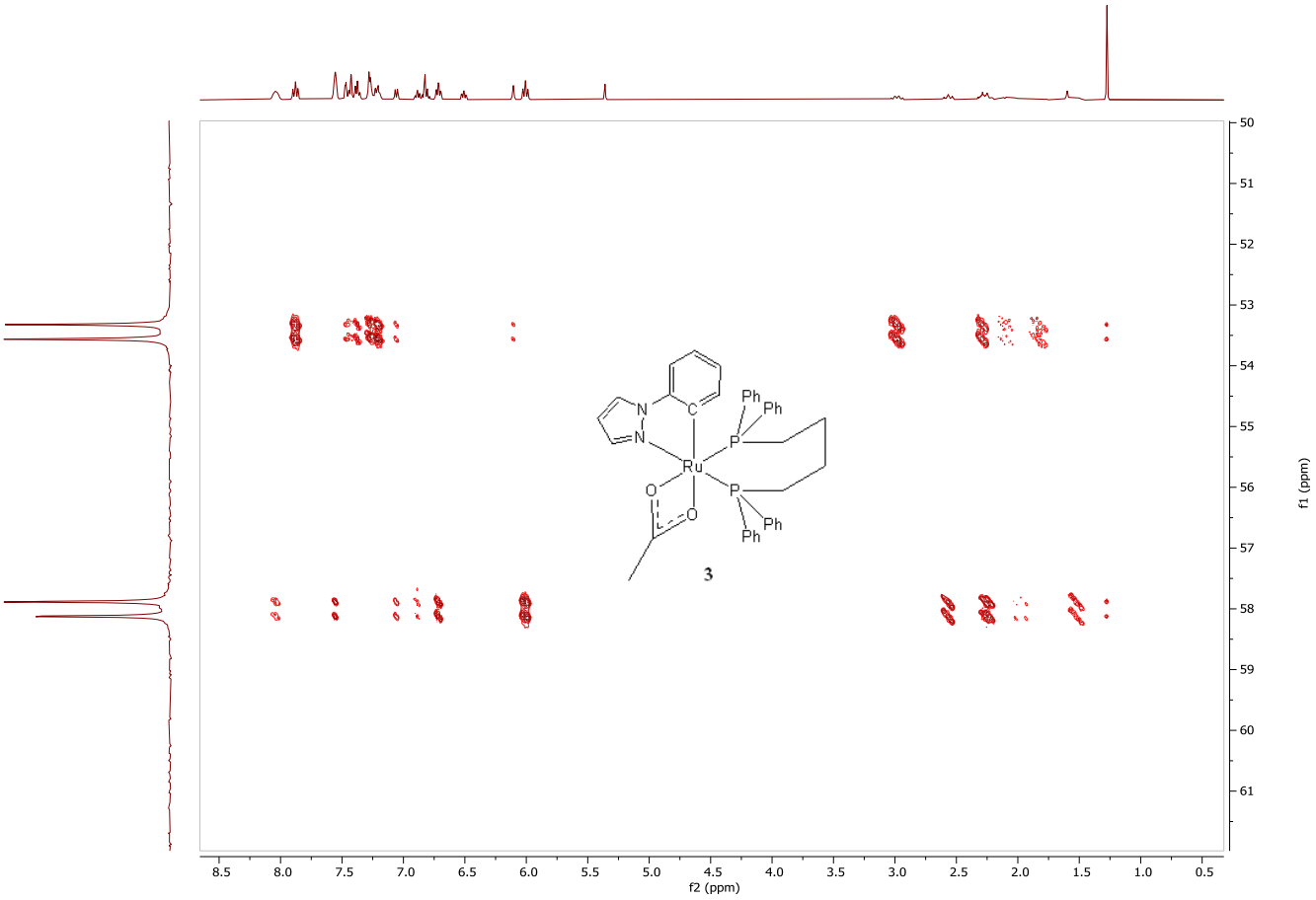

Figure S21. ^{1}H-^{31}P HMBC 2D NMR spectrum of [Ru(**c**)(η^{2}-OAc)(dppb)] (**3**) in CD_2Cl_2 at 25 °C.

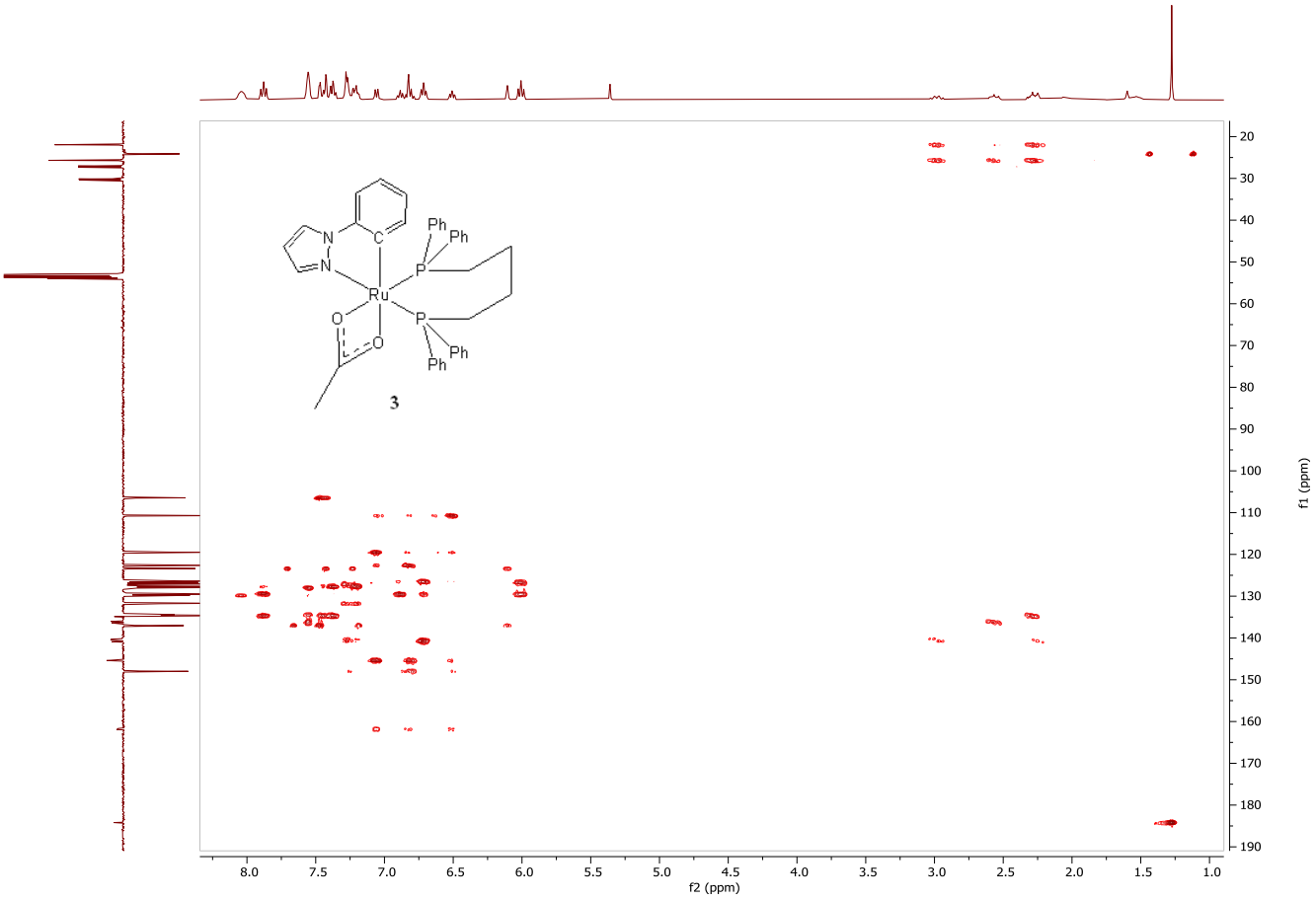

Figure S22. ^{1}H-^{13}C HMBC 2D NMR spectrum of [Ru(**c**)(η^2-OAc)(dppb)] (**3**) in CD_2Cl_2 at 25 °C.

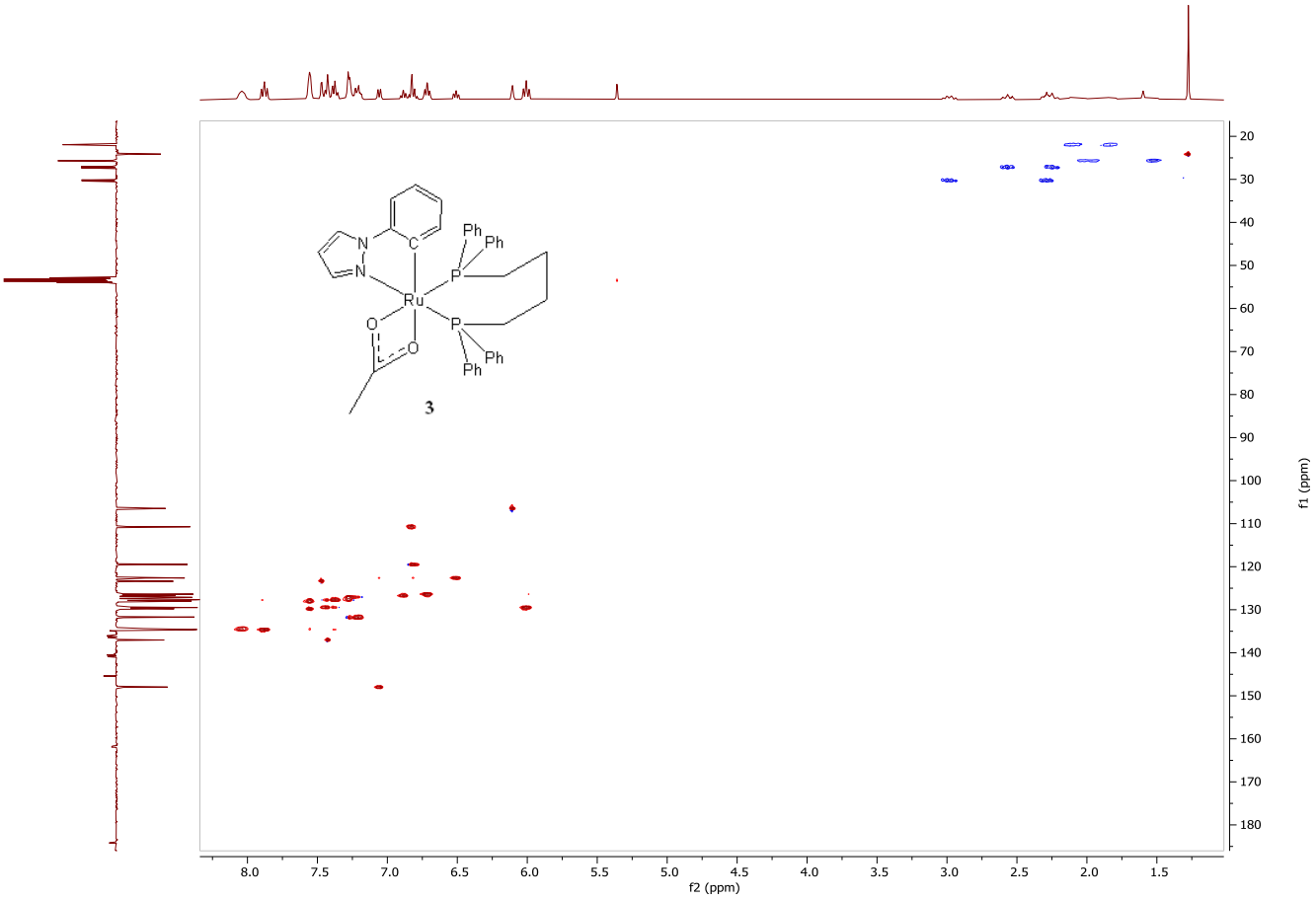

Figure S23. ^{1}H-^{13}C HSQC 2D NMR spectrum of [Ru(**c**)(η^2-OAc)(dppb)] (**3**) in CD_2Cl_2 at 25 °C.

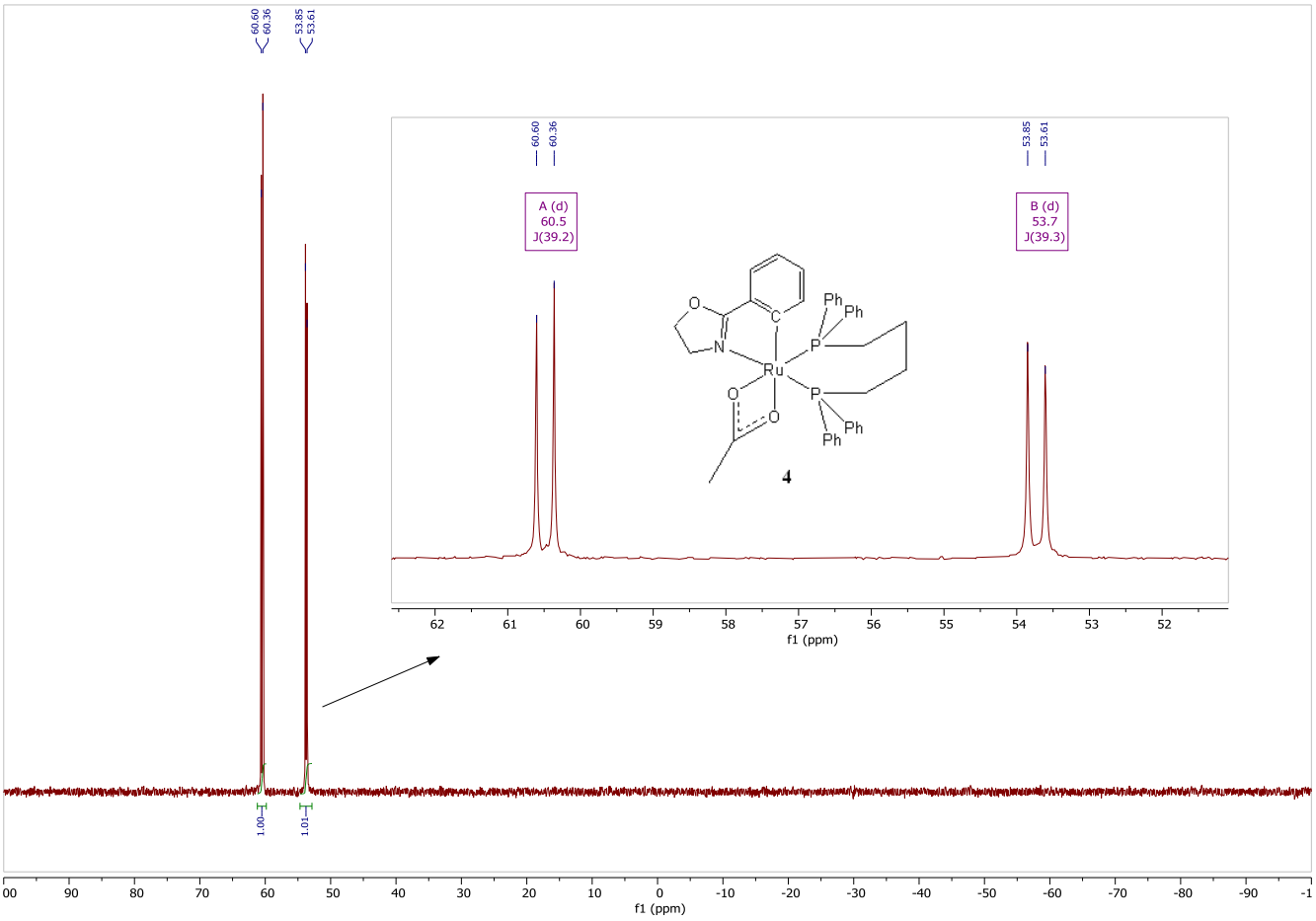

Figure S24. $^{31}P\{^{1}H\}$ NMR spectrum (162.0 MHz) of [Ru(**d**)(η^2-OAc)(dppb)] (**4**) in CD_2Cl_2 at 25 °C.

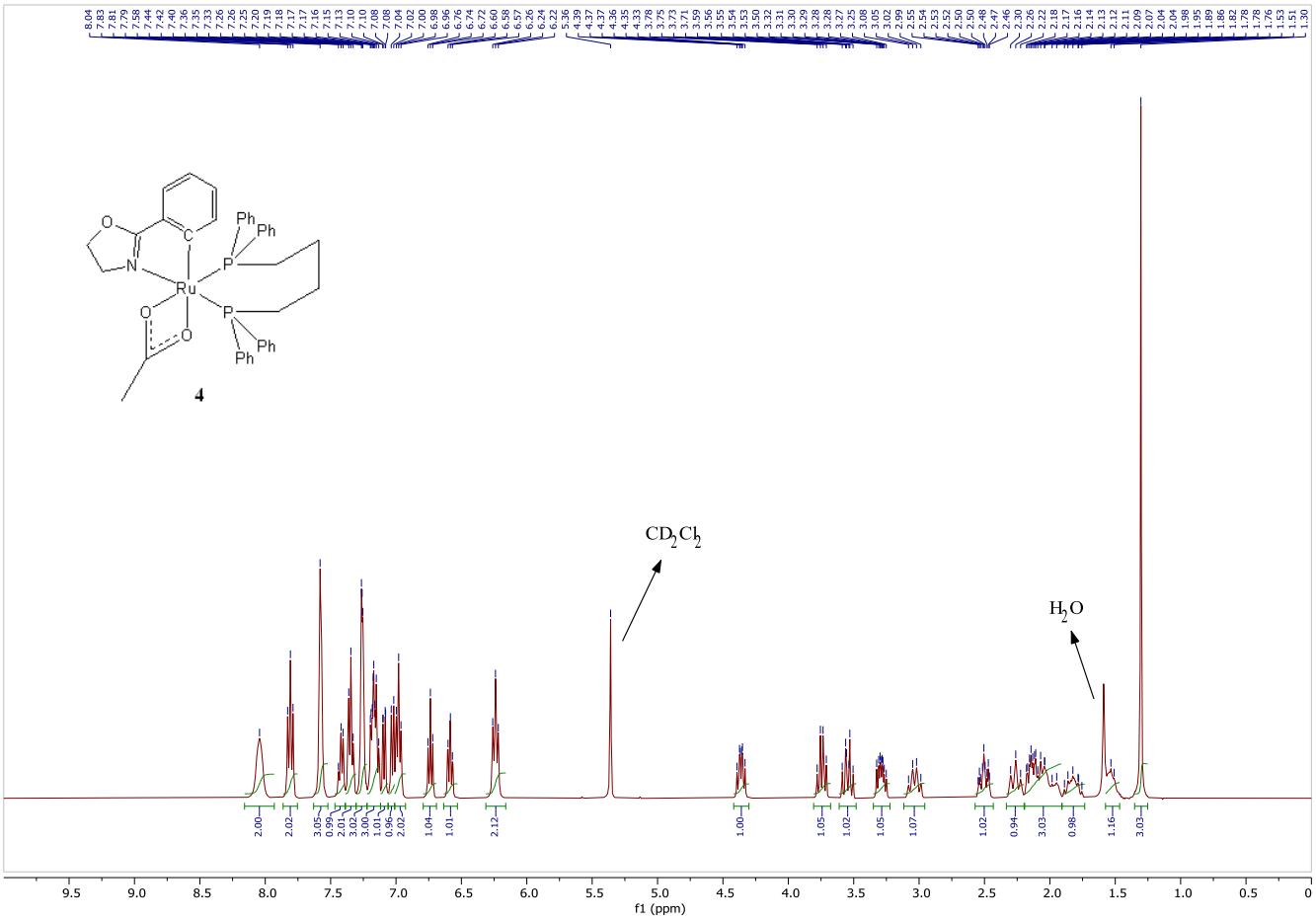

Figure S25. ^{1}H NMR spectrum (400.1 MHz) of [Ru(**d**)(η^2-OAc)(dppb)] (**4**) in CD_2Cl_2 at 25 °C.

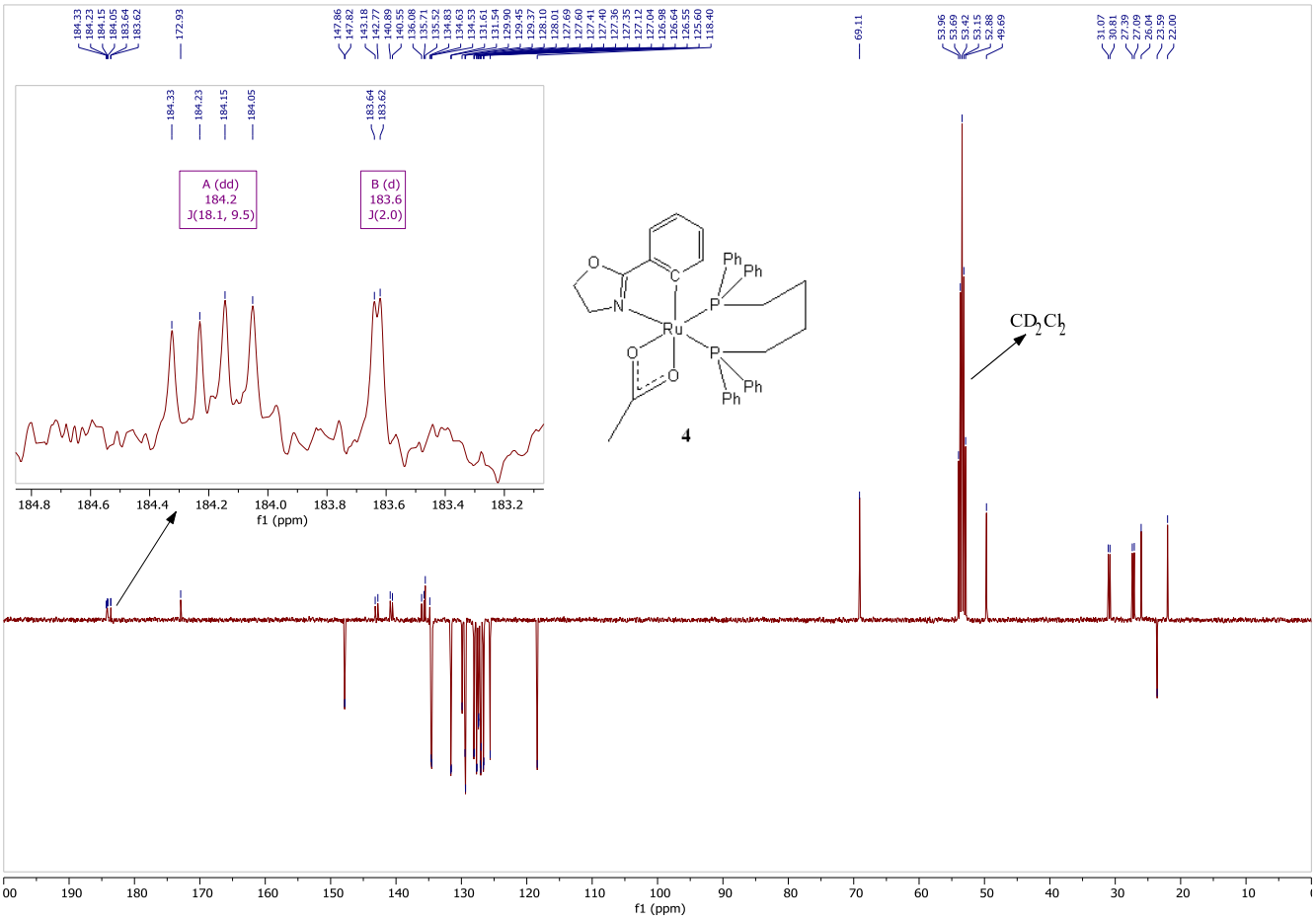

Figure S26. $^{13}C\{^{1}H\}$ DEPTQ NMR spectrum (100.6 MHz) of [Ru(**d**)(η^2-OAc)(dppb)] (**4**) in CD_2Cl_2 at 25 °C.

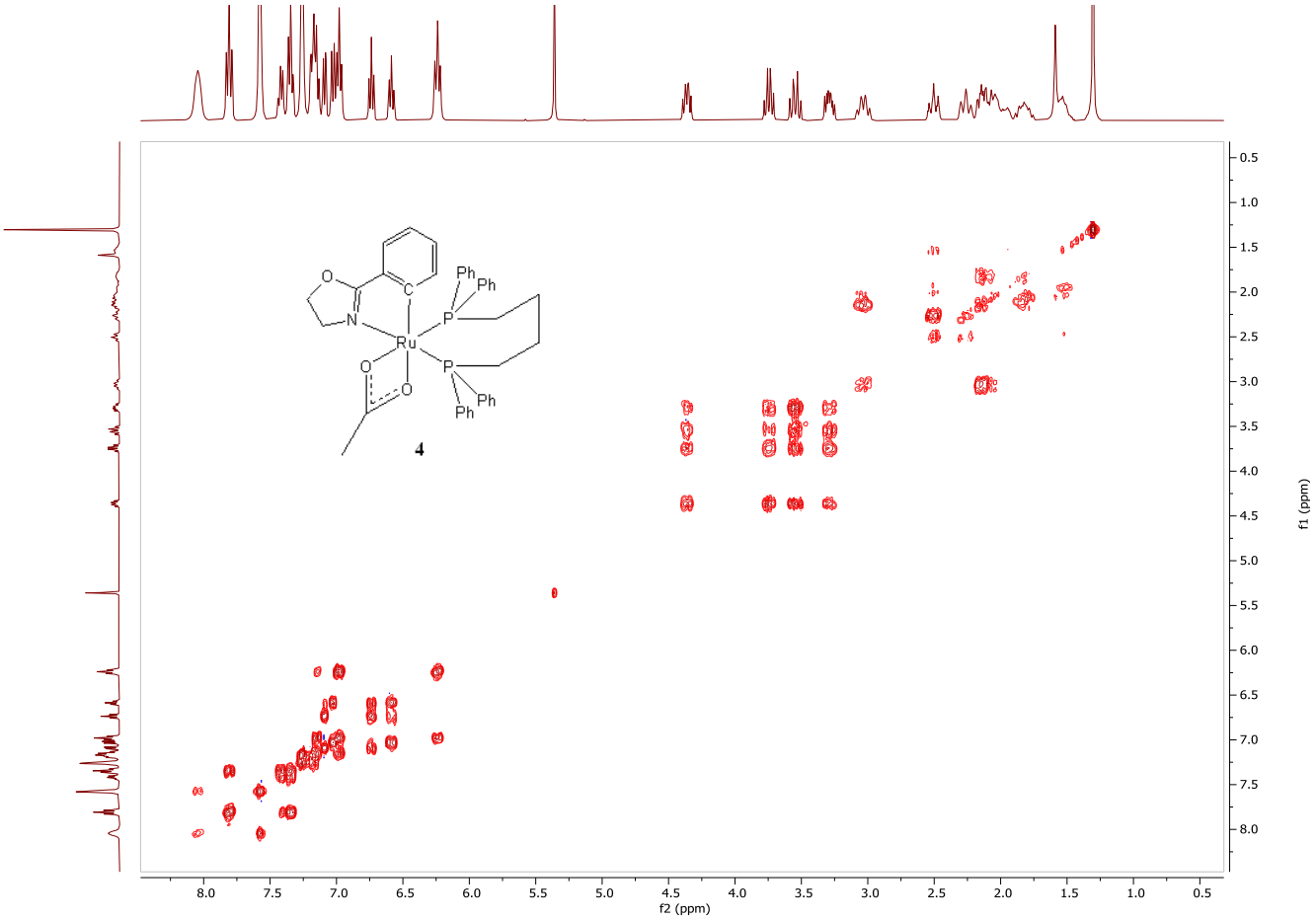

Figure S27. ^{1}H-^{1}H COSY 2D NMR spectrum of [Ru(**d**)(η^2-OAc)(dppb)] (**4**) in CD_2Cl_2 at 25 °C.

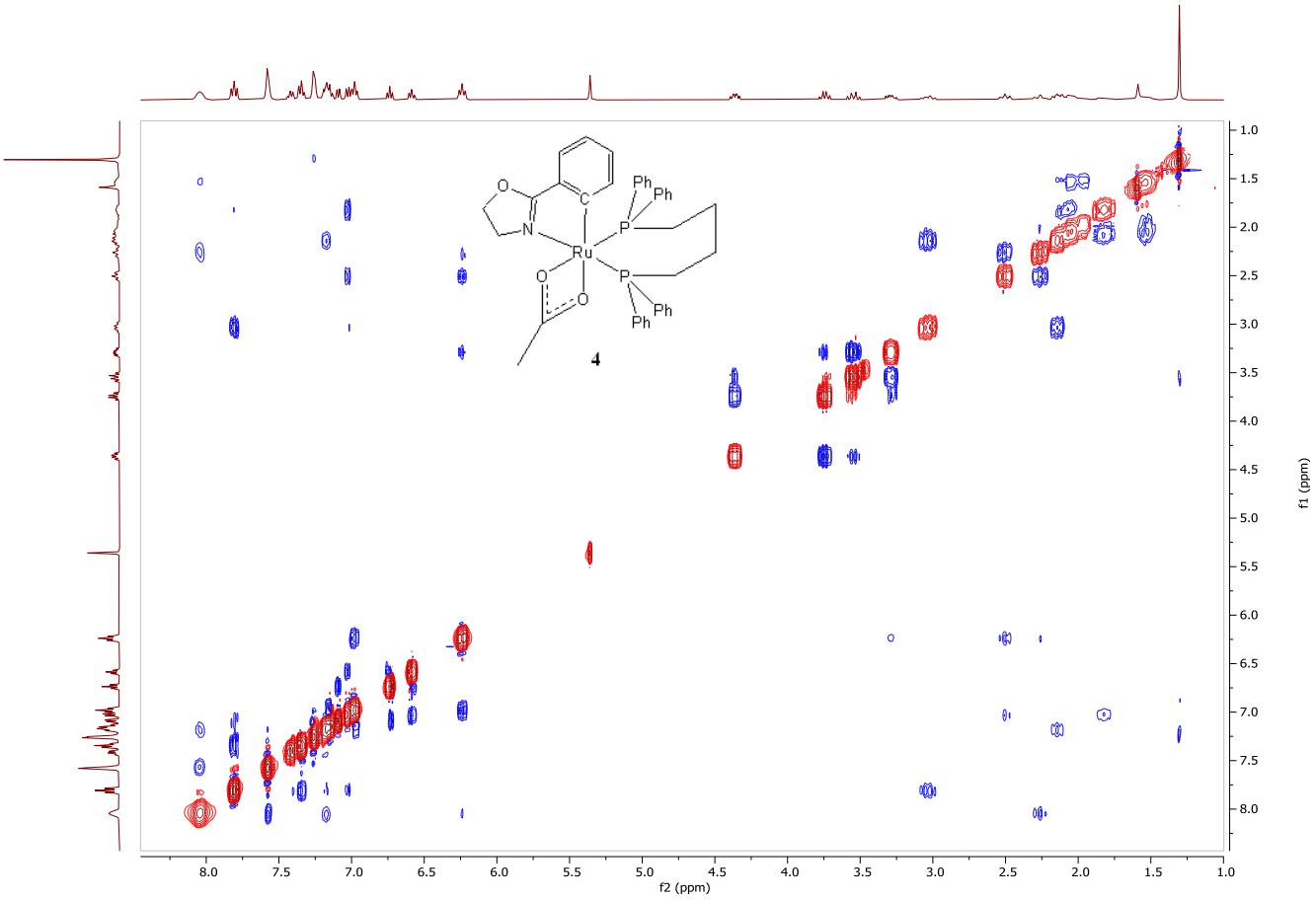

Figure S28. ^{1}H-^{1}H NOESY 2D NMR spectrum of [Ru(**d**)(η^{2}-OAc)(dppb)] (**4**) in CD_2Cl_2 at 25 °C.

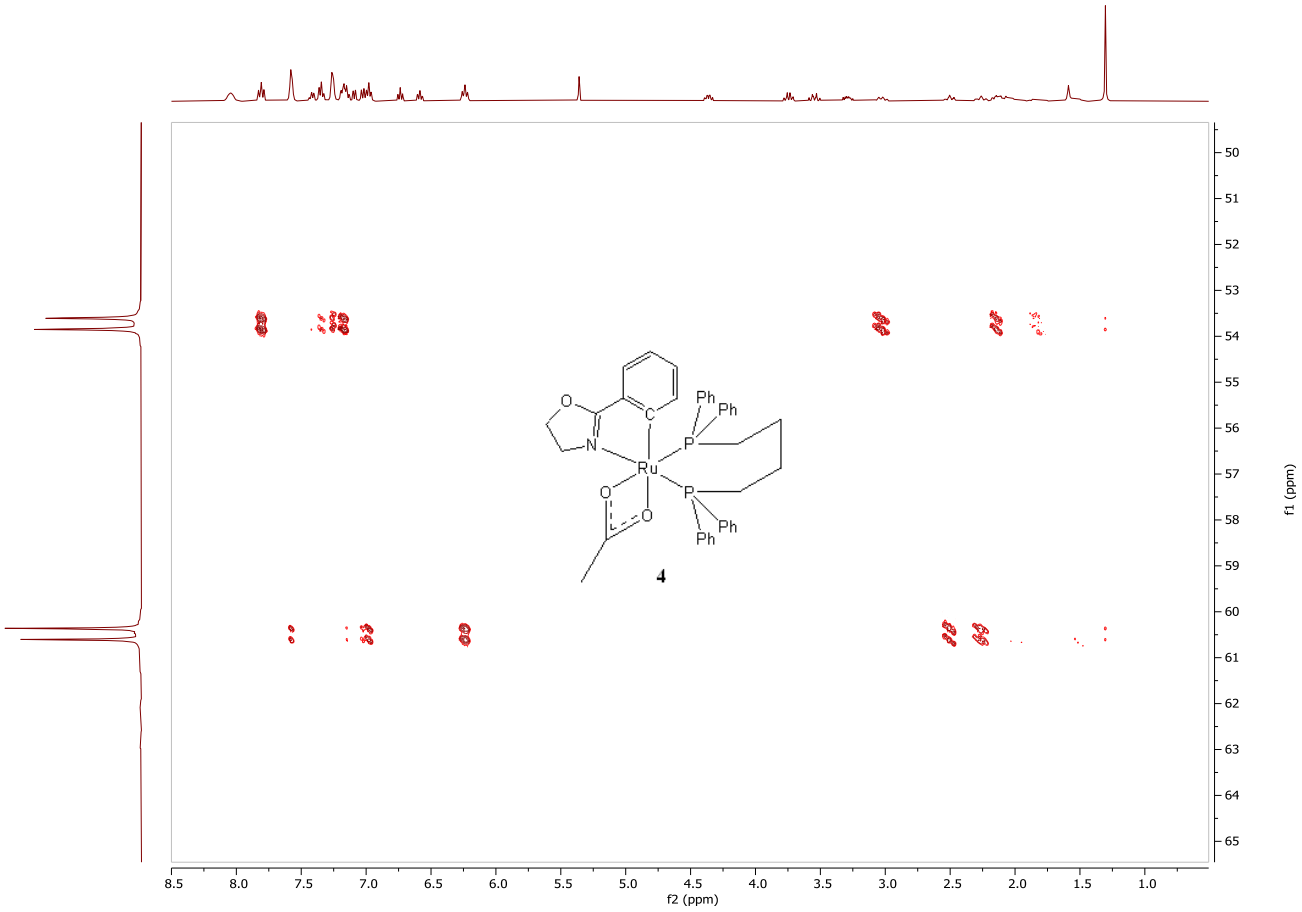

Figure S29. ^{1}H-^{31}P HMBC 2D NMR spectrum of [Ru(**d**)(η^{2}-OAc)(dppb)] (**4**) in CD_2Cl_2 at 25 °C.

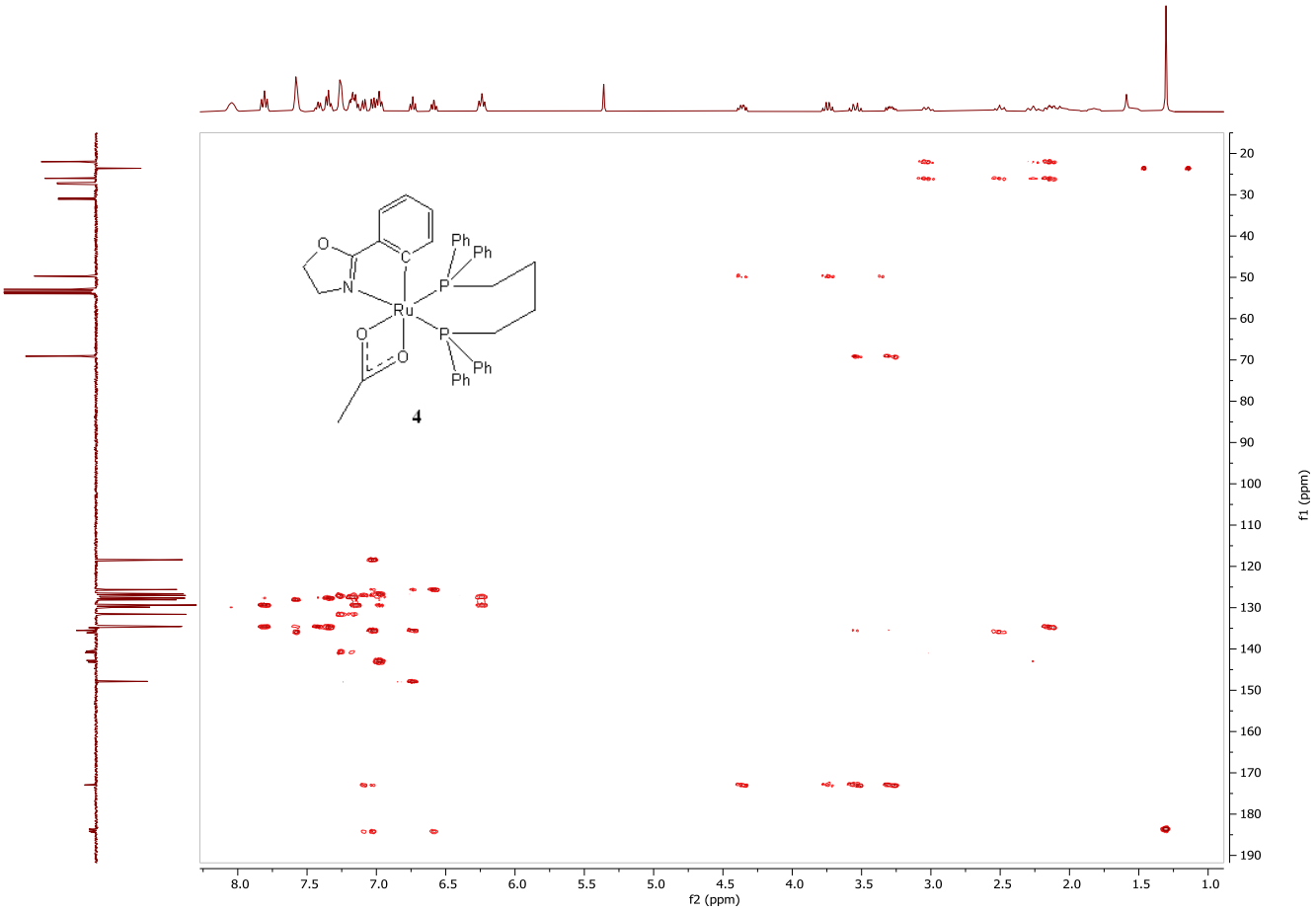

Figure S30. ^{1}H-^{13}C HMBC 2D NMR spectrum of [Ru(**d**)(η^{2}-OAc)(dppb)] (**4**) in CD_2Cl_2 at 25 °C.

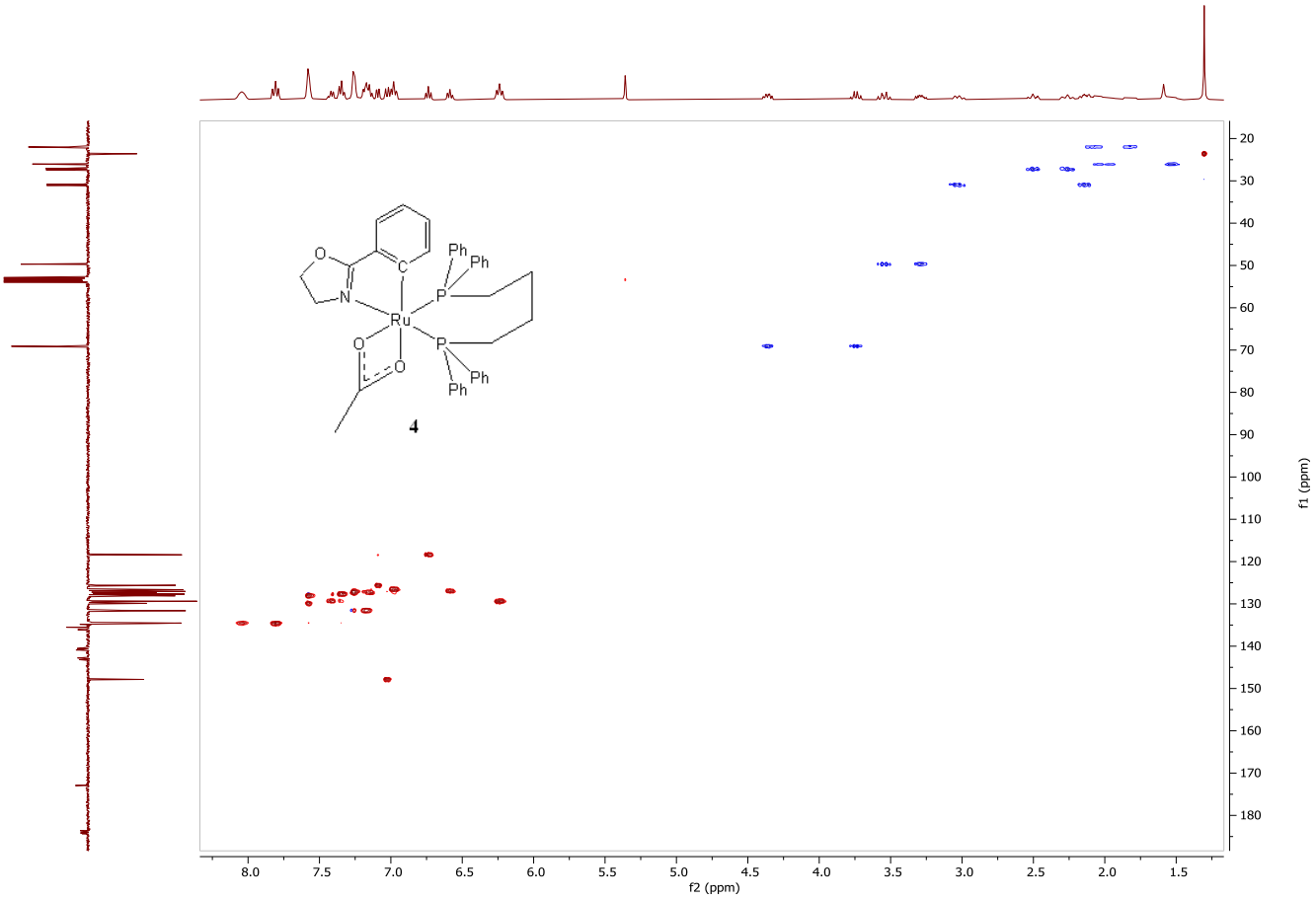

Figure S31. ^{1}H-^{13}C HSQC 2D NMR spectrum of [Ru(**d**)(η^2-OAc)(dppb)] (**4**) in CD_2Cl_2 at 25 °C.

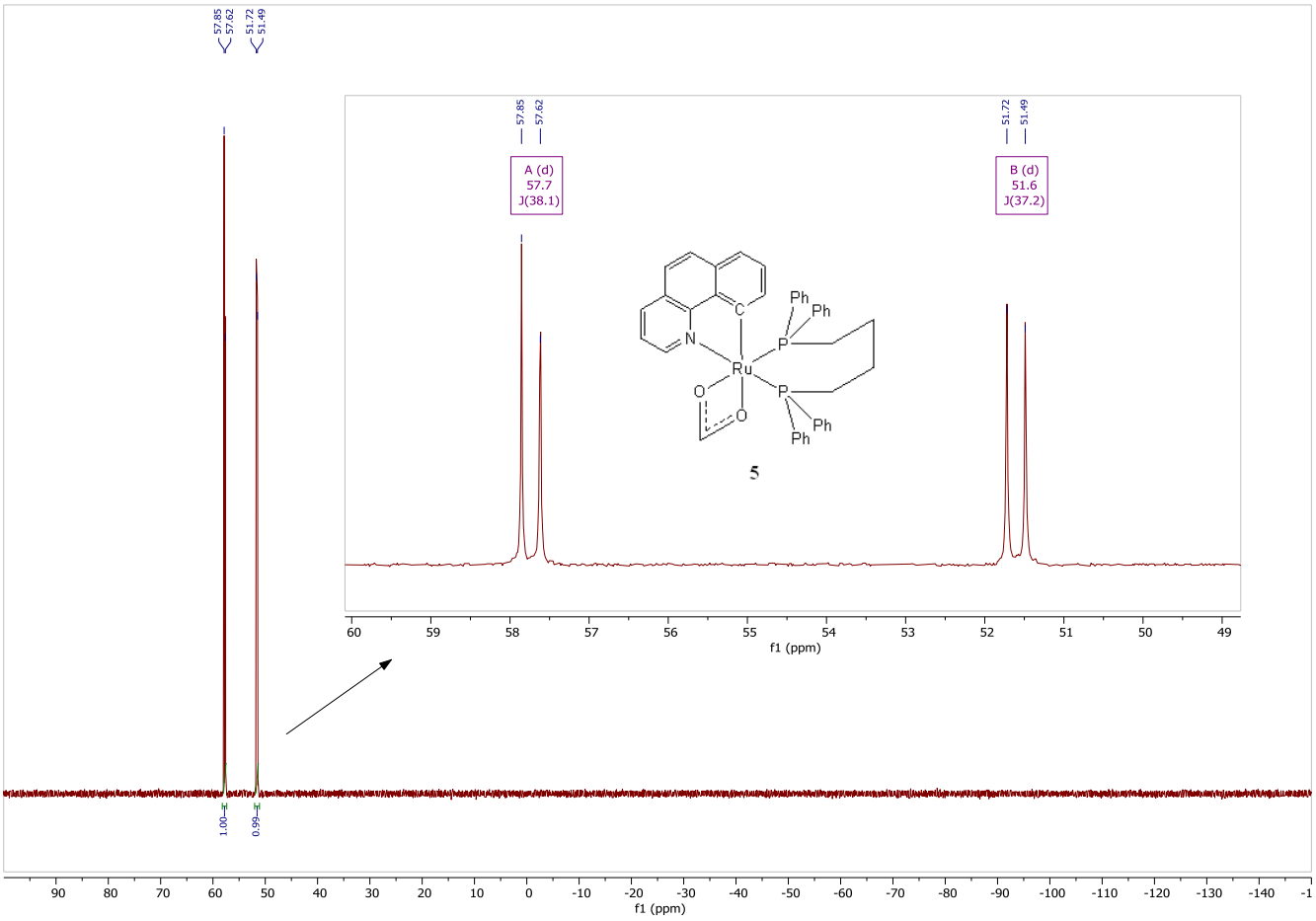

Figure S32. $^{31}P\{^{1}H\}$ NMR spectrum (162.0 MHz) of [Ru(**b**)(η^2-HCOO)(dppb)] (**5**) in CD_2Cl_2 at 25 °C.

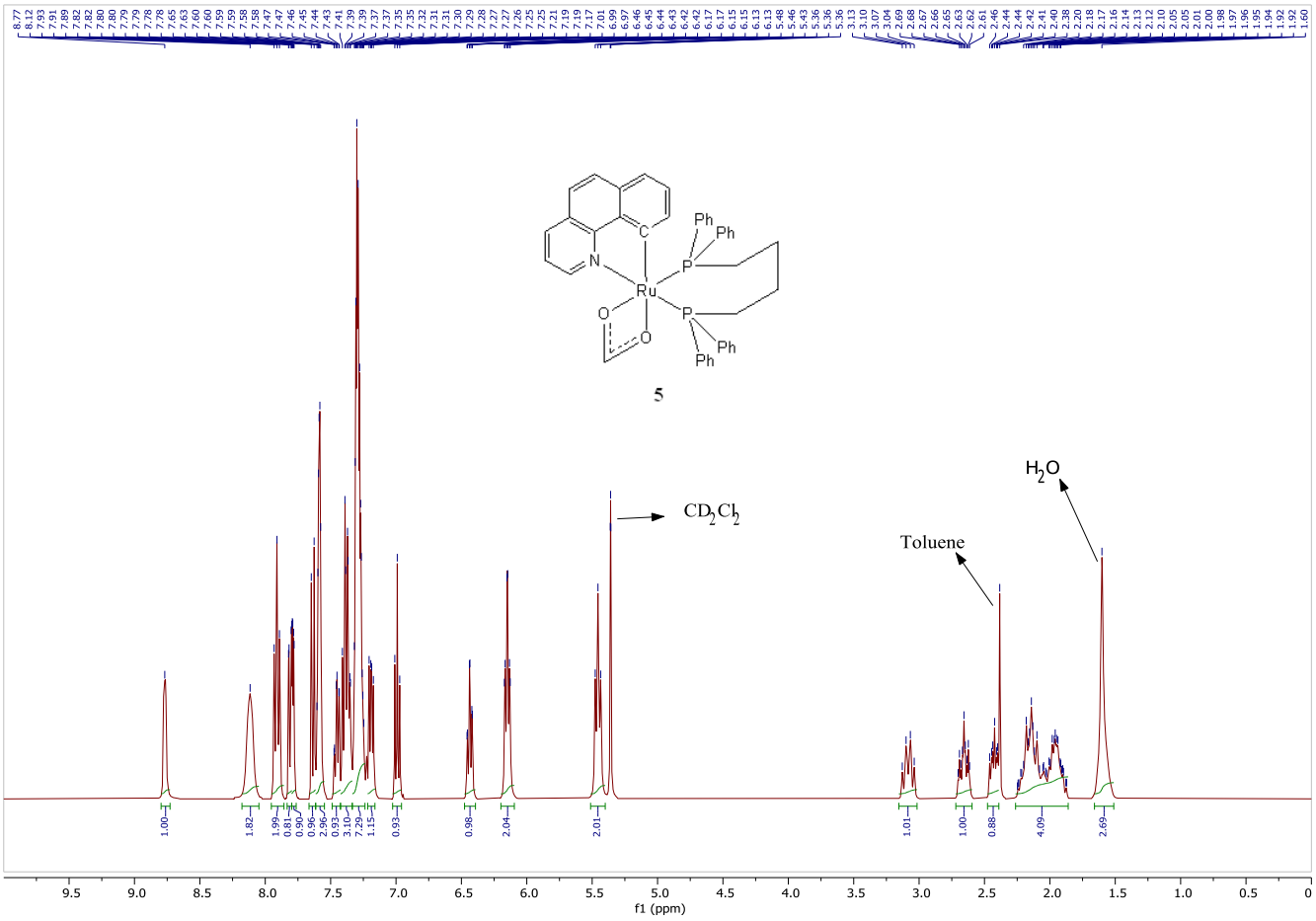

Figure S33. ^{1}H NMR spectrum (400.1 MHz) of [Ru(**b**)(η^2-HCOO)(dppb)] (**5**) in CD_2Cl_2 at 25 °C.

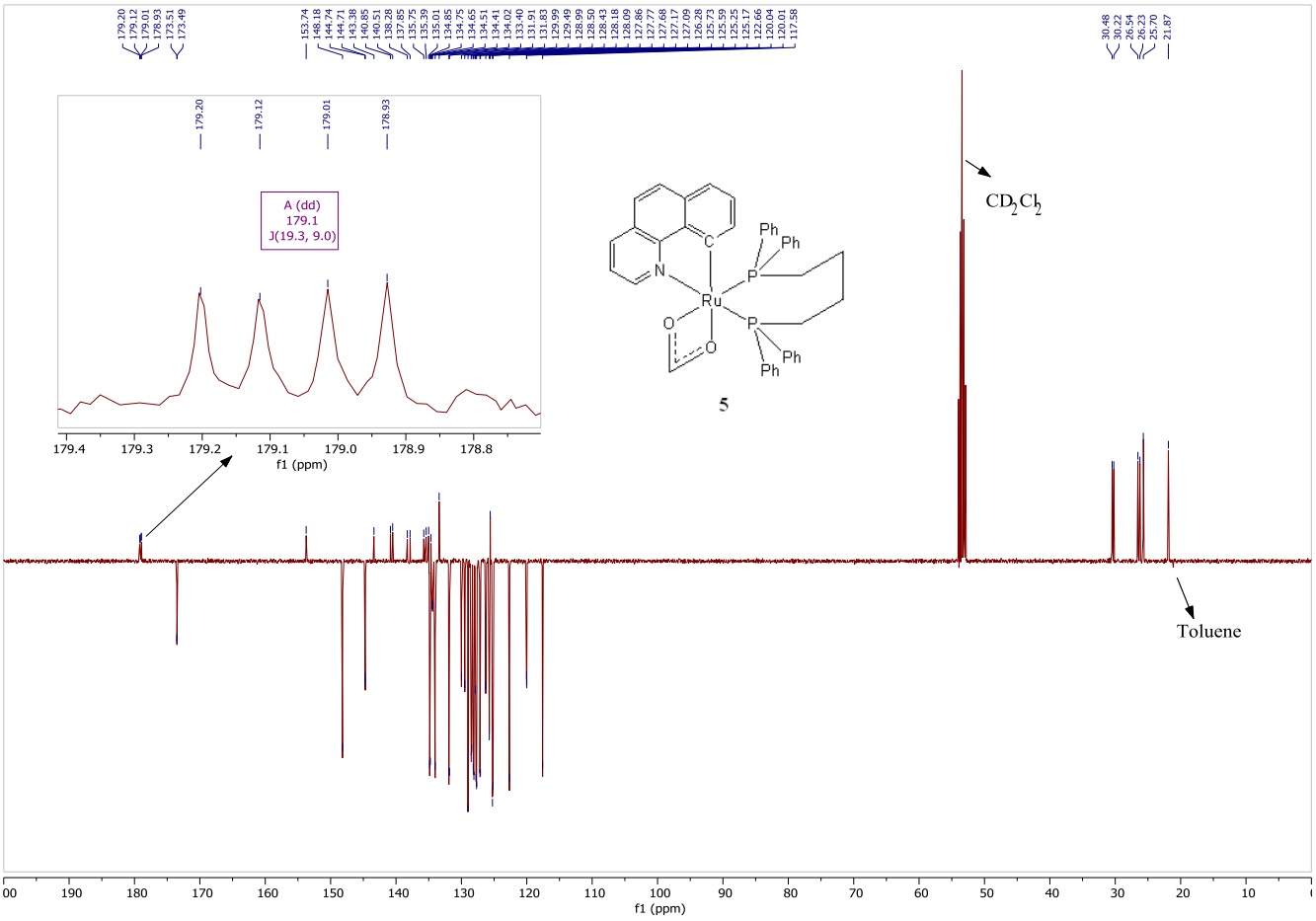

Figure S34. $^{13}C\{^{1}H\}$ DEPTQ NMR spectrum (100.6 MHz) of [Ru(**b**)(η^2-HCOO)(dppb)] (**5**) in CD_2Cl_2 at 25 °C.

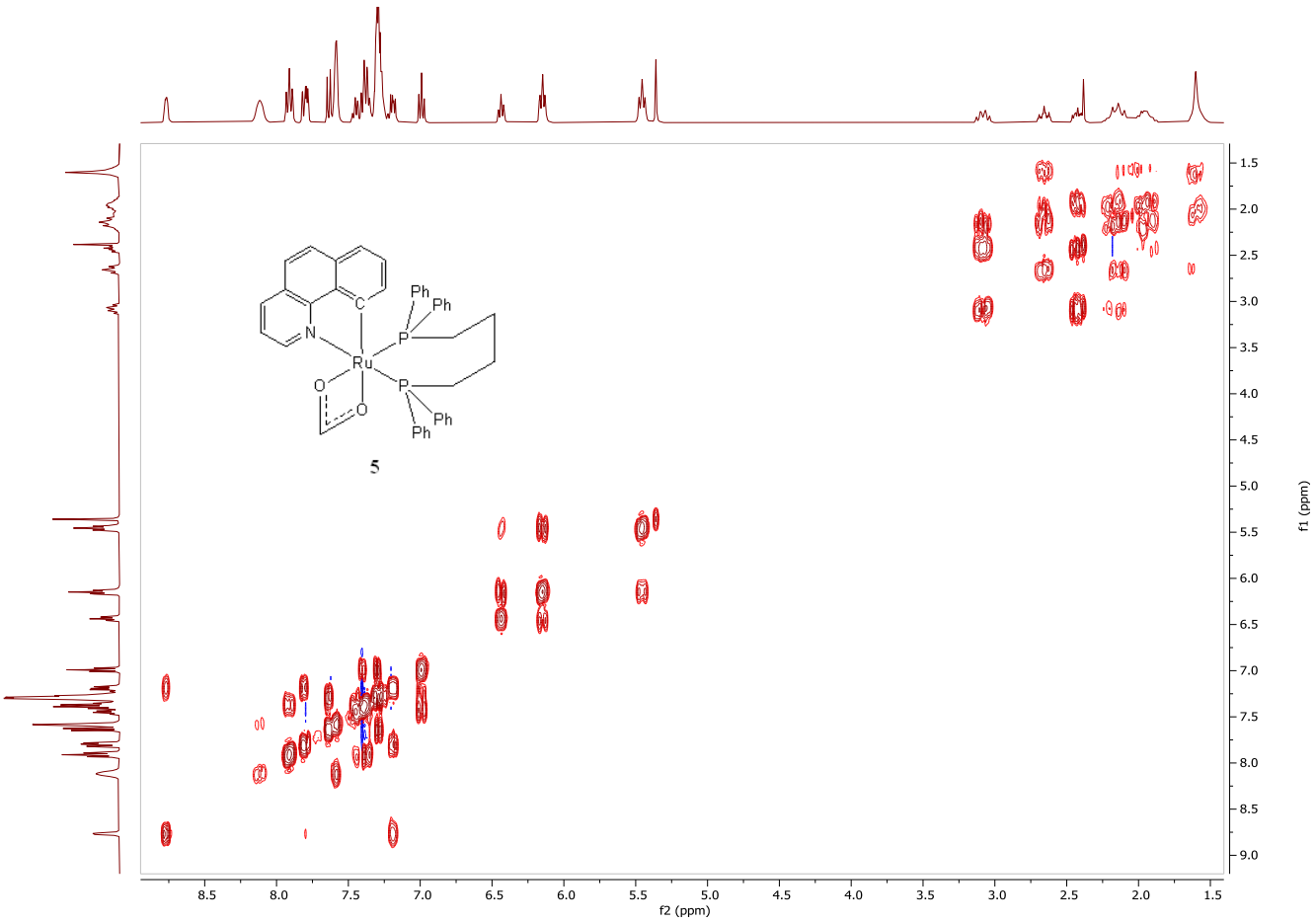

Figure S35. ^{1}H-^{1}H COSY 2D NMR spectrum of [Ru(**b**)(η^2-HCOO)(dppb)] (**4**) in CD_2Cl_2 at 25 °C.

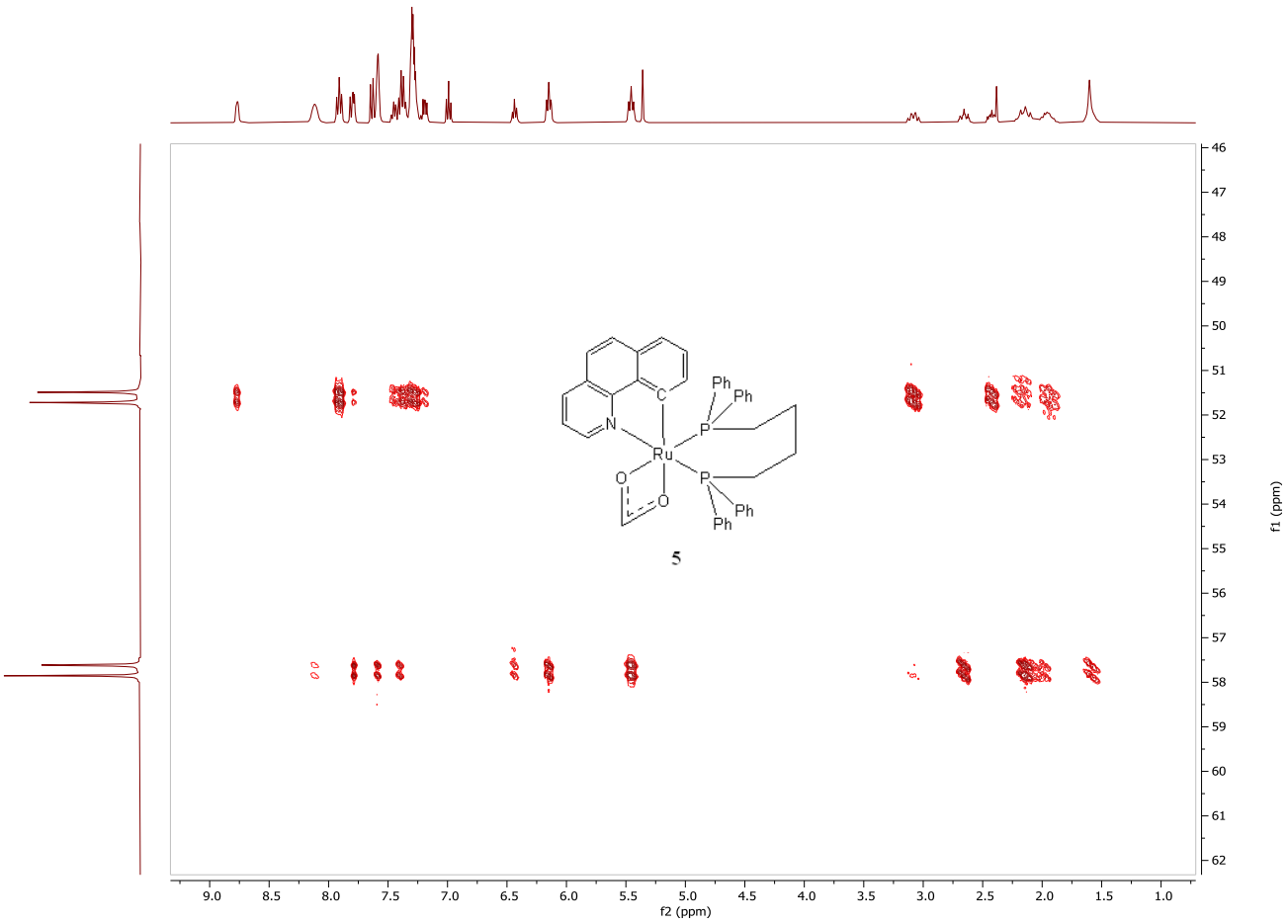

Figure S36. ^{1}H-^{31}P HMBC 2D NMR spectrum of [Ru(**b**)(η^{2}-HCOO)(dppb)] (**5**) in CD_2Cl_2 at 25 °C.

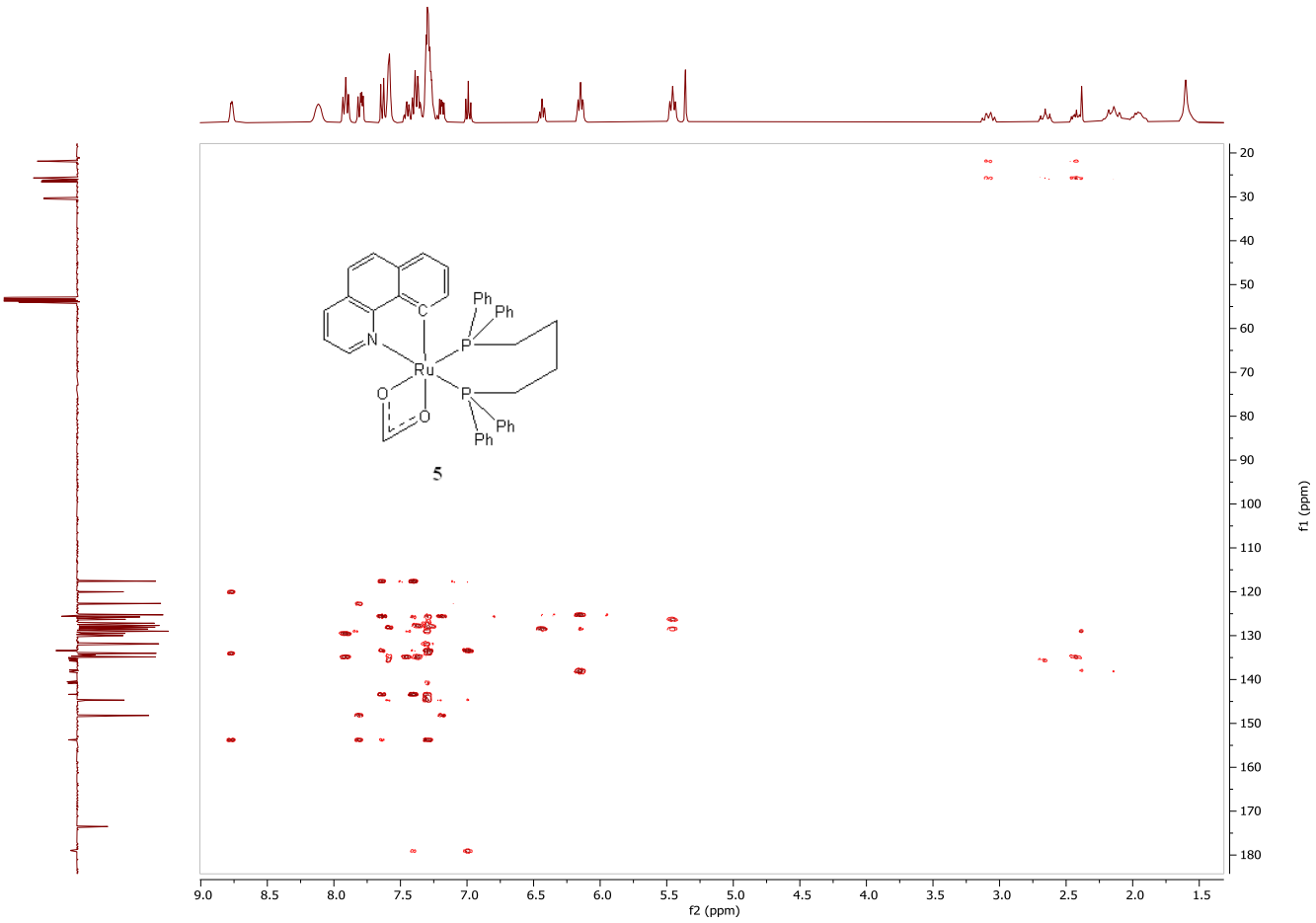

Figure S37. ^{1}H-^{13}C HMBC 2D NMR spectrum of [Ru(**b**)(η^{2}-HCOO)(dppb)] (**5**) in CD_2Cl_2 at 25 °C.

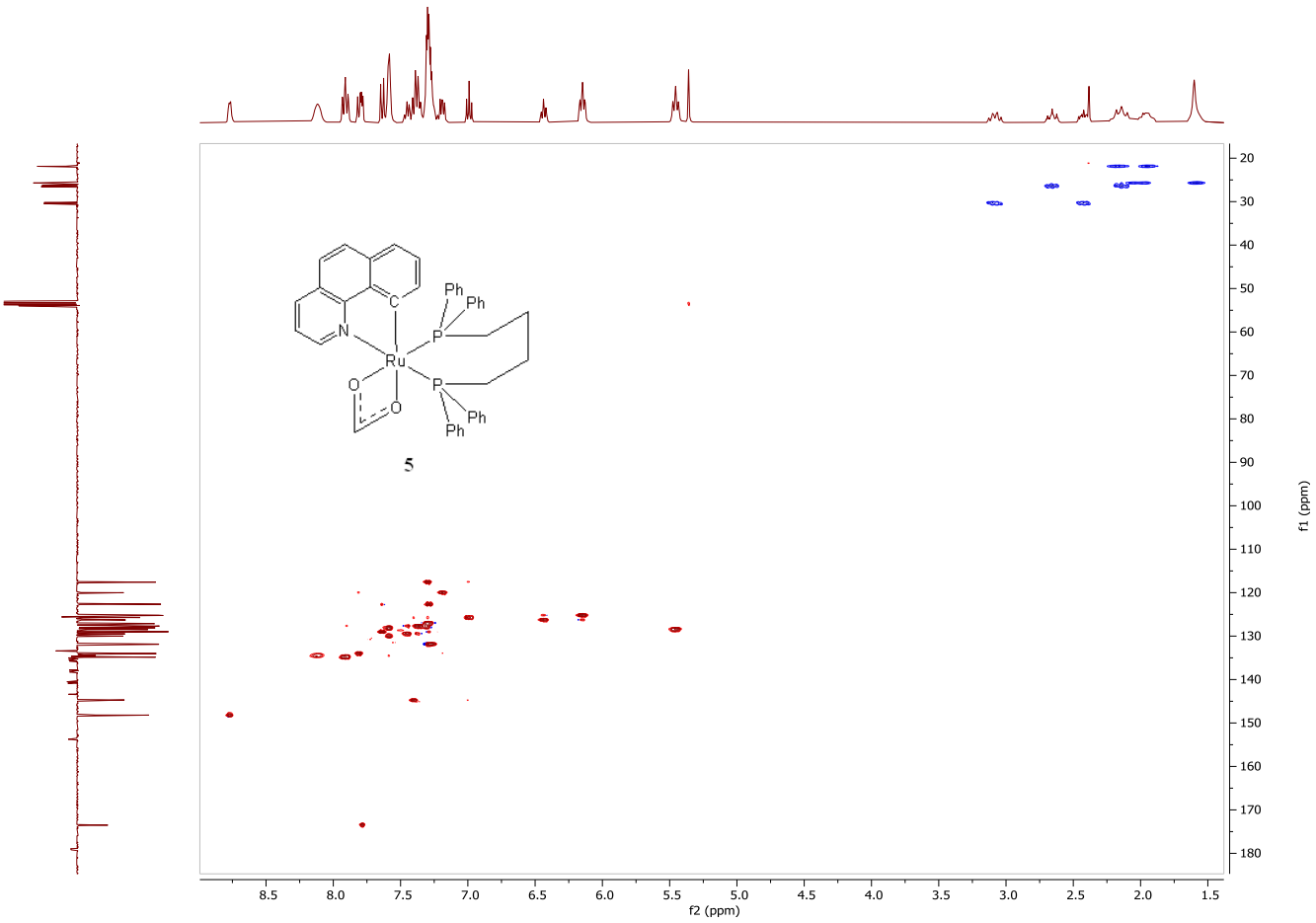

Figure S38. ^{1}H-^{13}C HSQC 2D NMR spectrum of [Ru(**b**)(η^2-HCOO)(dppb)] (**5**) in CD_2Cl_2 at 25 °C.

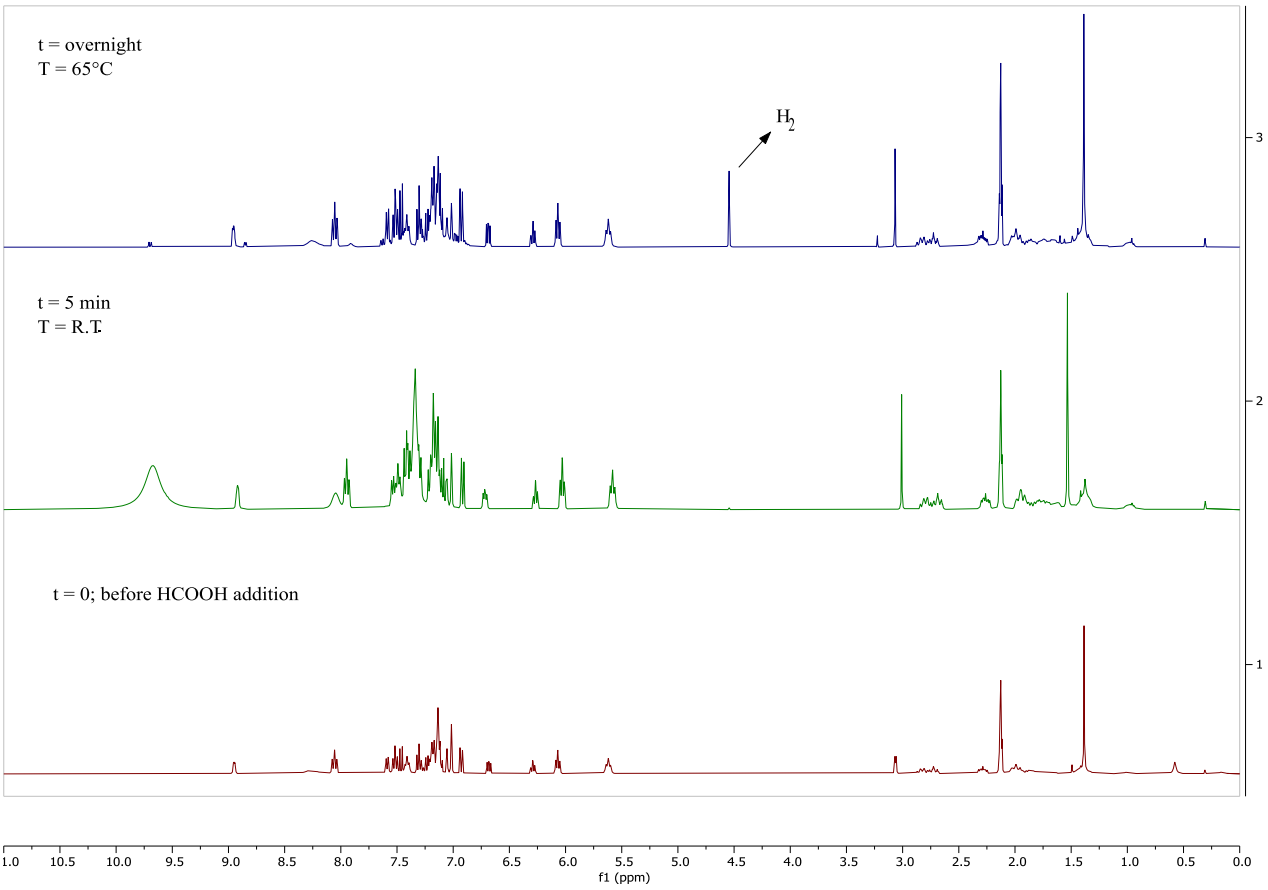

Figure S39. Evidence of H_2 formation from the decomposition of HCOOH promoted by [Ru(**b**)(η^2-OAc)(dppb)] (**2**) in the ^{1}H NMR spectra (400.1 MHz) in toluene-d^8.

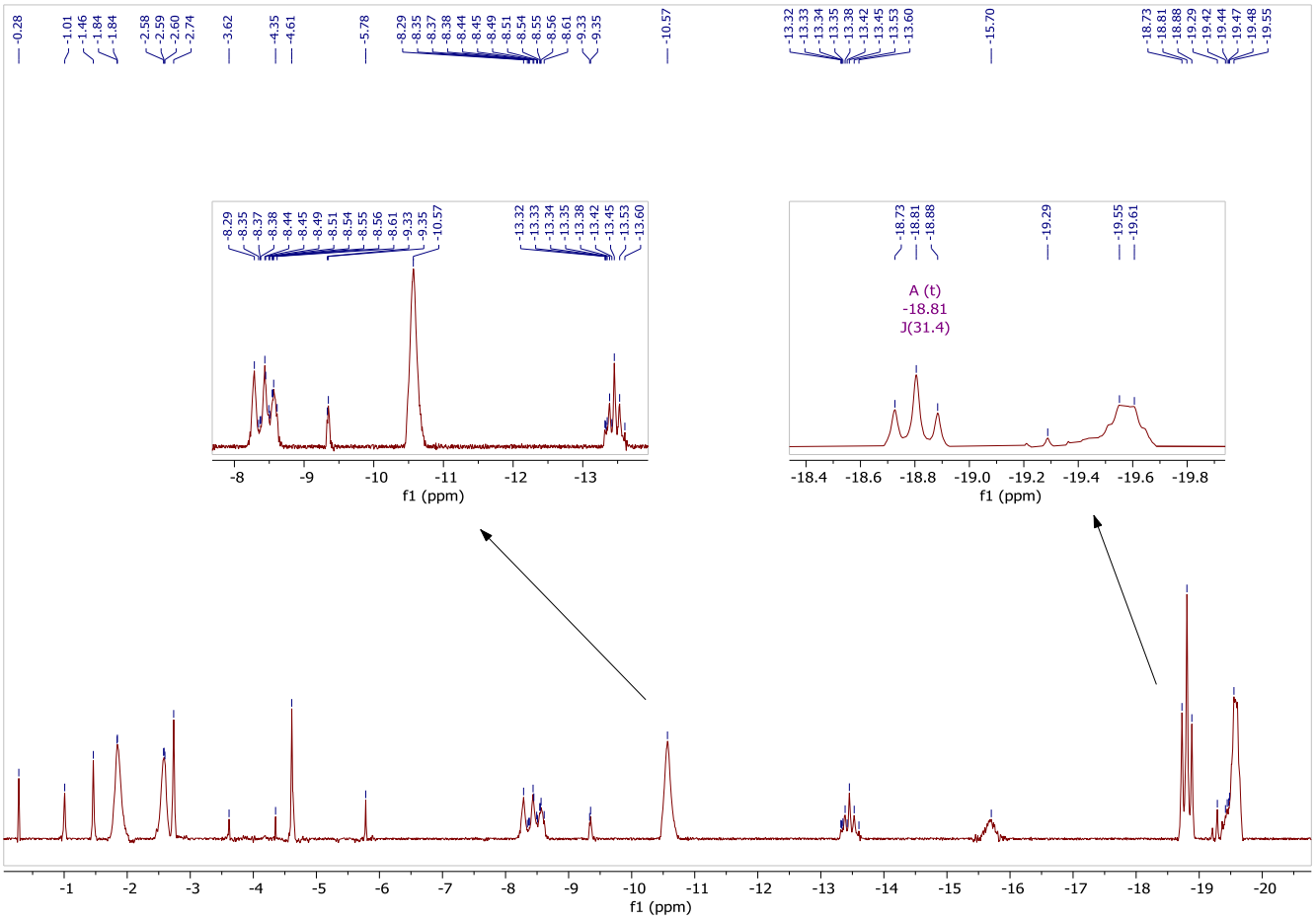

Figure S40. Evidence of formation of ruthenium monohydride species after treatment of [Ru(**d**)(η^2-OAc)(dppb)] (**4**) with NaO*i*Pr (2 equiv) at reflux in the ^{1}H NMR spectrum (400.1 MHz) in *i*PrOH/toluene-d^8 (4:1 (v/v)).

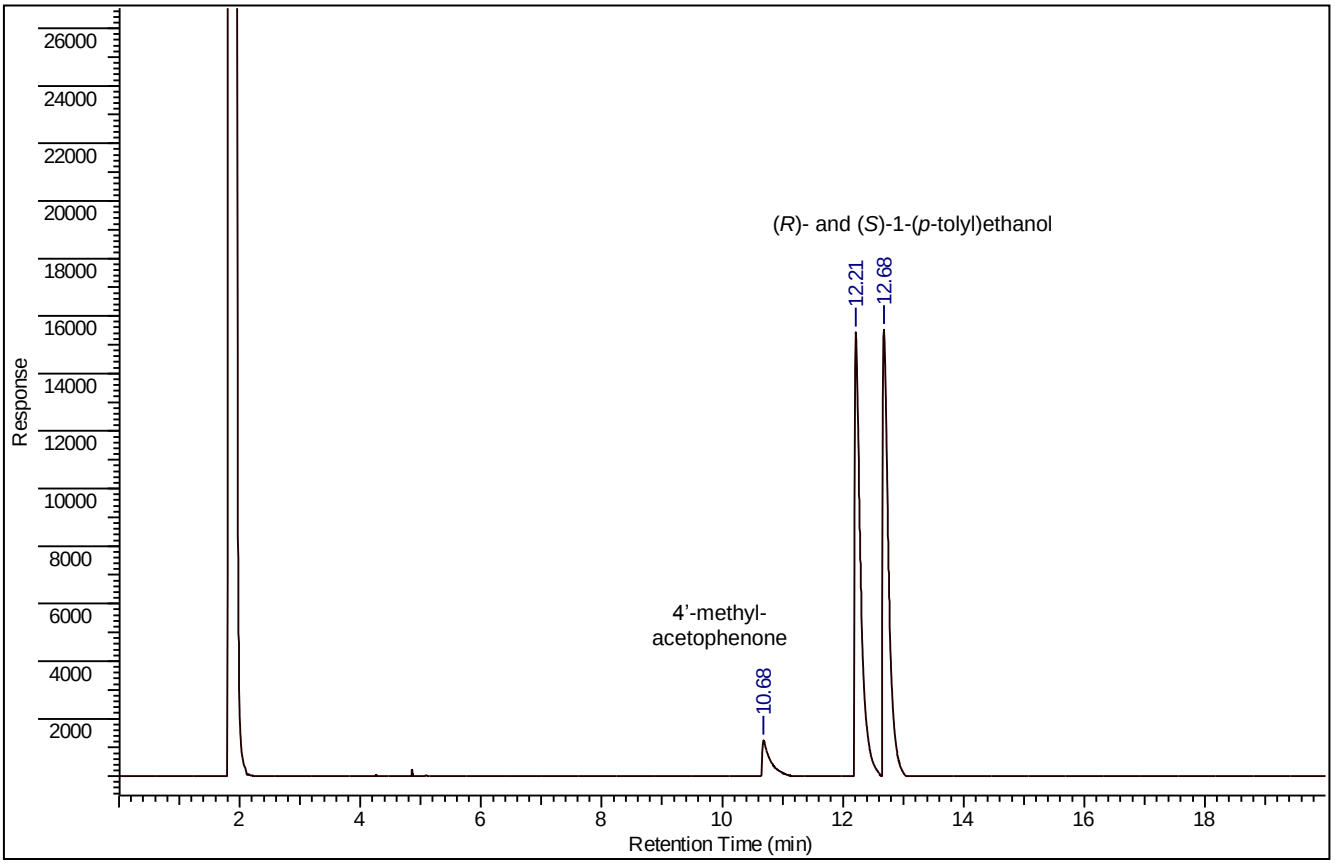

Figure S41. GC-FID chromatogram of the reaction mixture of the catalytic TH of 4'-methyl-acetophenone in 2-propanol at reflux and NaO*i*Pr 2 mol% promoted by complex **3** at S/C 1000 after 30 min. GC analyses were performed with a Varian CP-3380 gas chromatograph equipped with a 25 m length MEGADEX-ETTBDMS-β chiral column with hydrogen (5 psi) as the carrier gas and flame ionization detector (FID). The injector and detector temperature was 250 °C, with initial T = 95 °C ramped to 140 °C at 3 °C/min, then to 210 °C at 30 °C/min, which is maintained for other 3 min. for a total of 20 min of analysis.

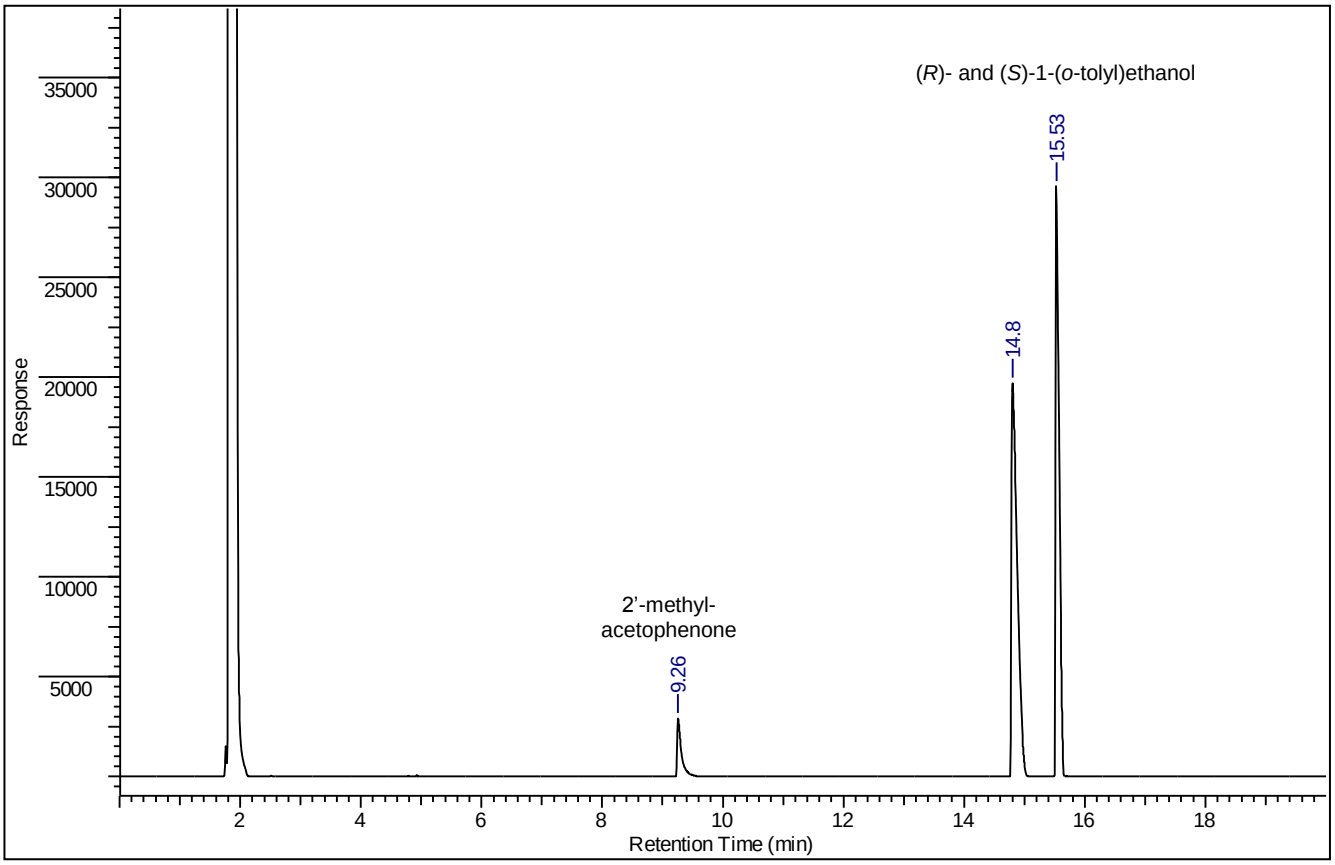

Figure S42. GC-FID chromatogram of the reaction mixture of the catalytic TH of 2'-methyl-acetophenone in 2-propanol at reflux and NaO*i*Pr 2 mol% promoted by complex **3** at S/C 1000 after 30 min. GC analyses were performed with a Varian CP-3380 gas chromatograph equipped with a 25 m length MEGADEX-ETTBDMS-β chiral column with hydrogen (5 psi) as the carrier gas and flame ionization detector (FID). The injector and detector temperature was 250 °C, with initial T = 95 °C ramped to 140 °C at 3 °C/min, then to 210 °C at 30 °C/min, which is maintained for other 3 min. for a total of 20 min of analysis.

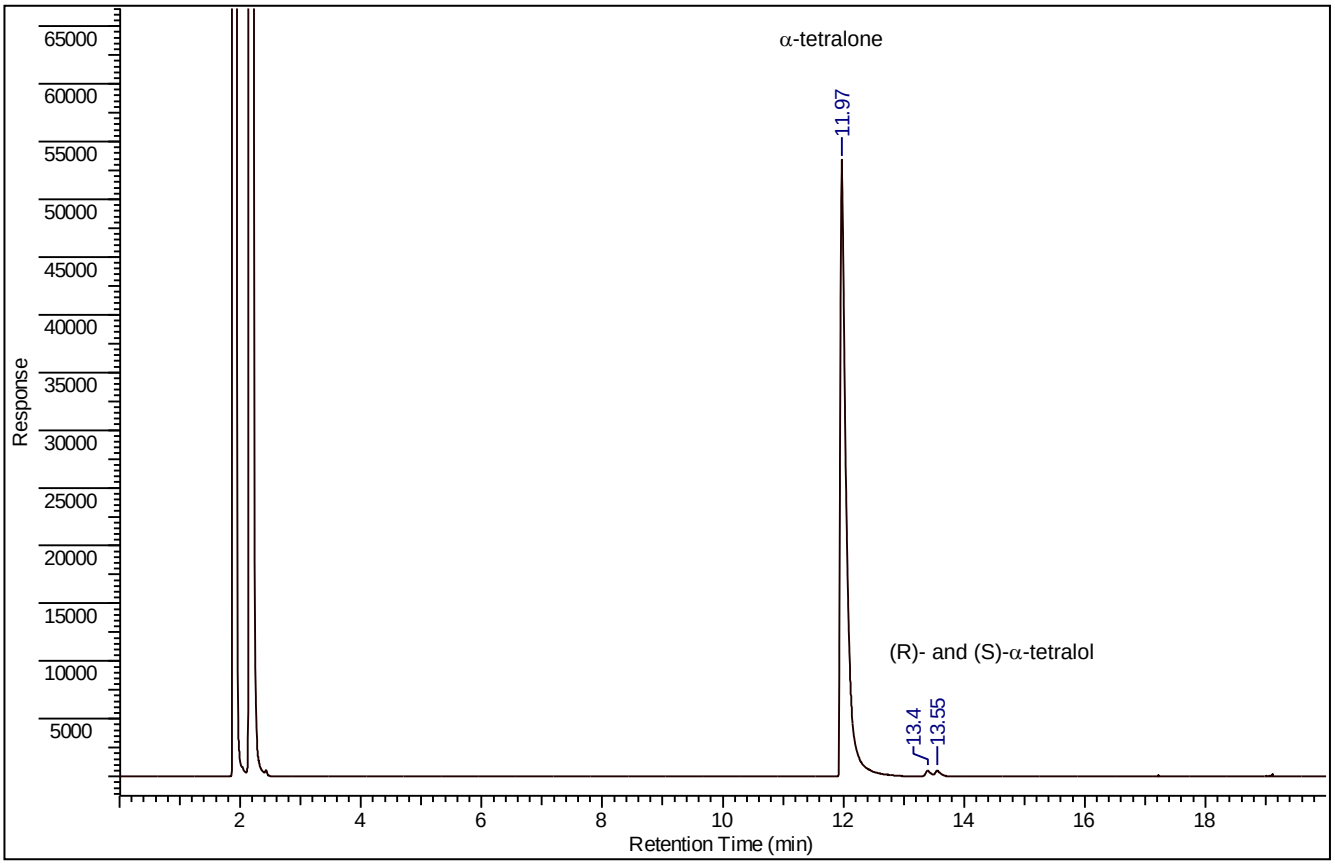

Figure S43. GC-FID chromatogram of the reaction mixture of the catalytic *Oppenauer*-type oxidation of *rac*-α-tetralol in toluene at reflux with KO*t*Bu 5 mol% and in presence of acetone (10 equiv) promoted by complex **1** at S/C 1000 after 20 min. GC analyses were performed with a Varian CP-3380 gas chromatograph equipped with a 25 m length MEGADEX-ETTBDMS-β chiral column with hydrogen (5 psi) as the carrier gas and flame ionization detector (FID). The injector and detector temperature was 250 °C, with initial T = 125 °C ramped to 155 °C at 2 °C/min, then to 195 °C at 20 °C/min, which is maintained for other 3 min. for a total of 20 min of analysis.

General Procedure for the *Oppenauer*-type oxidation of secondary alcohols

The ruthenium catalyst solutions used for these reactions were prepared by dissolving the complexes (**1**-**4**, 2 μmol) in toluene (2 mL). The alcohol substrate (1.0 mmol) was dissolved in toluene (8.26 mL (when acetone was used as proton acceptor) or 8.38 mL (when cyclohexanone was used)), and the catalyst solution (1.0 mL, 1.0 μmol) and KO*t*Bu (5.6 mg, 0.05 mmol) were added. After heating at reflux, acetone (740 μL, 580 mg, 10 mmol) or cyclohexanone (621 μL, 588.8 mg, 6.0 mmol) were added (final volume 10 mL). The reaction was sampled by removing an aliquot of the reaction mixture, which was quenched by addition of diethyl ether (1:1 v/v), filtered over a short silica pad and submitted to GC analysis. The ketone addition was considered as the start time of the reaction. The S/C molar ratio was 1000/1, whereas the base concentration was 5 mol% respect to the alcohol substrates (0.1 M). The same procedure was followed for the Oppenauer-type oxidation reactions with different S/C (250 - 1000), using the appropriate amount of catalyst.

For the isolation of ketones with **4**, the final mixture was filtered over a short silica pad and condensed under reduced pressure. The crude residue was dissolved with diethyl ether (5 mL) and the organic layer washed with a diluted solution of HCl (0.1 M; 3 x 3 mL), dried over anhydrous Na_2SO_4, and the solvent gently evaporated, affording the ketone products. In some cases, it was necessary to use a purification by flash silica gel column chromatography, using petroleum/ethyl acetate as eluent, to obtain the final products (yields: 44-95%). (1*R*)-(+)-camphor, on the other hand, was purified through a sublimation process. All compounds were characterized by ^{1}H and ^{13}C{^{1}H} NMR.

α-Tetralone:[1]

Clear amber oily liquid; yield: 95%.

^{1}H NMR (400.1 MHz, $CDCl_3$, 25 °C): δ = 7.96 (dd, $^3J_{HH}$ = 7.7 Hz, $^4J_{HH}$ = 1.3 Hz, 1H; aromatic proton), 7.40 (dd, $^3J_{HH}$ = 7.4 Hz, $^4J_{HH}$ =1.4 Hz, 1H; aromatic proton), 7.22 (t, $^3J_{HH}$ = 7.6 Hz, 1H; aromatic proton), 7.17 (d, $^3J_{HH}$ = 7.8 Hz, 1H; aromatic proton), 2.87 (t, $^3J_{HH}$ = 6.0 Hz, 2H; C*H*$_2$CH$_2$CH$_2$CO), 2.56 (t, $^3J_{HH}$ = 6.6 Hz, 2H; CH$_2$CH$_2$C*H*$_2$CO), 2.04 ppm (m, 2H; CH$_2$C*H*$_2$CH$_2$CO).

^{13}C{^{1}H} NMR (100.6 MHz, $CDCl_3$, 25 °C): δ = 198.3 (s; CO), 144.5 (s; aromatic ipso carbon), 133.4 (s; aromatic carbon atom), 132.6 (s; aromatic ipso carbon), 128.8 (s; aromatic carbon atom), 127.1 (s; aromatic carbon atom), 126.6 (s; aromatic carbon atom), 39.1 (s; CH$_2$CH$_2$*C*H$_2$CO), 29.6 (s; *C*H$_2$CH$_2$CH$_2$CO), 23.3 ppm (s; CH$_2$*C*H$_2$CH$_2$CO).

Benzophenone:[2]

White crystals; m.p. 47-49 °C (47-49 °C, lit.); yield: 71%.

^{1}H NMR (400.1 MHz, $CDCl_3$, 25 °C): δ = 7.75 (dd, $^{3}J_{HH}$ = 8.3 Hz, $^{4}J_{HH}$ = 1.2 Hz, 4H; aromatic protons), 7.52 (tt, $^{3}J_{HH}$ =7.3 Hz, $^{4}J_{HH}$ = 1.4 Hz, 2H; aromatic protons), 7.41 ppm (t, $^{3}J_{HH}$ = 7.7 Hz, 4H; aromatic protons);

^{13}C{^{1}H} NMR (100.6 MHz, $CDCl_3$, 25 °C): δ = 196.8 (s; CO), 137.6 (s; aromatic ipso carbons), 132.5 (s; aromatic carbon atoms), 130.1 (s; aromatic carbon atoms), 128.3 ppm (s; aromatic carbon atoms).

4'-Methylacetophenone:[3]

Colorless liquid; yield: 94%.

^{1}H NMR (400.1 MHz, $CDCl_3$, 25 °C): δ = 7.85 (d, $^{3}J_{HH}$ = 8.3 Hz, 2H; aromatic protons), 7.24 (d, $^{3}J_{HH}$ = 8.3 Hz, 2H; aromatic protons), 2.56 (s, 3H; $COCH_3$), 2.39 ppm (s, 3H, CH_3);

^{13}C{^{1}H} NMR (100.6 MHz, $CDCl_3$, 25 °C): δ = 197.8 (s; CO), 143.9 (s; aromatic ipso carbon), 134.7 (s; aromatic ipso carbon), 129.2 (s; aromatic carbon atoms), 128.4 (s; aromatic carbon atoms), 26.5 (s; CO*C*H_3), 21.6 ppm (s; *C*H_3).

Propiophenone:[2]

Colorless liquid; yield: 75%.

^{1}H NMR (400.1 MHz, $CDCl_3$, 25 °C): δ = 7.84 (m, 2H; aromatic protons), 7.44-7.39 (m, 1H; aromatic proton), 7.32 (m, 2H; aromatic protons), 2.86 (q, $^{3}J_{HH}$ = 7.3 Hz, 2H; C*H*$_2$CH$_3$), 1.10 ppm (t, $^{3}J_{HH}$ = 7.3 Hz, 3H; CH_2C*H*$_3$);

^{3}C{^{1}H} NMR (100.6 MHz, $CDCl_3$, 25 °C): δ = 200.7 (s; CO), 136.9 (s; aromatic ipso carbon), 132.8 (s; aromatic carbon atom), 128.5 (s; aromatic carbon atom), 127.9 (s; aromatic carbon atom), 31.7 (s; *C*H_2CH$_3$), 8.2 ppm (s; CH_2*C*H_3).

2-heptanone:[4]

Colorless liquid; yield: 83%.

^{1}H NMR (400.1 MHz, $CDCl_3$, 25 °C): δ = 2.41 (t, $^{3}J_{HH}$ = 7.1 Hz, 2H; C*H*$_2$COCH$_3$), 2.12 (s, 3H; COC*H*$_3$), 1.55 (m, 2H; C*H*$_2$CH$_2$CO), 1.27 (m, 4H; CH_2), 0.89 ppm (t, $^{3}J_{HH}$ = 6.5 Hz, 3H; CH_2C*H*$_3$).

^{3}C{^{1}H} NMR (100.6 MHz, $CDCl_3$, 25 °C): δ = 209.4 (s; CO), 43.9 (s; *C*H_2COCH$_3$), 31.2 (s; C*H*$_2$CH$_2$CO), 29.9 (s; CO*C*H_3), 22.8 (s; C*H*$_2$), 22.6 (s; C*H*$_2$), 13.9 ppm (s; CH_2*C*H_3).

(1*R*)-(+)-camphor:[5]

Colorless solid; m.p. 176 °C (175-177 °C, lit.); yield: 44%.

^{1}H NMR (400.1 MHz, $CDCl_3$, 25 °C): δ = 2.26 (dt, $^{2}J_{HH}$ = 18.2 Hz, $^{3}J_{HH}$ = 3.9 Hz, 1H; C*H*$_2$CO), 2.00 (t, $^{3}J_{HH}$ = 4.5 Hz, 1H; CH_2C*H*(CMe_2)CH_2), 1.86 (ddt, $^{2}J_{HH}$ = 12.1 Hz, $^{2}J_{HH}$ = 7.8 Hz, $^{3}J_{HH}$ = 3.5 Hz, 1H; CH_2C*H*$_2$CH(CMe_2)), 1.75 (d, $^{2}J_{HH}$ = 18.2 Hz, 1H; C*H*$_2$CO), 1.59 (td, $^{2}J_{HH}$ = 12.1 Hz, $^{3}J_{HH}$ = 11.0 Hz, $^{3}J_{HH}$ = 3.3 Hz, 1H; CH_2C*H*$_2$(CMe)), 1.38-1.16 (m, 2H; C*H*$_2C$*H*$_2$(CMe)), 0.87 (s, 3H; C(C*H*$_3$)$_2$), 0.82 (s, 3H; CH_3), 0.75 ppm (s, 3H; C(C*H*$_3$)$_2$)).

^{13}C{^{1}H} NMR (100.6 MHz, $CDCl_3$, 25 °C): δ = 219.7 (s; CO), 57.7 (s; *C*Me_2), 46.8 (s; *C*Me), 43.3 (s; *C*H_2CO), 43.0 (s; CH_2*C*H(CMe_2)CH_2), 29.9 (s; *C*H_2(CMe)), 27.1 (s; *C*H_2CH(CMe_2)CH_2), 19.8 (s; C(*C*H_3)$_2$), 19.2 (s; C(*C*H_3)$_2$), 9.3 ppm (s; C(*C*H_3)).

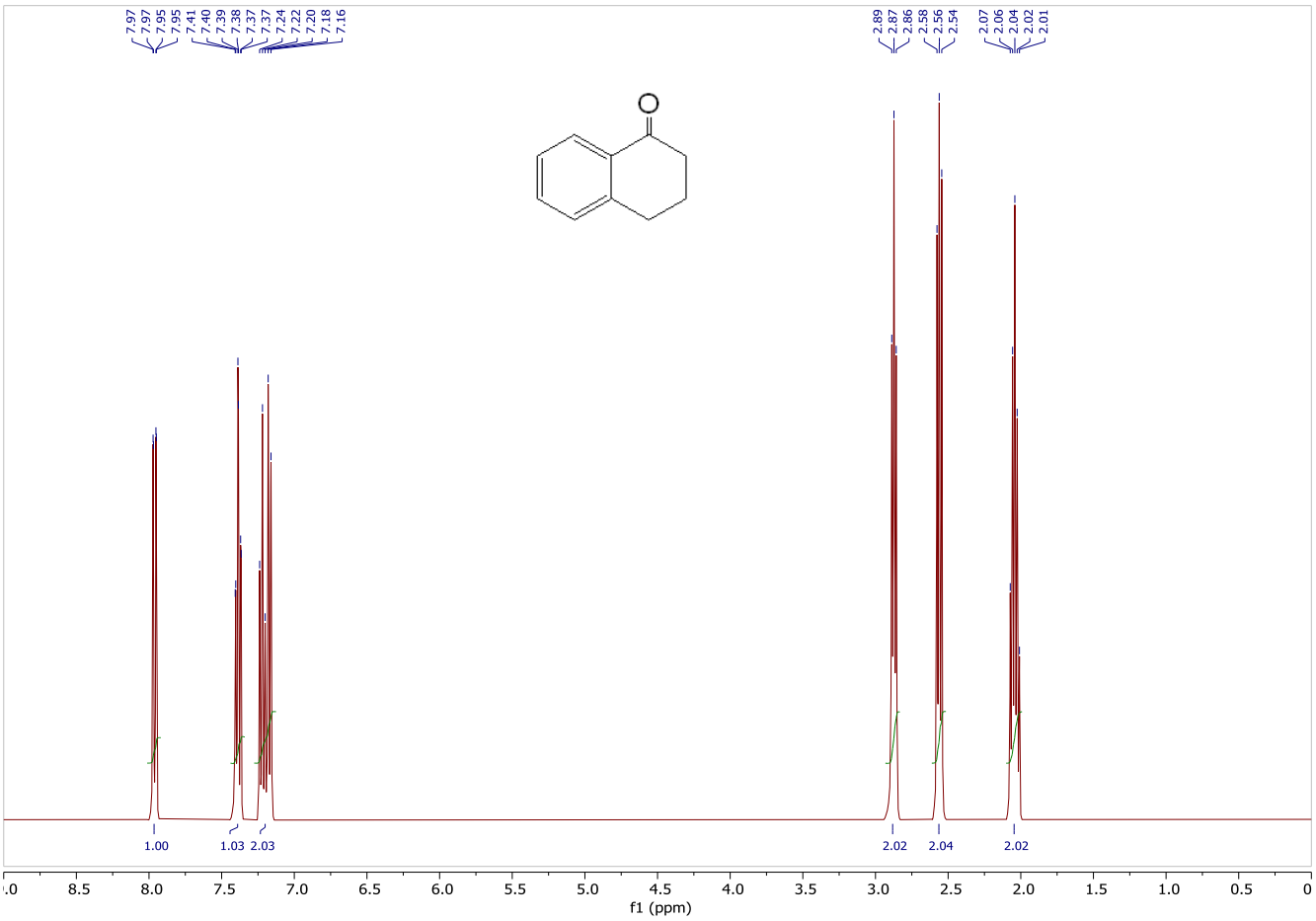

Figure S44. ^{1}H NMR spectrum (400.1 MHz) of α-tetralone obtained from catalytic *Oppenauer*-type oxidation of α-tetralol in $CDCl_3$ at 25 °C.

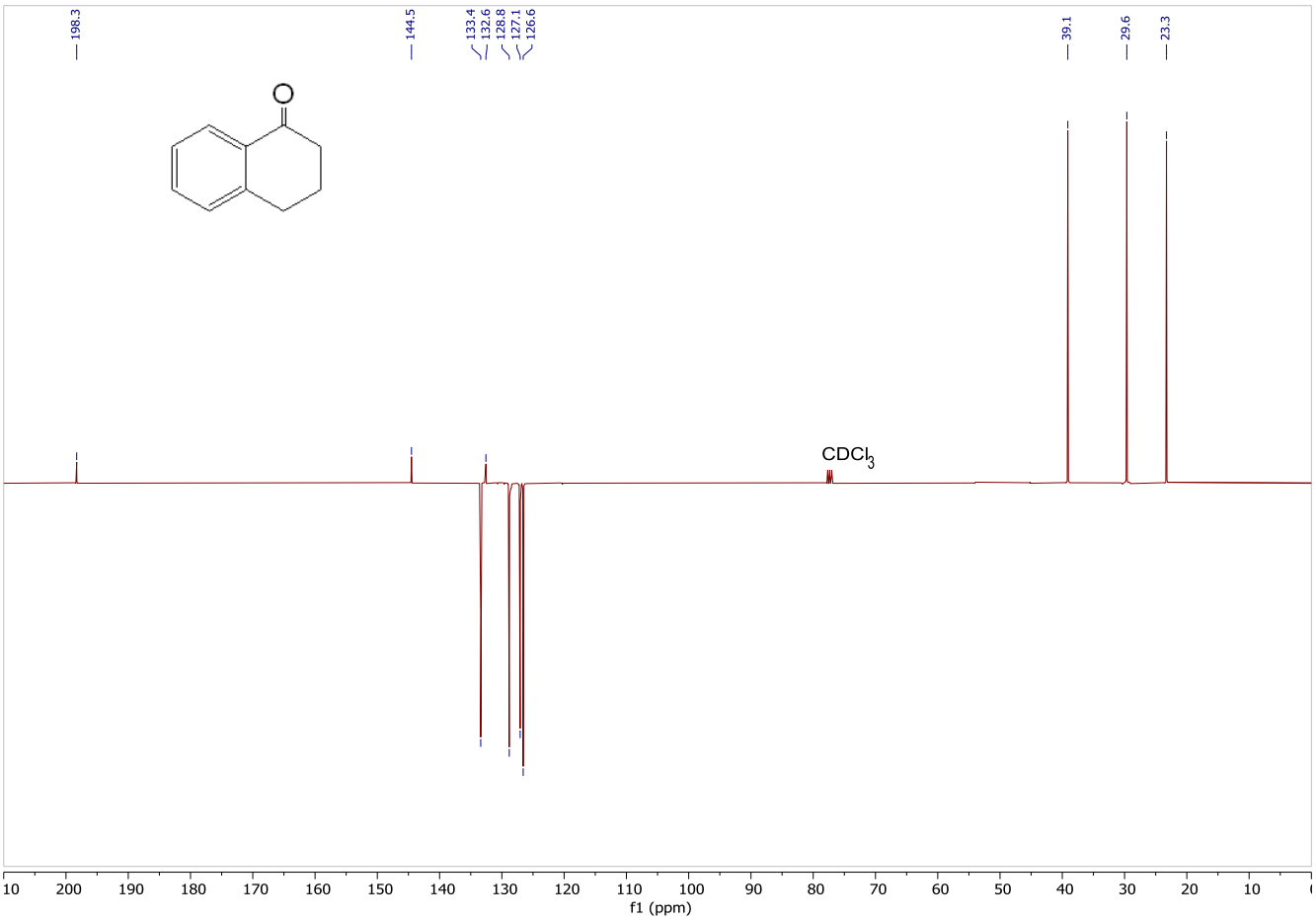

Figure S45. $^{13}C\{^{1}H\}$ DEPTQ NMR spectrum (100.6 MHz) of α-tetralone obtained from catalytic *Oppenauer*-type oxidation of α-tetralol in $CDCl_3$ at 25 °C.

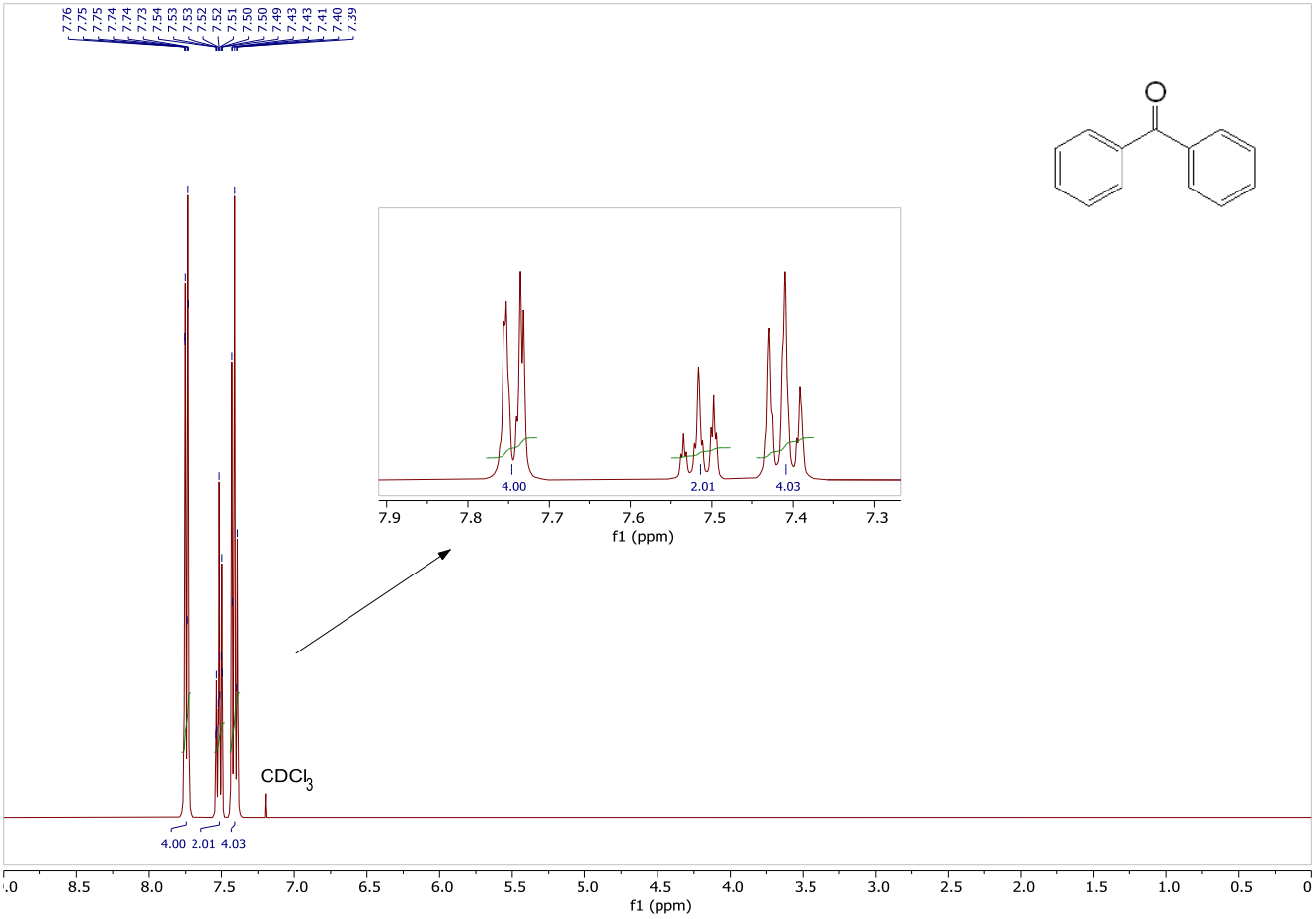

Figure S46. ^{1}H NMR spectrum (400.1 MHz) of benzophenone obtained from catalytic *Oppenauer*-type oxidation of benzhydrol in $CDCl_3$ at 25 °C.

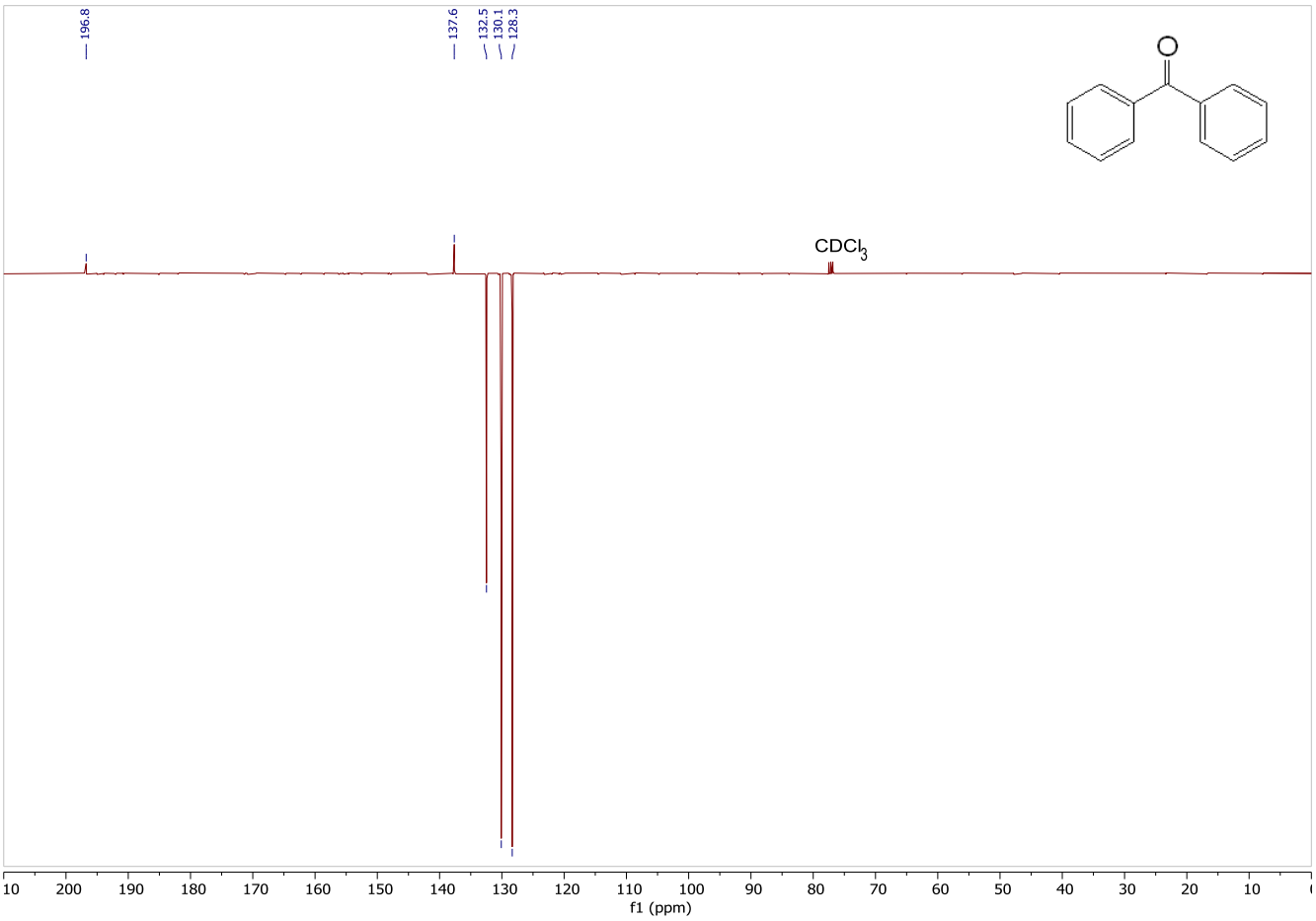

Figure S47. $^{13}C\{^{1}H\}$ DEPTQ NMR spectrum (100.6 MHz) of benzophenone obtained from catalytic *Oppenauer*-type oxidation of benzhydrol in $CDCl_3$ at 25 °C.

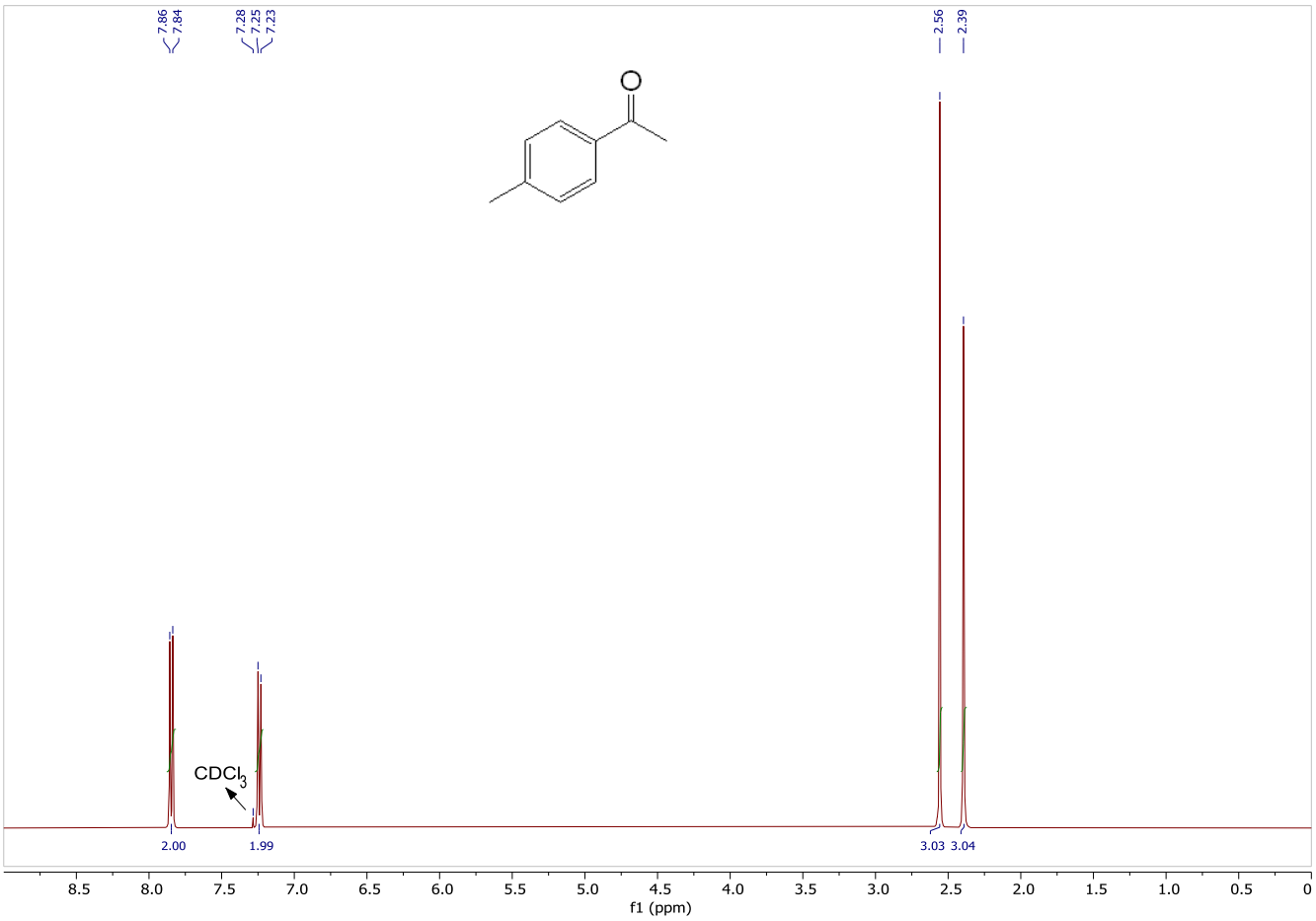

Figure S48. ^{1}H NMR spectrum (400.1 MHz) of 4'-methylacetophenone obtained from catalytic *Oppenauer*-type oxidation of 1-(*p*-tolyl)ethanol in $CDCl_3$ at 25 °C.

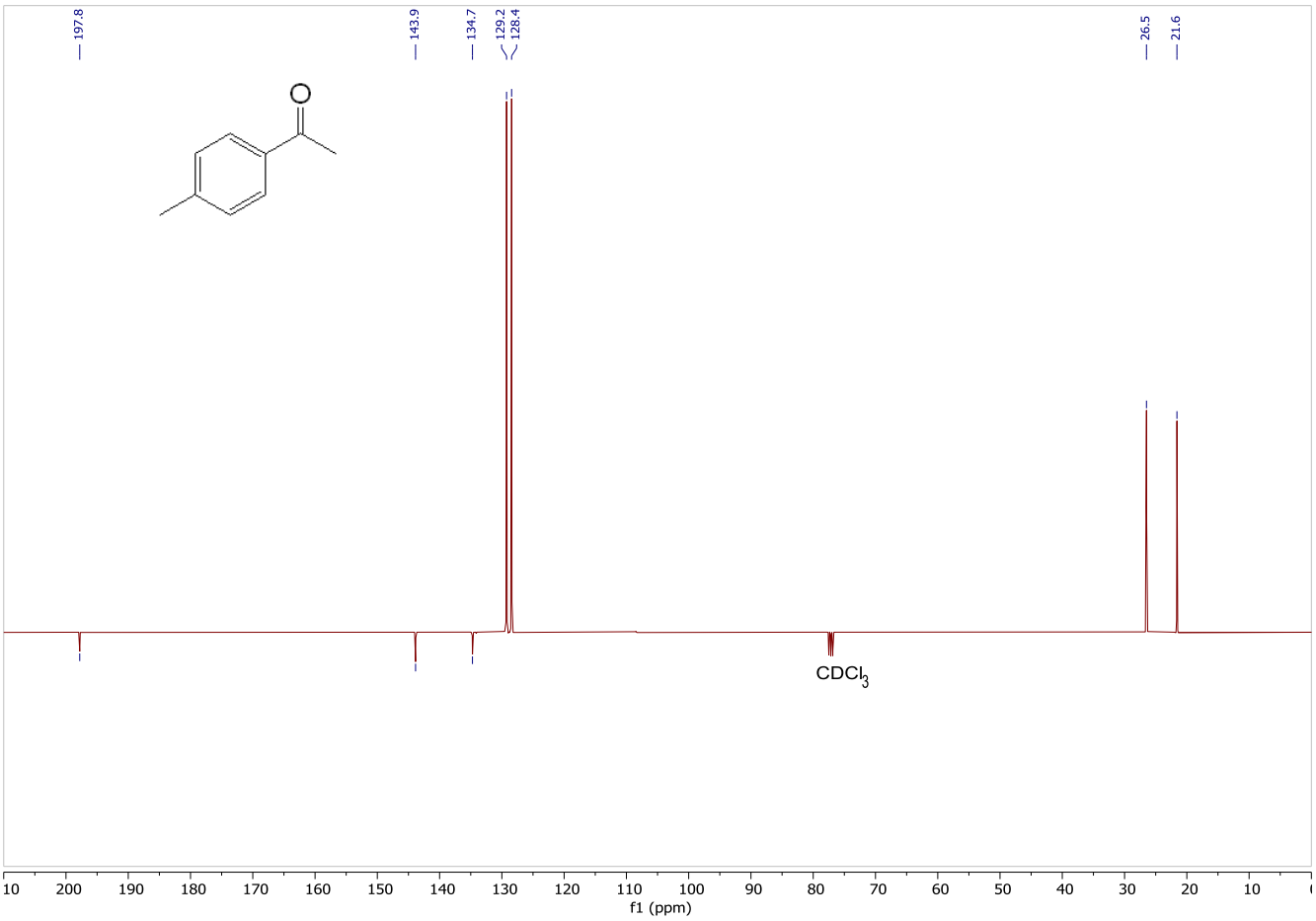

Figure S49. $^{13}C\{^{1}H\}$ DEPTQ NMR spectrum (100.6 MHz) of 4'-methylacetophenone obtained from catalytic *Oppenauer*-type oxidation of 1-(*p*-tolyl)ethanol in $CDCl_3$ at 25 °C.

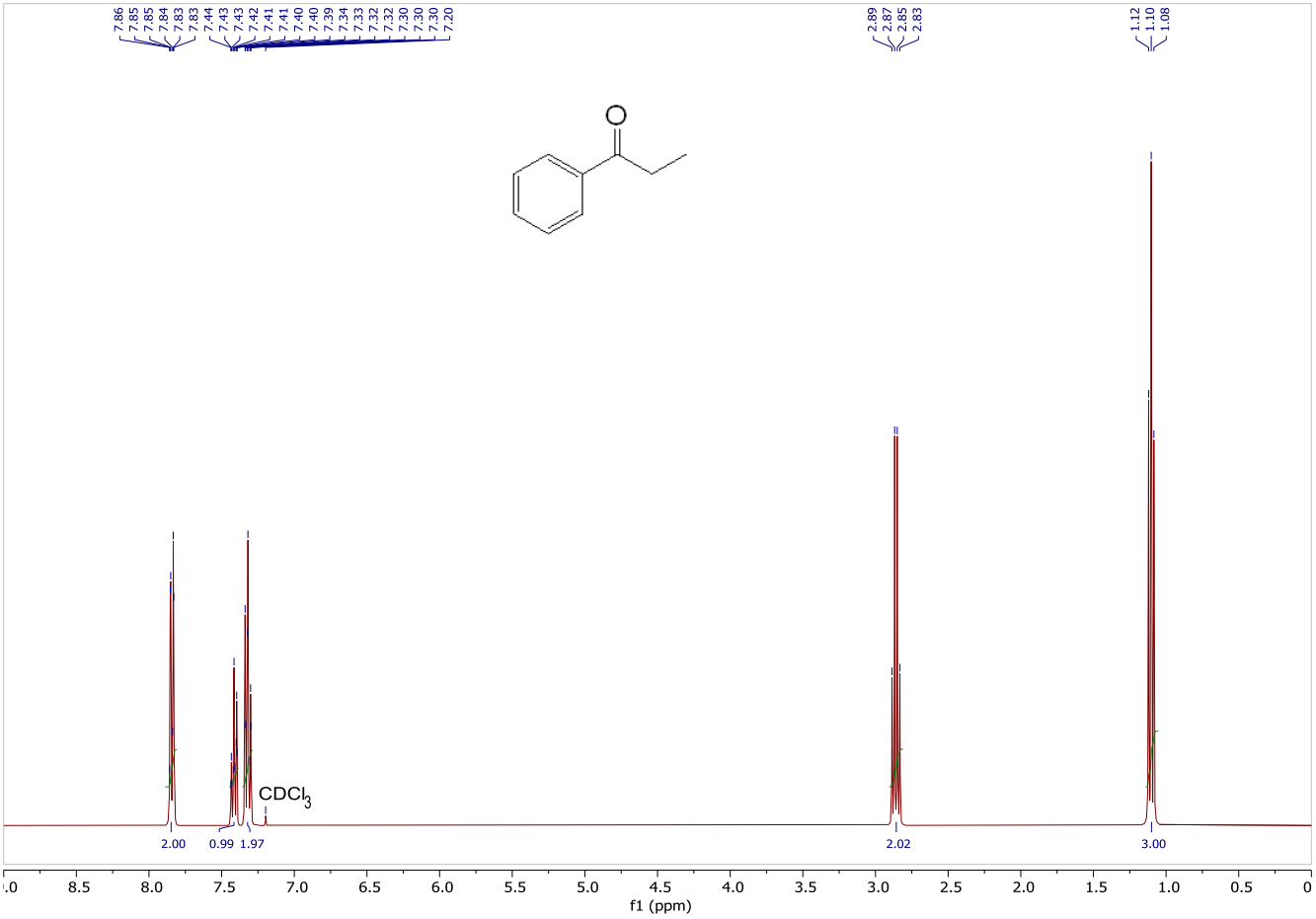

Figure S50. ^{1}H NMR spectrum (400.1 MHz) of propiophenone obtained from catalytic *Oppenauer*-type oxidation of 1-phenyl-1-propanol in $CDCl_3$ at 25 °C.

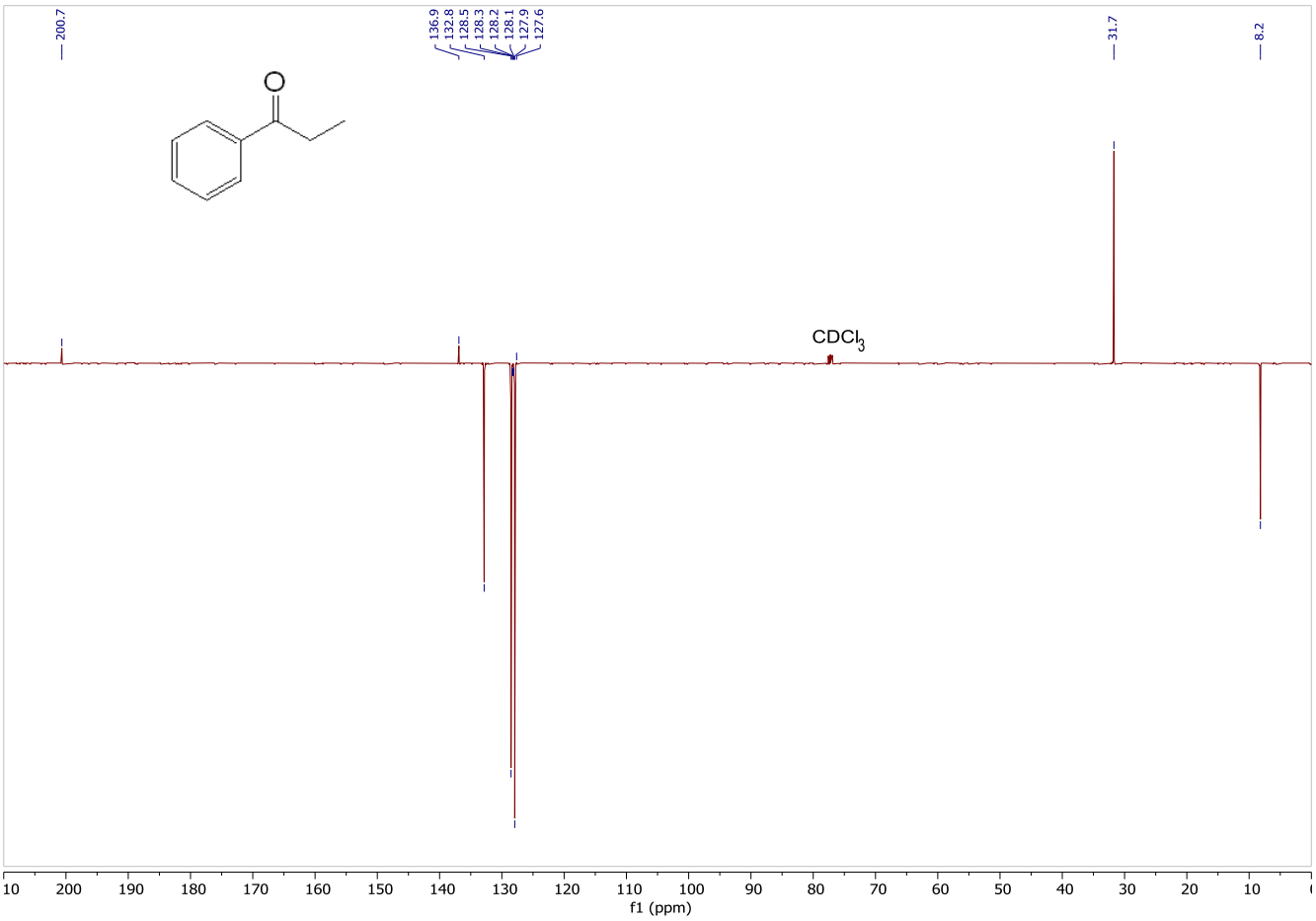

Figure S51. $^{13}C\{^{1}H\}$ DEPTQ NMR spectrum (100.6 MHz) of propiophenone obtained from catalytic *Oppenauer*-type oxidation of 1-phenyl-1-propanol in $CDCl_3$ at 25 °C.

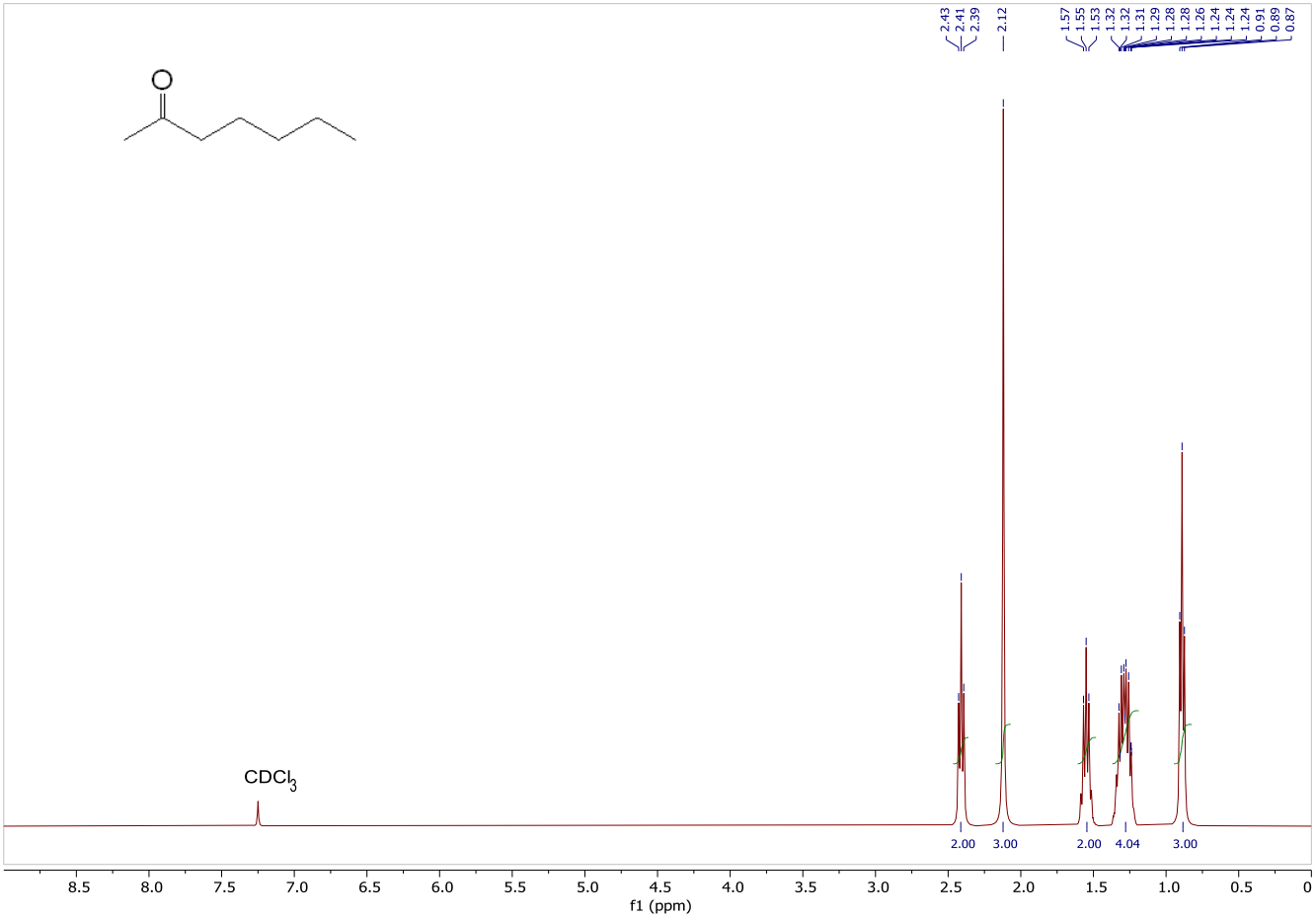

Figure S52. ^{1}H NMR spectrum (400.1 MHz) of 2-heptanone obtained from catalytic *Oppenauer*-type oxidation of 2-heptanol in $CDCl_3$ at 25 °C.

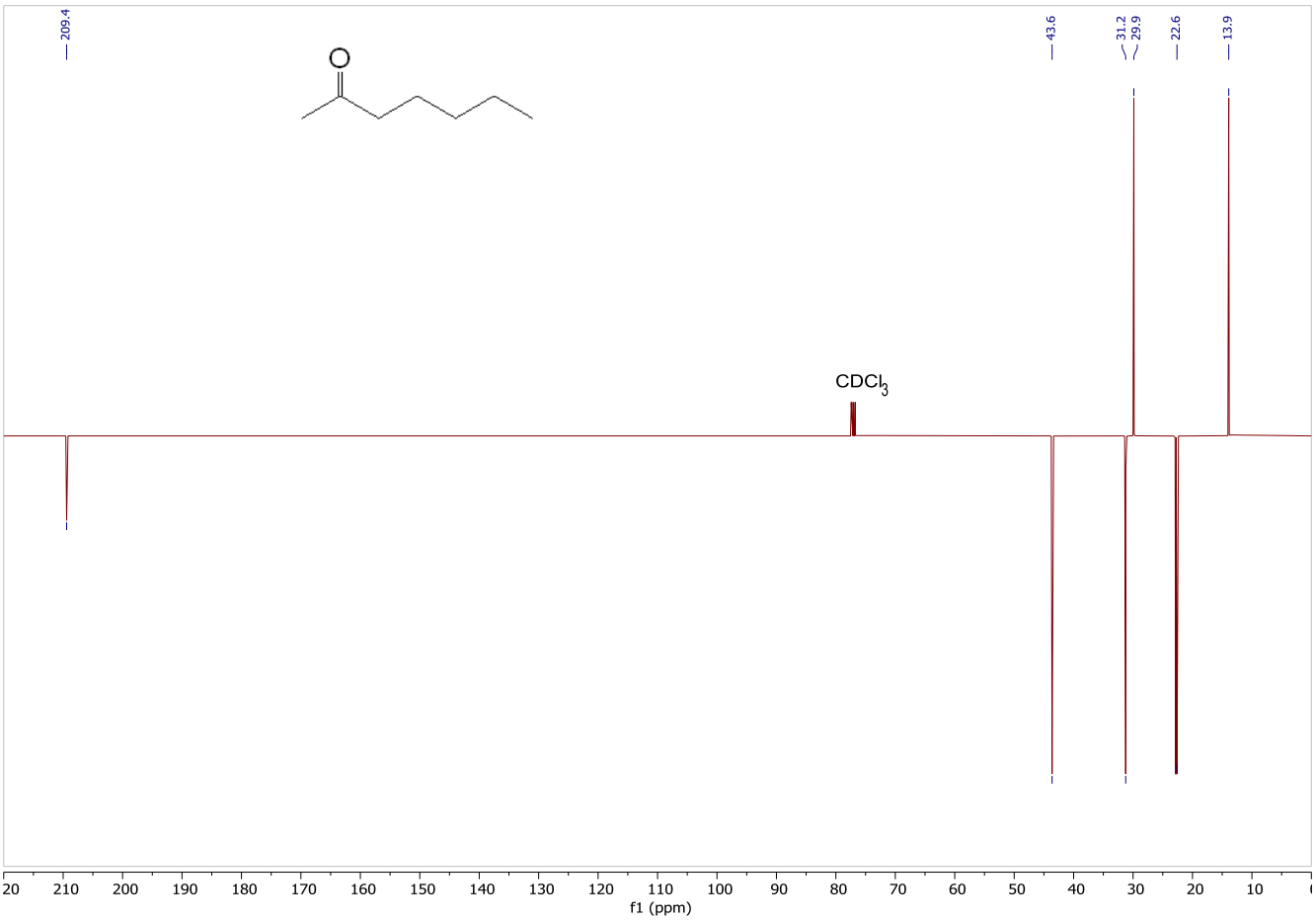

Figure S53. $^{13}C\{^{1}H\}$ DEPTQ NMR spectrum (100.6 MHz) of 2-heptanone obtained from catalytic *Oppenauer*-type oxidation of 2-heptanol in $CDCl_3$ at 25 °C.

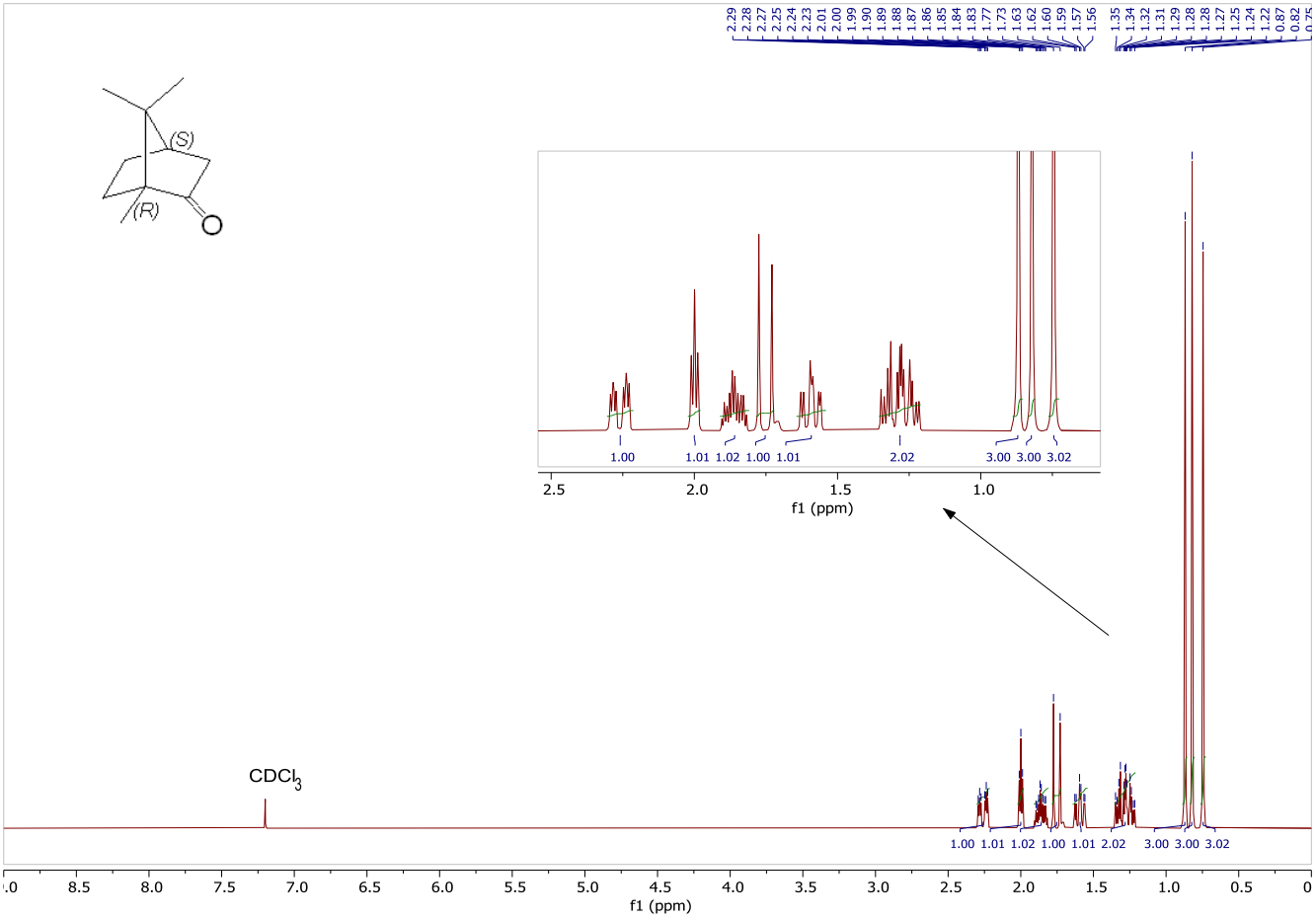

Figure S54. ^{1}H NMR spectrum (400.1 MHz) of (1*R*)-(+)-camphor obtained from catalytic *Oppenauer*-type oxidation of (1*R*)-(+)-borneol in $CDCl_3$ at 25 °C.

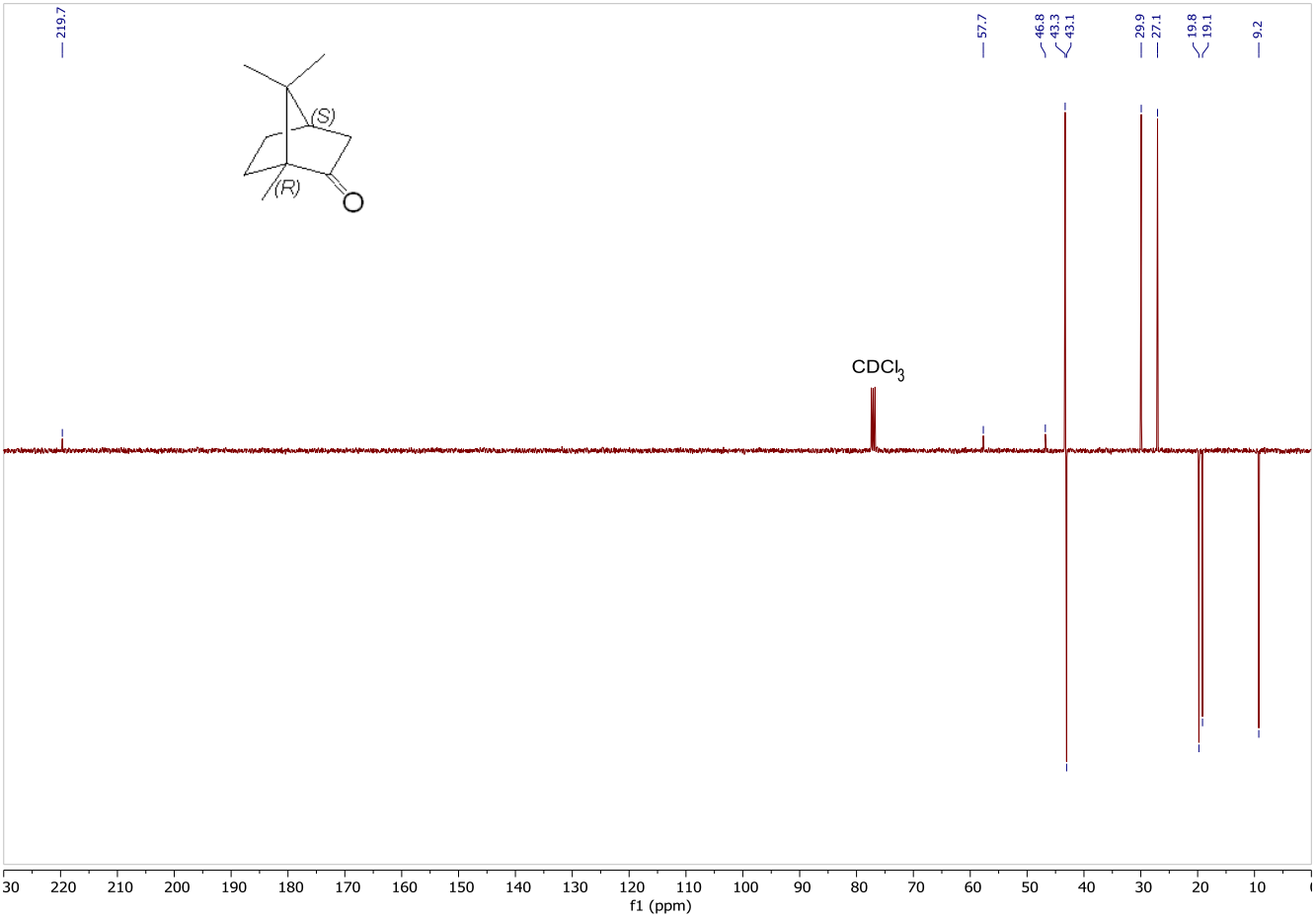

Figure S55. $^{13}C\{^{1}H\}$ DEPTQ NMR spectrum (100.6 MHz) of (1*R*)-(+)-camphor obtained from catalytic *Oppenauer*-type oxidation of (1*R*)-(+)-borneol in $CDCl_3$ at 25 °C.

General Procedure for the catalytic transfer hydrogenation (TH) of carbonyl compounds

The ruthenium catalyst solutions used for the catalytic TH were prepared by dissolving the complexes (**1**-**4**, 2 μmol) in 2-propanol (2 mL). The catalyst solution (1.0 mL, 1.0 μmol) and a 0.1 M solution of NaO*i*Pr (200 μL, 20 μmol) in 2-propanol were added subsequently to the carbonyl substrate (1.0 mmol) dissolved in 2-propanol (final volume 10 mL), and the mixture was heated at reflux. The reaction was sampled by removing an aliquot of the reaction mixture, which was quenched by addition of diethyl ether (1:1 v/v), filtered over a short silica pad and submitted to GC analysis. The base addition was considered as the start time of the reaction. The S/C molar ratio was 1000/1, whereas the base concentration was 2 mol% respect to the carbonyl substrates (0.1 M). The same procedure was followed for the TH reactions with different S/C (1000-10000), using the appropriate amount of catalyst.
For the isolation of alcohols with **4**, the final mixture was filtered over a short silica pad and evaporated under reduced pressure. The crude residue was dissolved with diethyl ether (5 mL) and the organic layer washed with a diluted solution of HCl (0.1 M; 3 x 5 mL), dried over anhydrous Na_2SO_4, and the solvent gently evaporated, affording the alcohol products (yields: 72-94%). In some cases, it was necessary to use a purification by flash silica gel column chromatography, using petroleum ether 40-60 °C/ethyl acetate or chloroform/methanol as eluents, to obtain the final products. All compounds were characterized by ^{1}H and ^{13}C{^{1}H} NMR.

1-Phenylethanol:[6]

Colorless liquid; Yield, 94%.

^{1}H NMR (400.1 MHz, $CDCl_3$, 25 °C): δ = 7.34-7.19 (m, 5H; aromatic protons), 4.78 (q, $^3J_{HH}$ = 6.5 Hz, 1H; C*H*CH_3), 2.79 (s, 1H; OH), 1.41 ppm (d, $^3J_{HH}$ = 6.5 Hz, 3H; CHC*H*$_3$);

^{13}C{^{1}H} NMR (100.6 MHz, $CDCl_3$, 25 °C): δ = 146.0 (s; aromatic ipso carbon), 128.5 (s; aromatic carbon atom), 127.4 (s; aromatic carbon atom), 125.5 (s; aromatic carbon atom), 70.3 (s; *C*HCH_3), 25.2 ppm (s; CH*C*H_3).

1-(*o*-tolyl)ethanol:[6b, c]

Colorless oil; Yield, 91%.

^{1}H NMR (400.1 MHz, $CDCl_3$, 25 °C): δ = 7.46 (dd, $^3J_{HH}$ = 7.7 Hz, $^4J_{HH}$ = 1.0 Hz, 1H; aromatic proton), 7.28-7.04 (m, 3H; aromatic protons), 5.02 (q, $^3J_{HH}$ = 6.4, 1H; C*H*CH_3), 2.87 (s, 1H; OH), 2.29 (s, 3H; CH_3), 1.40 ppm (d, $^3J_{HH}$ = 6.4 Hz, 3H; CHC*H*$_3$);

$^{13}C\{^{1}H\}$ NMR (100.6 MHz, $CDCl_3$, 25 °C): δ = 144.0 (s; aromatic ipso carbon), 134.2 (s; aromatic ipso carbon), 130.4 (s; aromatic carbon atom), 127.1 (s; aromatic carbon atom), 126.4 (s; aromatic carbon atom), 124.7 (s; aromatic carbon atom), 66.7 (s; *C*HCH$_3$), 24.0 (s; CH*C*H$_3$), 19.0 ppm (s; *C*H$_3$).

1-(*p*-tolyl)ethan-1-ol:[6c, 7]

Colorless oil; Yield, 89%.

^{1}H NMR (400.1 MHz, $CDCl_3$, 25 °C): δ = 7.21 (d, $^{3}J_{HH}$ = 8.1 Hz, 2H; aromatic protons), 7.12 (d, $^{3}J_{HH}$ = 8.1 Hz, 2H; aromatic protons), 4.76 (q, $^{3}J_{HH}$ = 6.5, 1H; C*H*CH$_3$), 2.96 (s, 1H; OH), 2.33 (s, 3H; CH$_3$), 1.42 ppm (d, $^{3}J_{HH}$ = 6.5 Hz, 3H; CHC*H*$_3$);

$^{13}C\{^{1}H\}$ NMR (100.6 MHz, $CDCl_3$, 25 °C): δ = 143.1 (s; aromatic ipso carbon), 136.9 (s; aromatic ipso carbon), 129.1 (s; aromatic carbon atoms), 125.5 (s; aromatic carbon atoms), 70.0 (s; *C*HCH$_3$), 25.2 (s; CH*C*H$_3$), 21.1 ppm (s; *C*H$_3$).

1-(2'-Methoxyphenyl)ethanol:[6a, 8]

Colorless oil; Yield, 92%.

^{1}H NMR (400.1 MHz, $CDCl_3$, 25 °C): δ = 7.31 (dd, $^{3}J_{HH}$ = 7.5 Hz, $^{4}J_{HH}$ = 1.7 Hz, 1H; aromatic proton), 7.18 (td, $^{3}J_{HH}$ = 8.0 Hz, $^{4}J_{HH}$ = 1.7 Hz, 1H; aromatic proton), 6.90 (td, $^{3}J_{HH}$ = 7.5 Hz, $^{4}J_{HH}$ = 0.9 Hz, 1H; aromatic proton), 6.80 (d, $^{3}J_{HH}$ = 8.0 Hz, 1H; aromatic proton), 5.05 (q, $^{3}J_{HH}$ = 6.5 Hz, 1H; C*H*CH$_3$), 3.76 (s, 3H; OCH$_3$), 3.11 (s, 1H; OH), 1.42 ppm (d, $^{3}J_{HH}$ = 6.5 Hz, 3H; CHC*H*$_3$);

$^{13}C\{^{1}H\}$ NMR (100.6 MHz, $CDCl_3$, 25 °C): δ = 156.4 (s; aromatic ipso carbon), 133.8 (s; aromatic ipso carbon), 128.2 (s; aromatic carbon atom), 126.0 (s; aromatic carbon atom), 120.8 (s; aromatic carbon atom), 110.4 (s; aromatic carbon atom), 66.0 (s; *C*HCH$_3$), 55.2 (s; O*C*H$_3$), 23.1 ppm (s; CH*C*H$_3$)

Benzhydrol (Diphenylmethanol):[6c]

White crystals; m.p. 68 °C (69 °C, lit.); Yield, 90%.

^{1}H NMR (400.1 MHz, $CDCl_3$, 25 °C): δ = 7.44-7.34 (m, 8H; aromatic protons), 7.32-7.27 (m, 2H; aromatic protons), 5.87 (d, $^{3}J_{HH}$ = 3.5 Hz, 1H; C*H*OH), 2.28 ppm (d, $^{3}J_{HH}$ = 3.5 Hz, 1H; OH);

$^{13}C\{^{1}H\}$ NMR (100.6 MHz, $CDCl_3$, 25 °C): δ = 143.8 (s; aromatic ipso carbons), 128.5 (s; aromatic carbon atoms), 127.6 (s; aromatic carbon atoms), 126.6 (s; aromatic carbon atoms), 76.3 ppm (s; *C*HOH).

Cyclohexanol:[7]

Colorless oil; Yield, 95%.

^{1}H NMR (400.1 MHz, $CDCl_3$, 25 °C): δ = 3.57 (tt, $^{3}J_{HH}$ = 8.8 Hz, $^{3}J_{HH}$ = 4.2 Hz, 1H; C*H*OH), 2.00 (s, 1H; OH), 1.90-1.82 (m, 2H; CH_2CHOH), 1.75-1.65 m, 2H; CH_2), 1.56-1.47 (m, 1H; CH_2), 1.31-1.07 ppm (m, 5H; CH_2);

^{13}C{^{1}H} NMR (100.6 MHz, $CDCl_3$, 25 °C): δ = 70.3 (s; *C*HOH), 35.5 (s; *C*H_2CHOH), 25.5 (s; *C*H_2), 24.1 ppm (s; *C*H_2).

Benzyl alcohol:[7, 9]

Colorless liquid; Yield, 72%.

^{1}H NMR (400.1 MHz, $CDCl_3$, 25 °C): δ = 7.35-7.22 (m, 5H; aromatic protons), 4.55 (br s, 2H; CH_2OH), 2.98 ppm (br s, 1H; OH);

^{13}C{^{1}H} NMR (100.6 MHz, $CDCl_3$, 25 °C): δ = 141.0 (s; aromatic ipso carbon), 128.6 (s; aromatic carbon atoms), 127.6 (s; aromatic carbon atoms), 127.1 (s; aromatic carbon atoms), 65.0 ppm (s; *C*H_2OH).

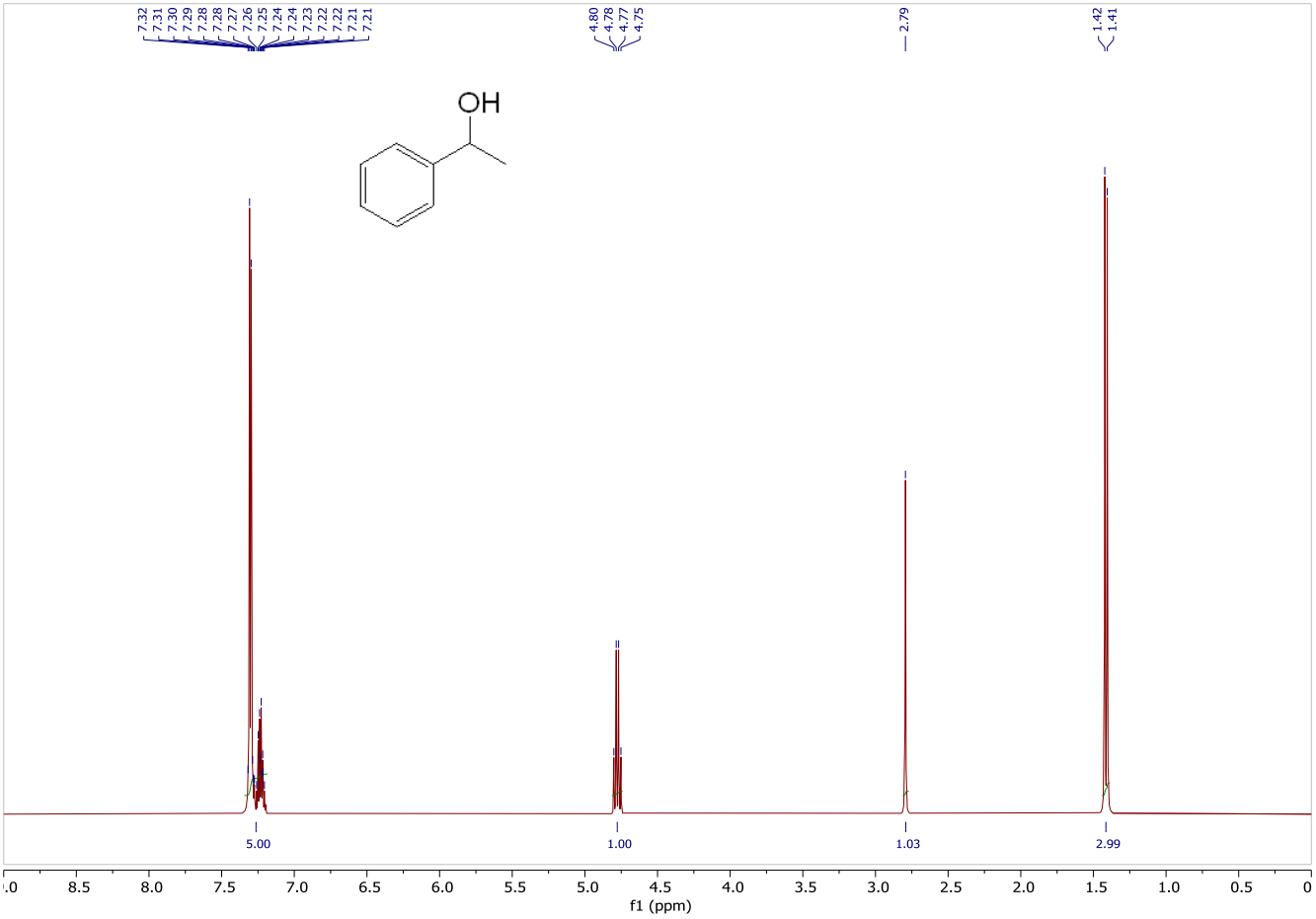

Figure S56. ^{1}H NMR spectrum (400.1 MHz) of 1-Phenylethanol obtained from catalytic TH of acetophenone in $CDCl_3$ at 25 °C.

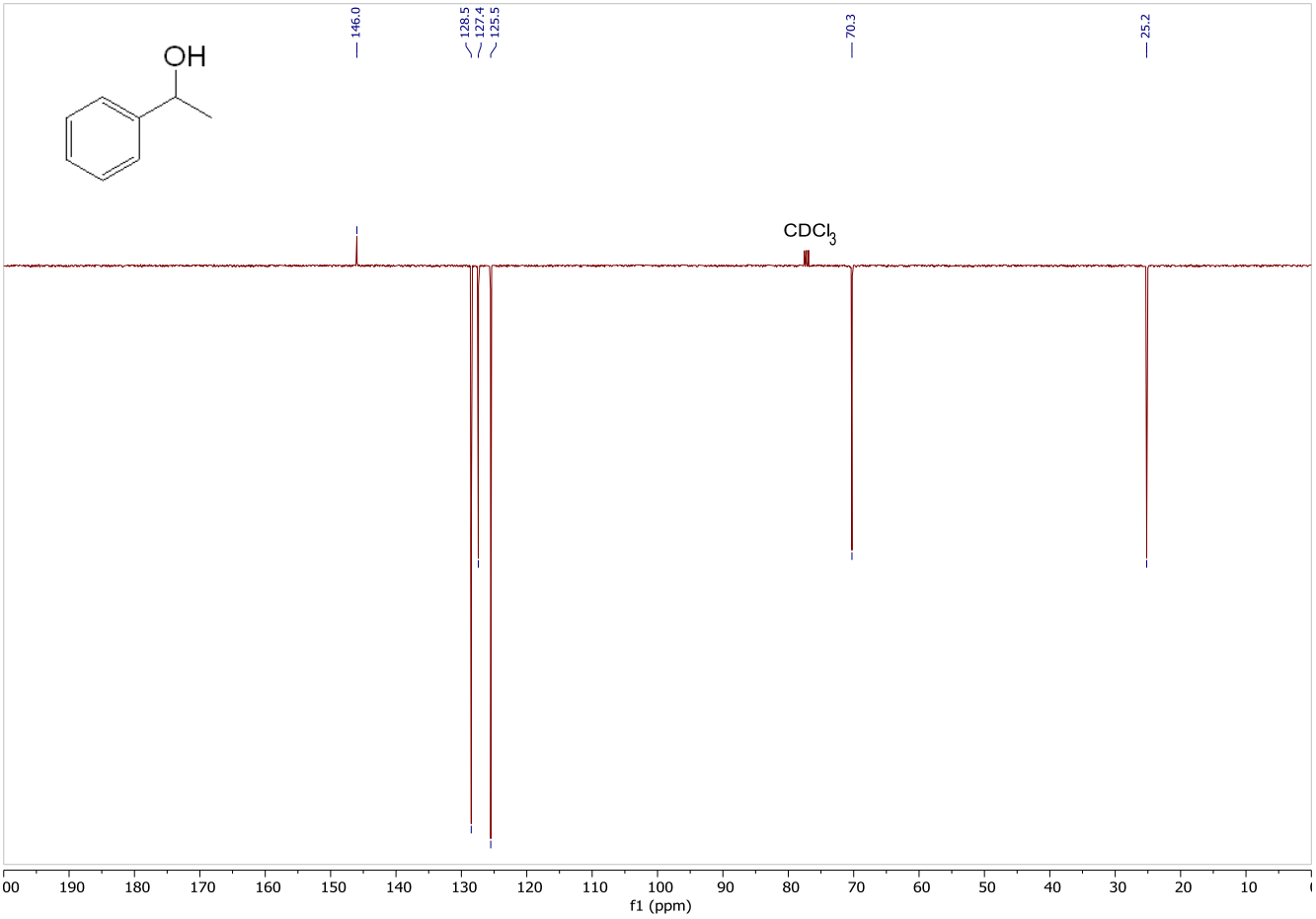

Figure S57. $^{13}C\{^{1}H\}$NMR spectrum (100.6 MHz) of 1-Phenylethanol obtained from catalytic TH of acetophenone in $CDCl_3$ at 25 °C.

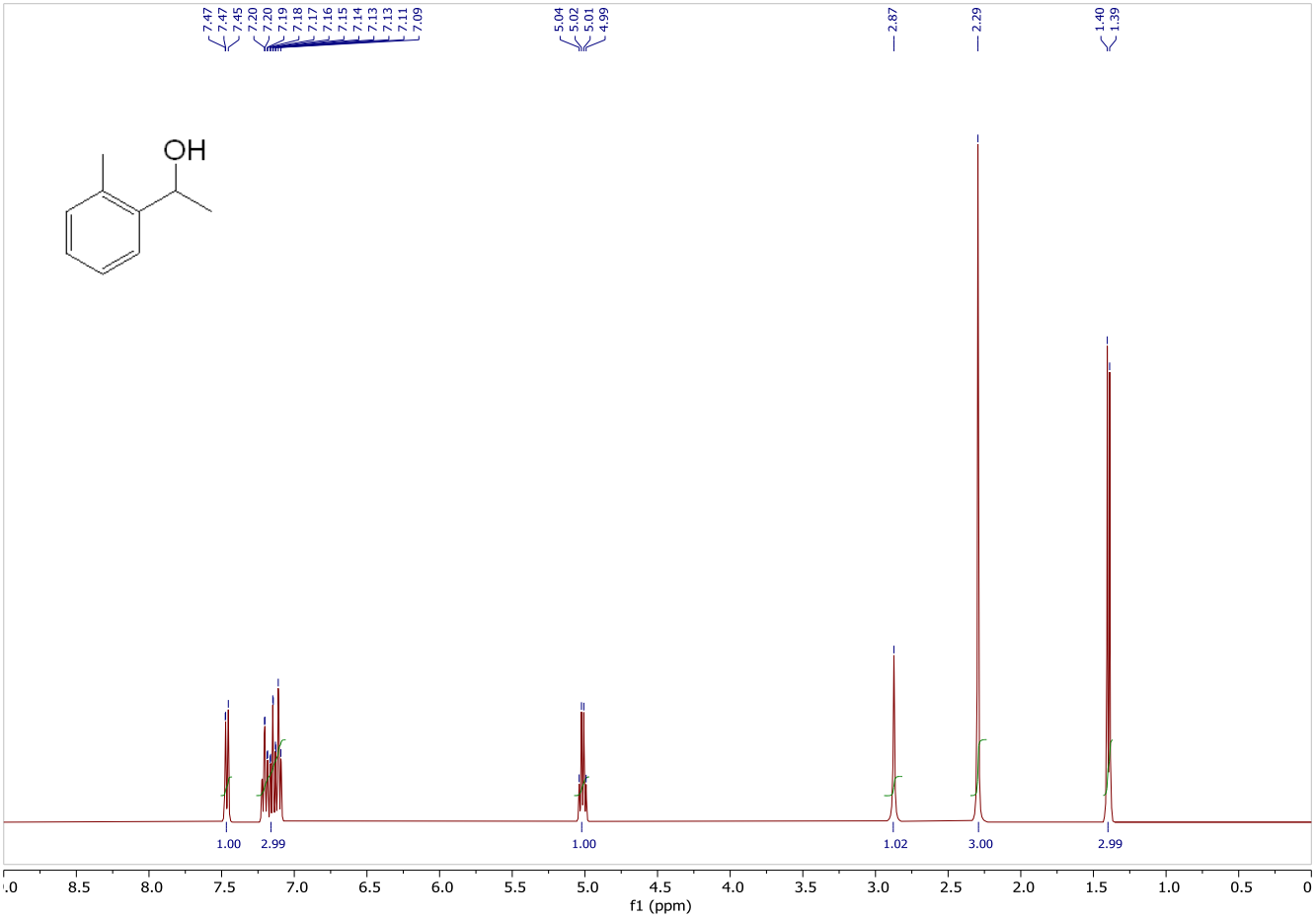

Figure S58. ^{1}H NMR spectrum (400.1 MHz) of 1-(*o*-tolyl)ethanol obtained from catalytic TH of 2'-methylacetophenone in $CDCl_3$ at 25 °C.

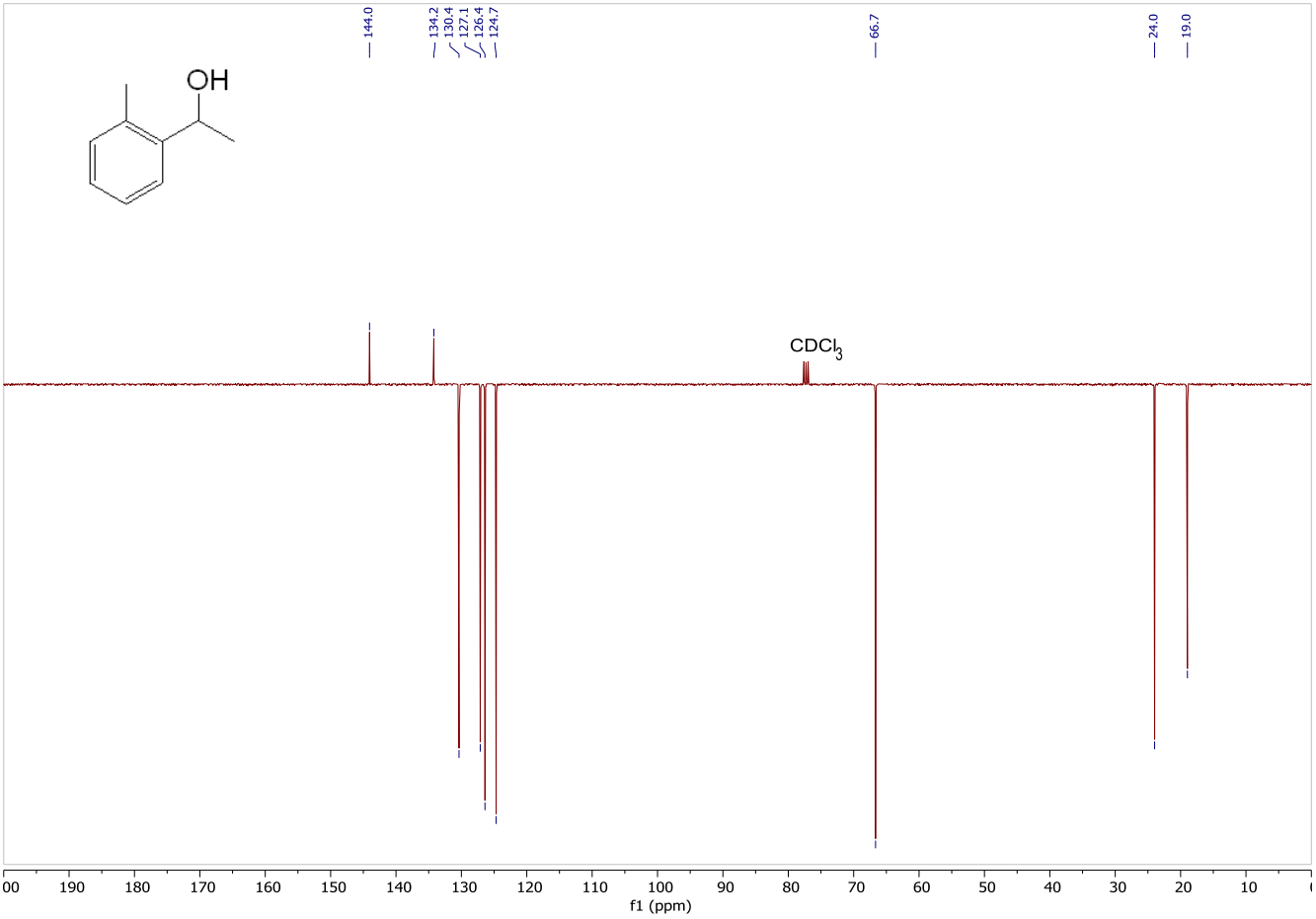

Figure S59. $^{13}C\{^{1}H\}$NMR spectrum (100.6 MHz) of 1-(*o*-tolyl)ethanol obtained from catalytic TH of 2'-methylacetophenone in $CDCl_3$ at 25 °C.

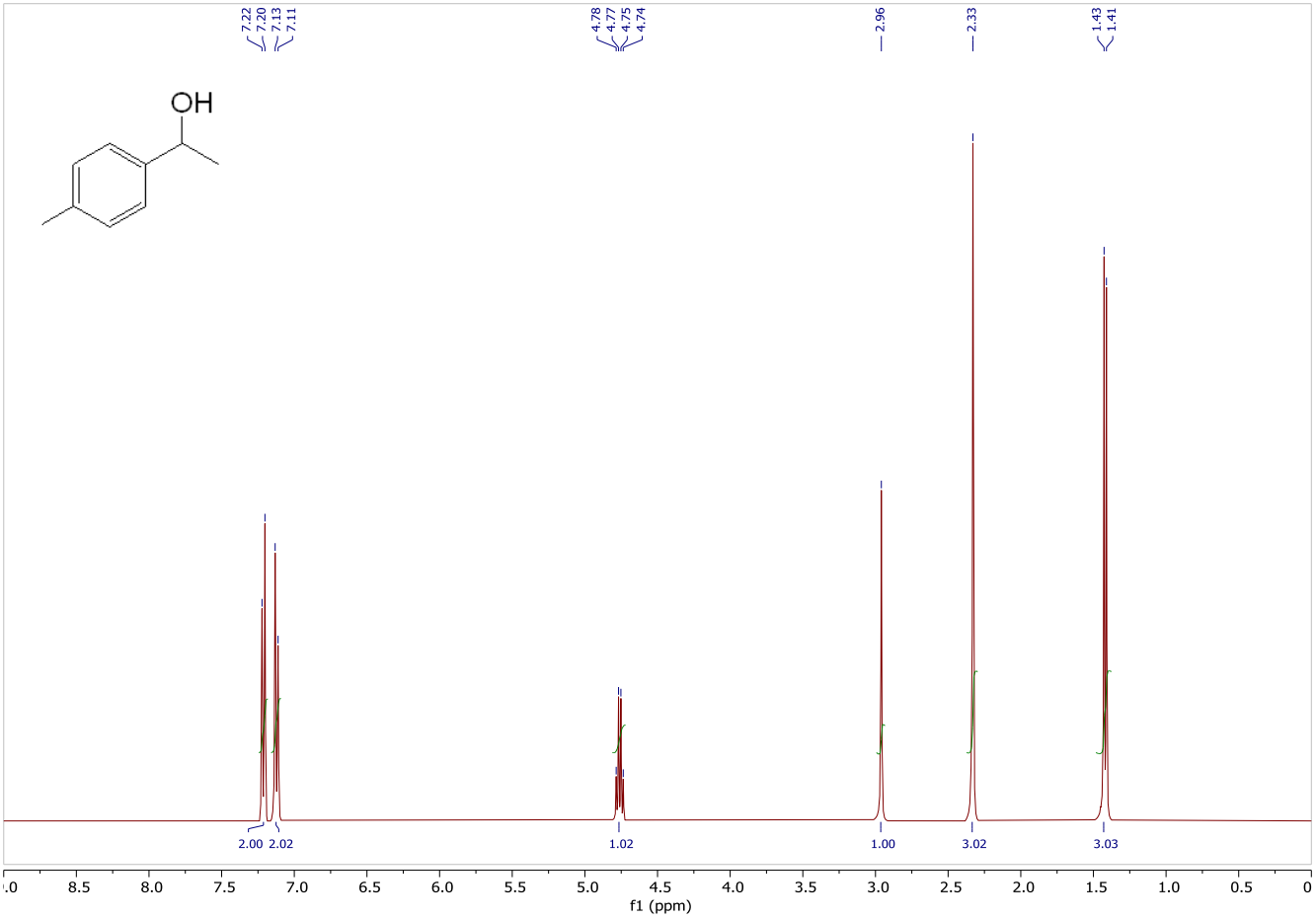

Figure S60. ^{1}H NMR spectrum (400.1 MHz) of 1-(*p*-tolyl)ethanol obtained from catalytic TH of 4'-methylacetophenone in $CDCl_3$ at 25 °C.

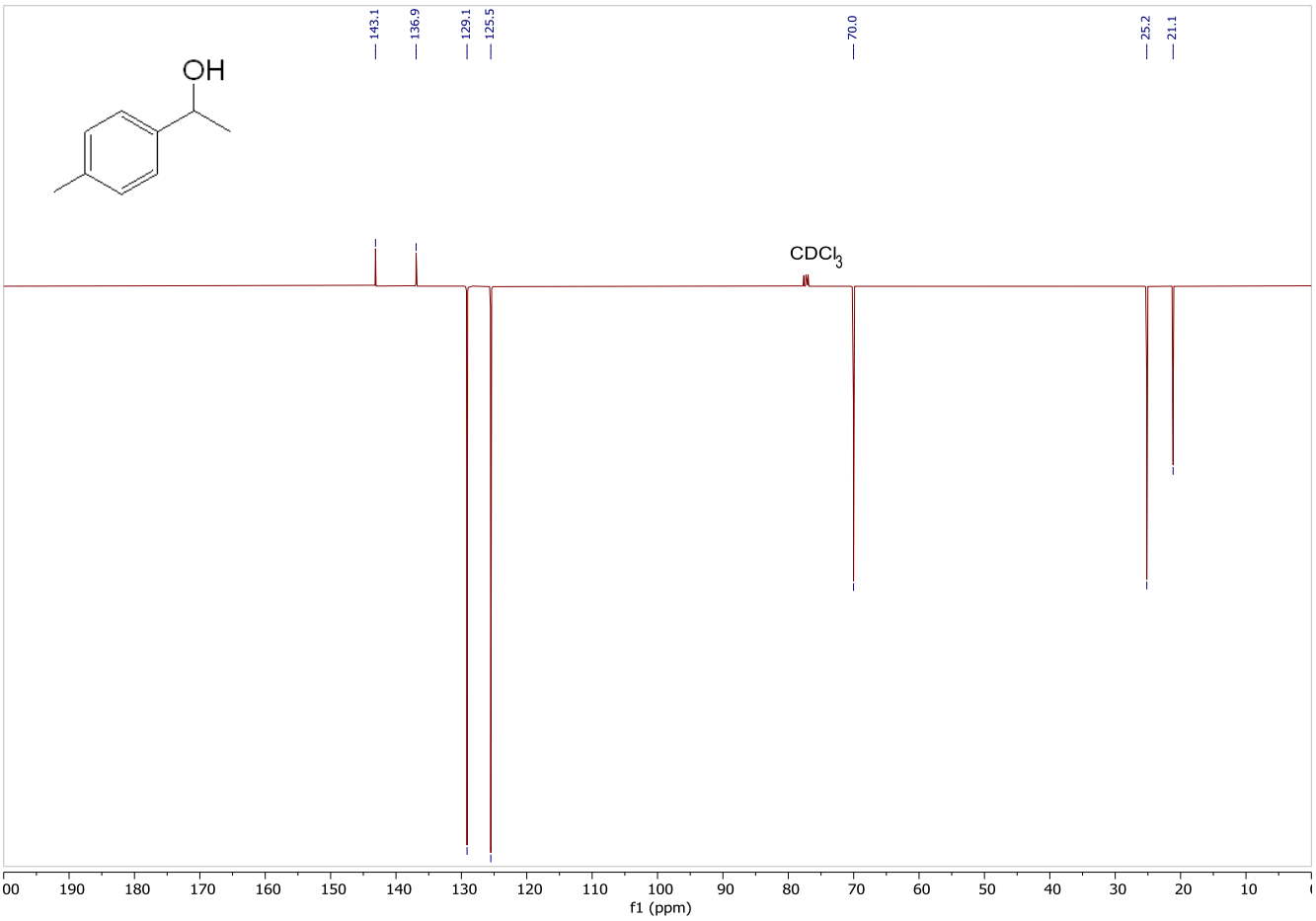

Figure S61. $^{13}C\{^{1}H\}$NMR spectrum (100.6 MHz) of 1-(*p*-tolyl)ethanol obtained from catalytic TH of 4'-methylacetophenone in $CDCl_3$ at 25 °C.

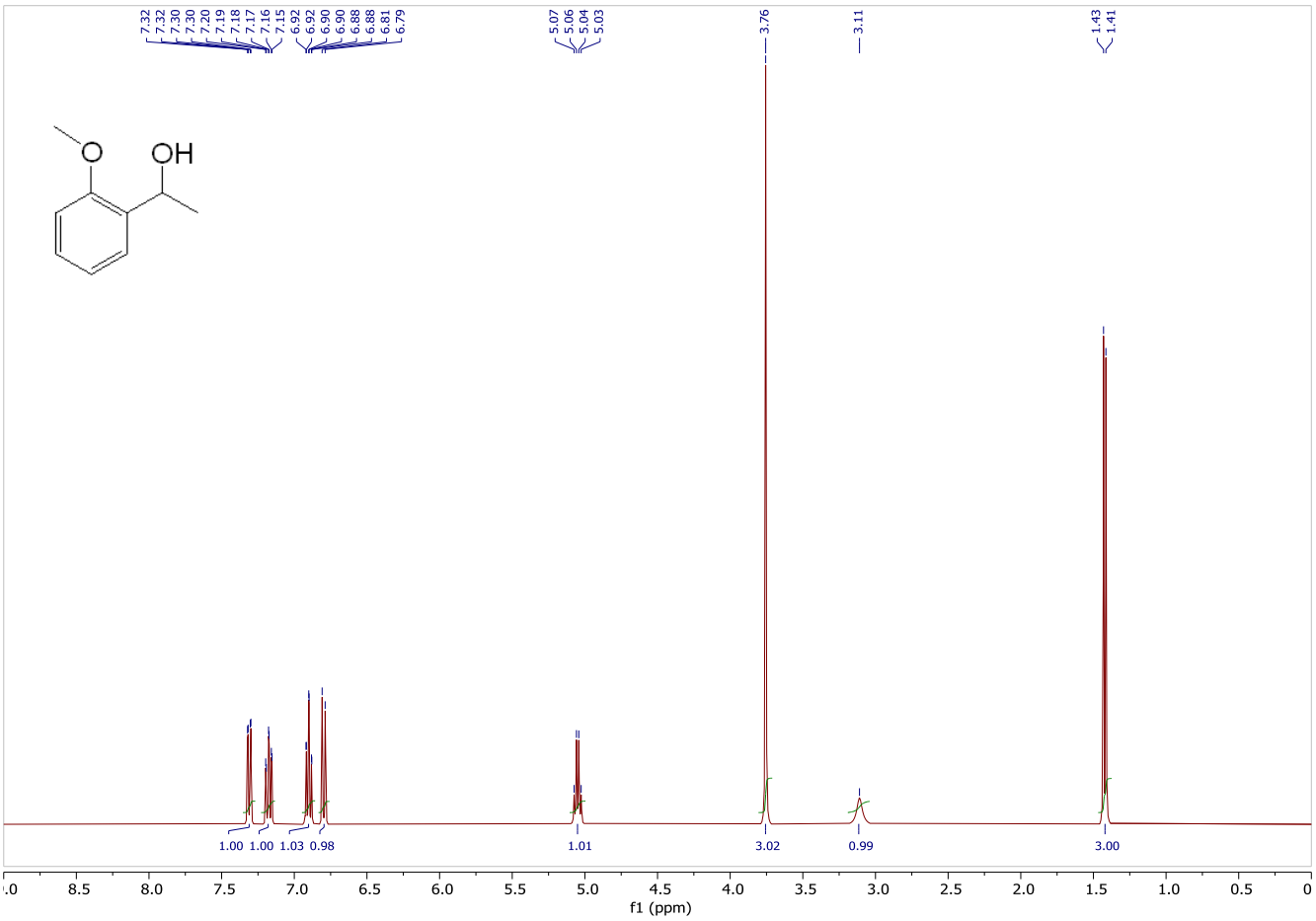

Figure S62. ^{1}H NMR spectrum (400.1 MHz) of 1-(*2*'-methoxy-phenyl)ethanol obtained from catalytic TH of 2'-methoxyacetophenone in $CDCl_3$ at 25 °C.

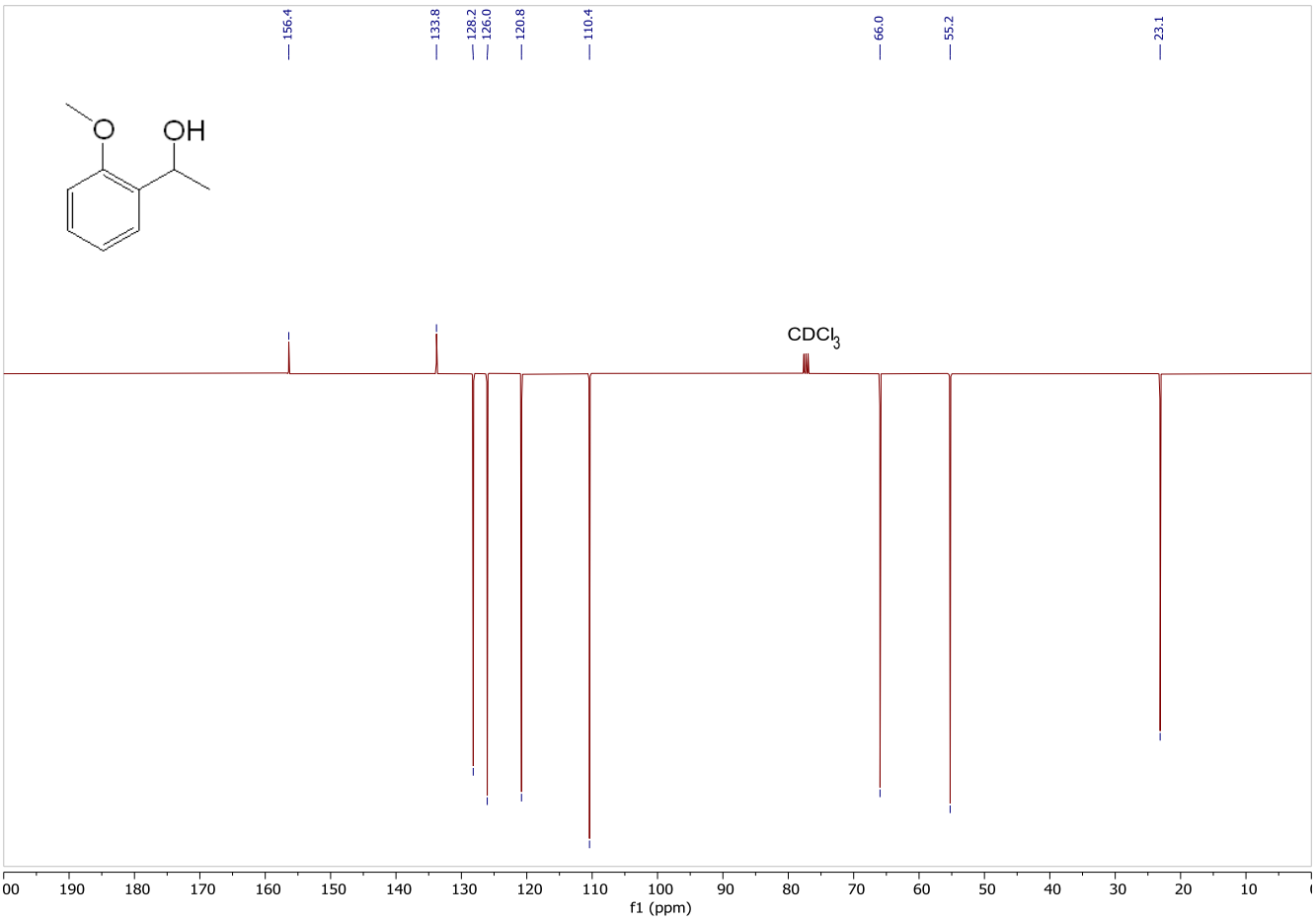

Figure S63. $^{13}C\{^{1}H\}$NMR spectrum (100.6 MHz) of 1-(*2*'-methoxy-phenyl)ethanol obtained from catalytic TH of 2'-methoxyacetophenone in $CDCl_3$ at 25 °C.

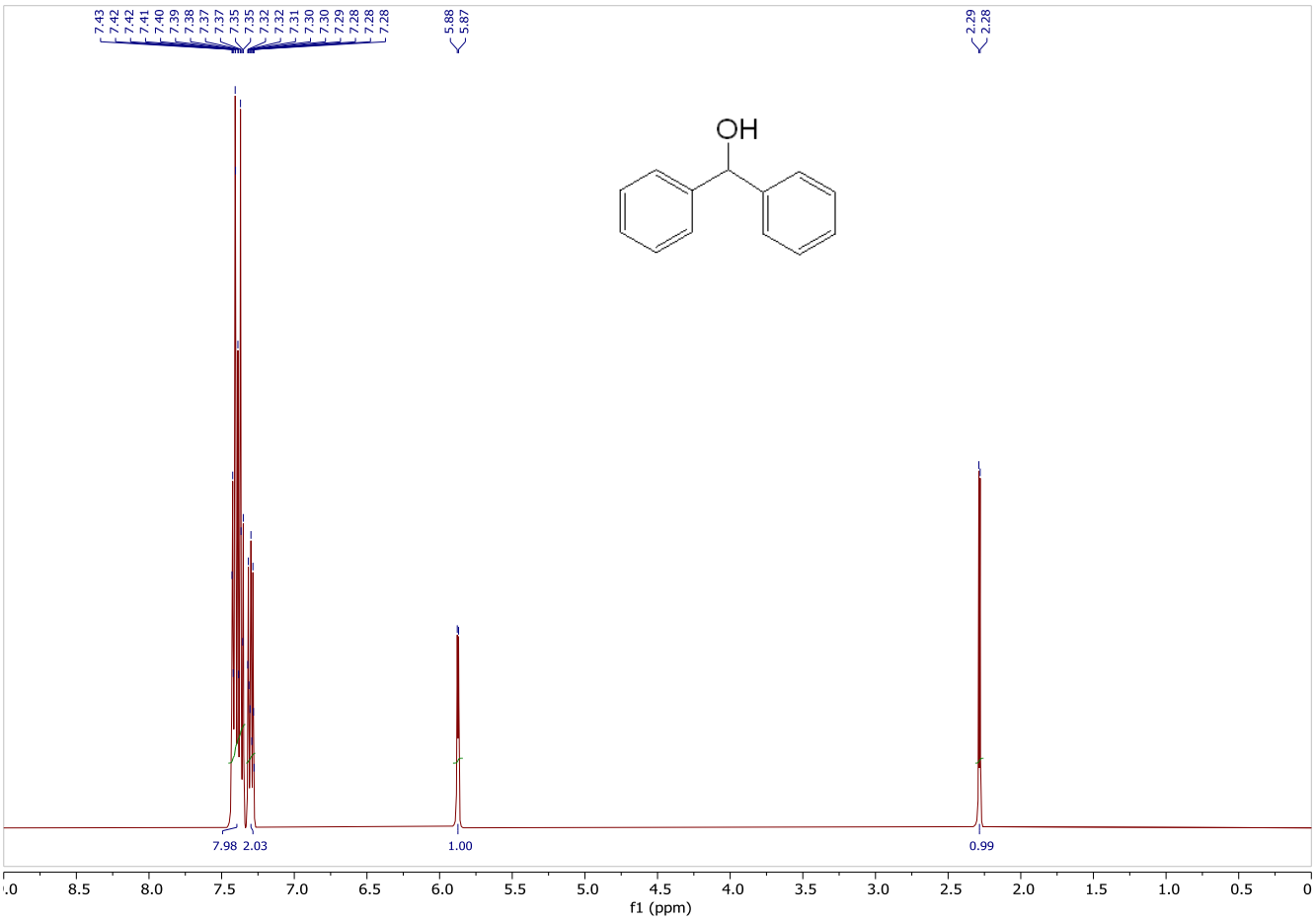

Figure S64. ^{1}H NMR spectrum (400.1 MHz) of benzhydrol obtained from catalytic TH of benzophenone in $CDCl_3$ at 25 °C.

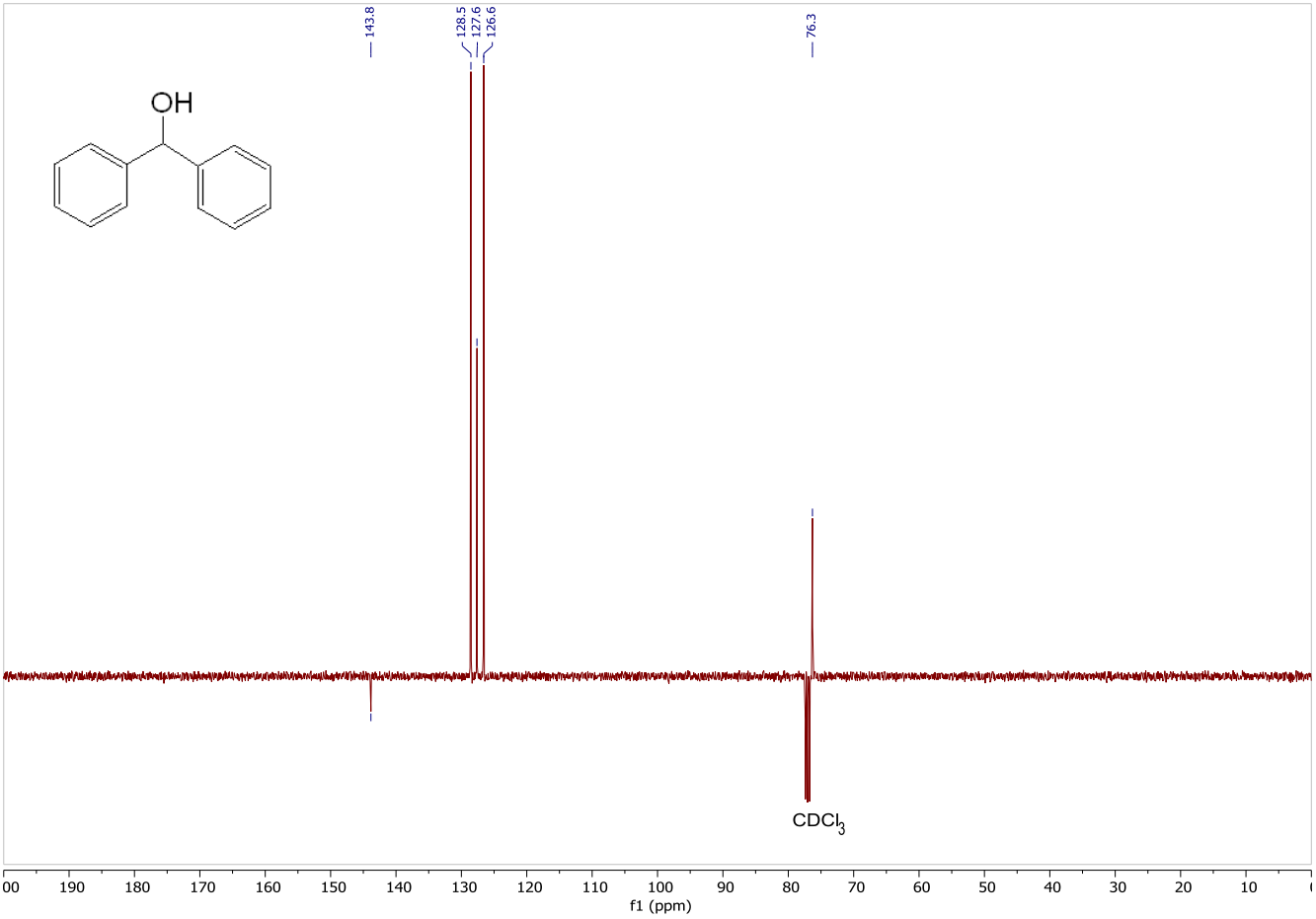

Figure S65. $^{13}C\{^{1}H\}$NMR spectrum (100.6 MHz) of benzhydrol obtained from catalytic TH of benzophenone in $CDCl_3$ at 25 °C.

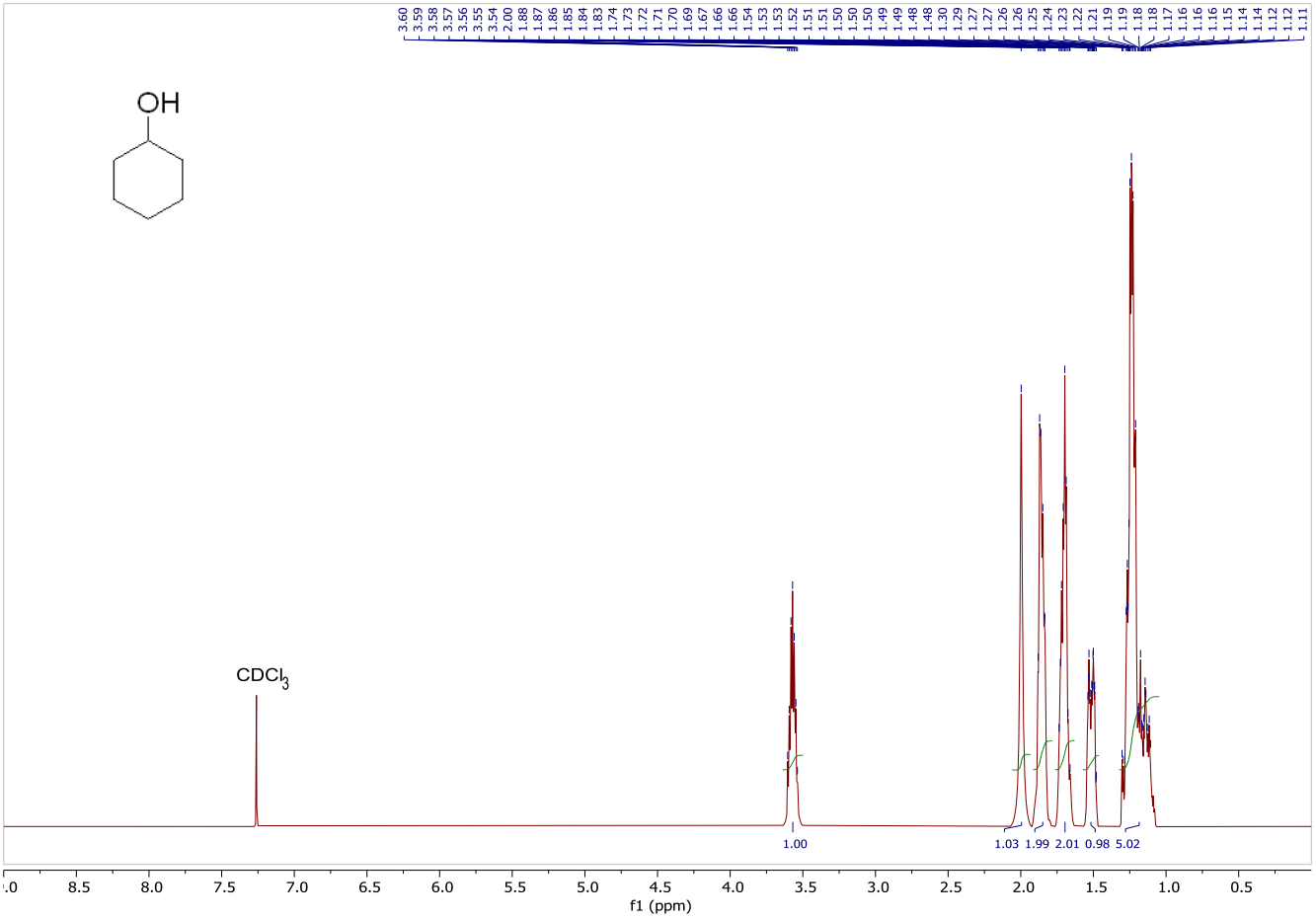

Figure S66. ^{1}H NMR spectrum (400.1 MHz) of cyclohexanol obtained from catalytic TH of cyclohexanone in $CDCl_3$ at 25 °C.

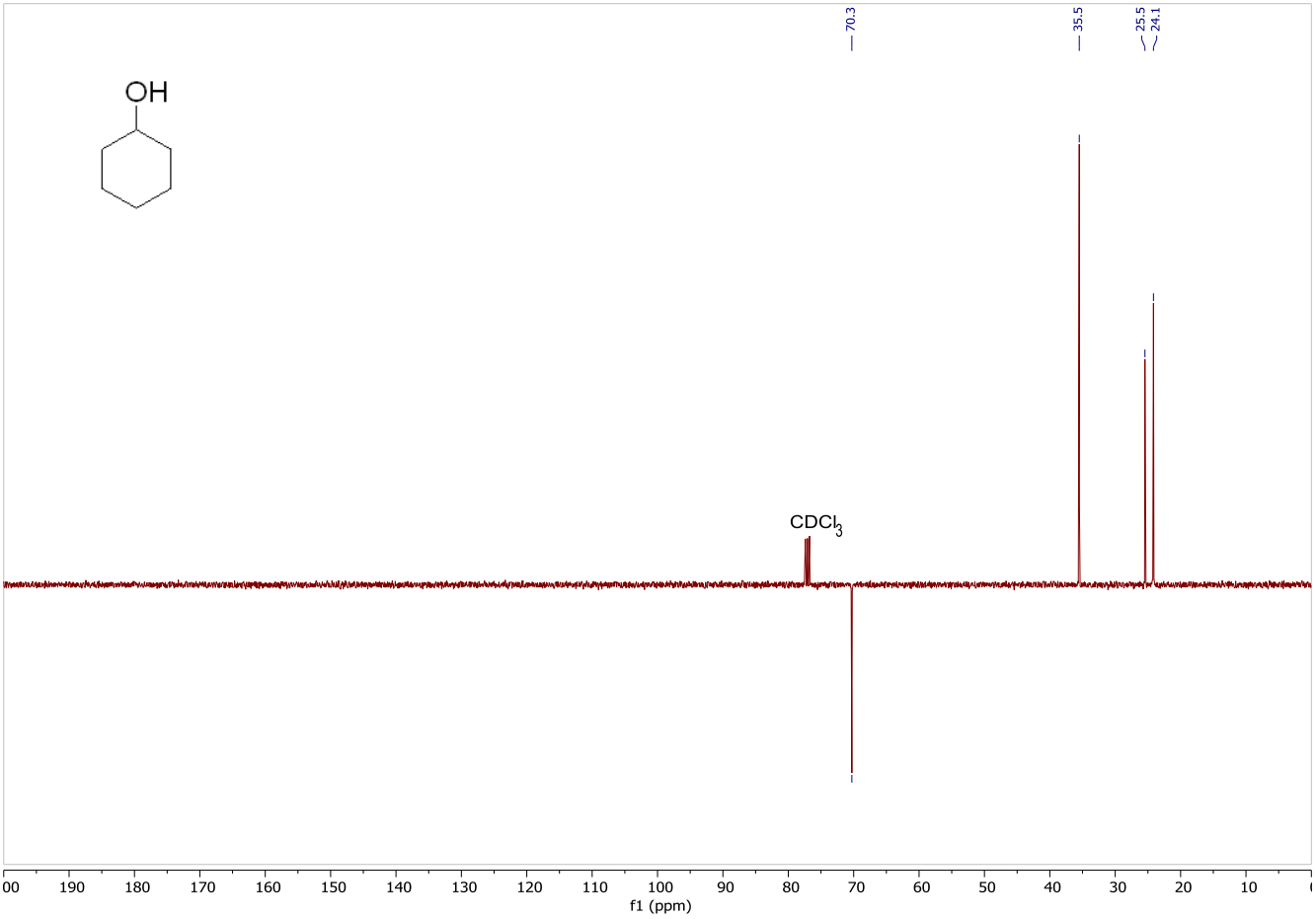

Figure S67. $^{13}C\{^{1}H\}$NMR spectrum (100.6 MHz) of cyclohexanol obtained from catalytic TH of cyclohexanone in $CDCl_3$ at 25 °C.

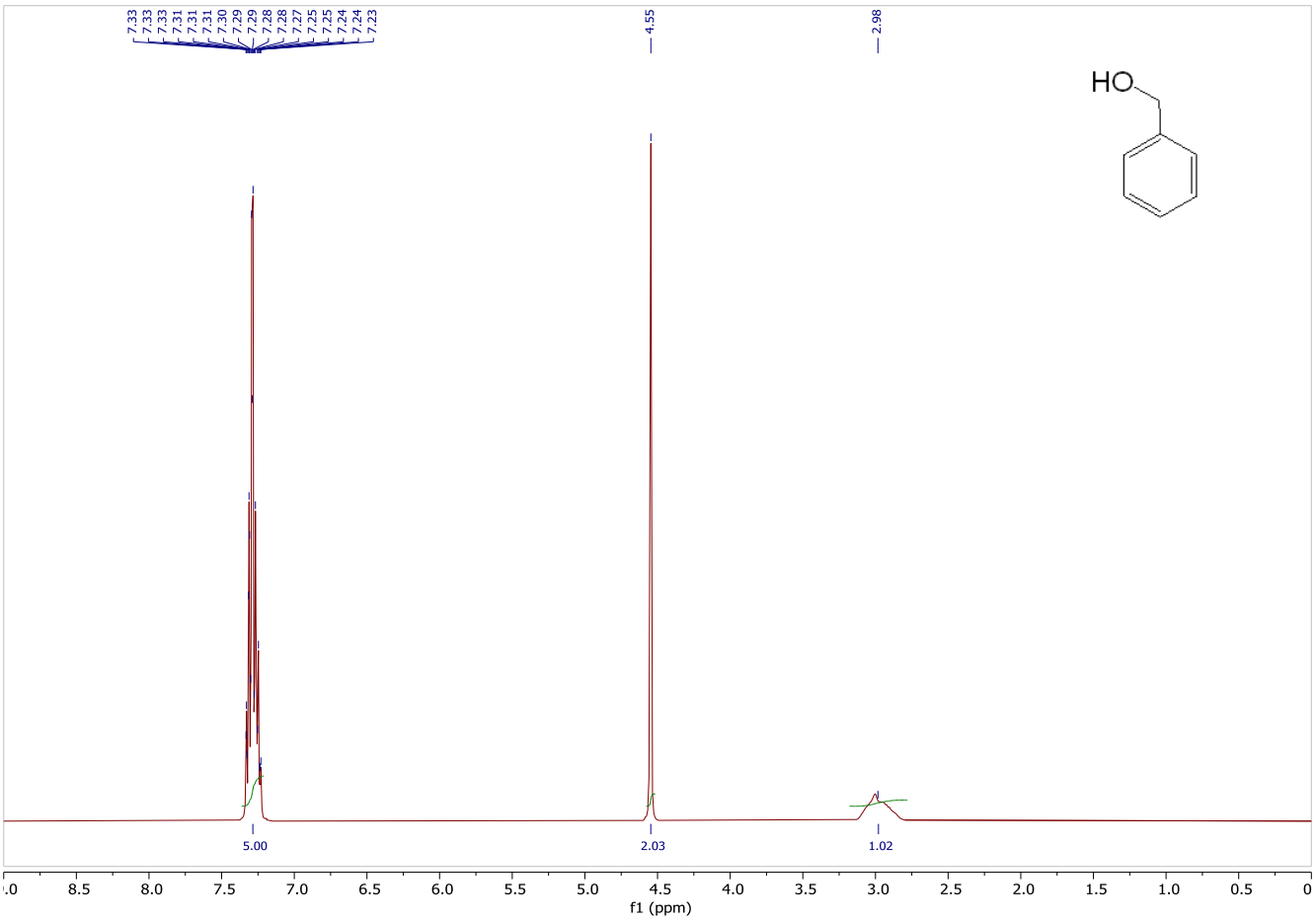

Figure S68. ^{1}H NMR spectrum (400.1 MHz) of benzyl alcohol obtained from catalytic TH of benzaldehyde in $CDCl_3$ at 25 °C.

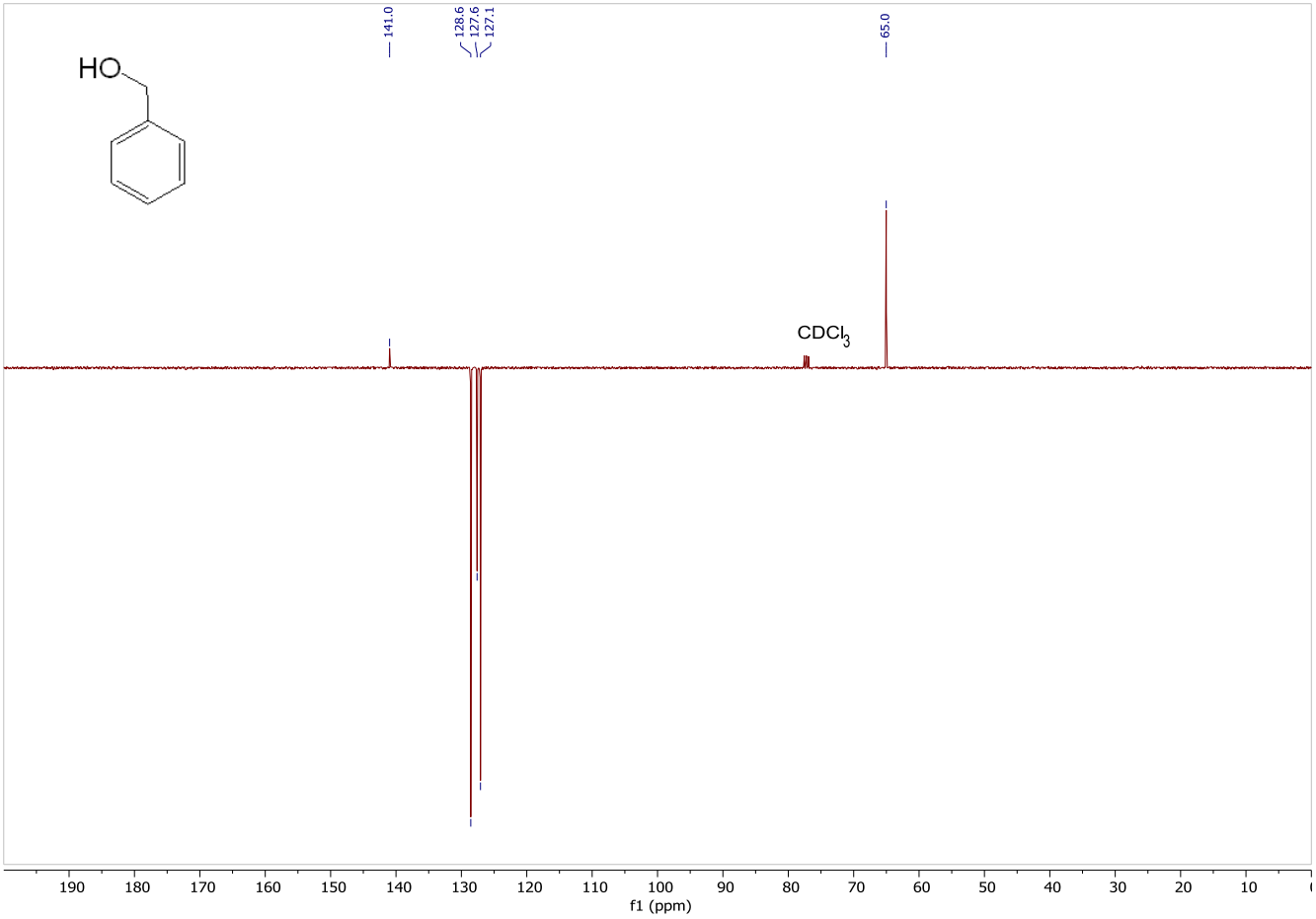

Figure S69. $^{13}C\{^{1}H\}$NMR spectrum (100.6 MHz) of benzyl alcohol obtained from catalytic TH of benzaldehyde in $CDCl_3$ at 25 °C.

Single Crystal X-Ray Structure Determination of Compounds 1-4 (CCDC 2253558-2253561)

General Data

X-ray diffraction data were collected at 100 K on an X-ray single crystal diffractometer equipped with a CPAD detector (Bruker Photon-II CPAD), an IMS microsource with MoK_α radiation (λ = 0.71073 Å) and a Helios optic using the APEX4 software package.[10] Measurements were performed on a single crystal coated with perfluorinated ether and the crystal was fixed on top of a Kapton micro sampler, transferred to the diffractometer and frozen under a stream of cold nitrogen. A matrix scan was used to determine the initial lattice parameters. Reflections were merged and corrected for Lorenz and polarization effects, scan speed and background using SAINT.[11] Absorption corrections, including odd and even ordered spherical harmonics were performed using SADABS.[11] Based on systematic absences, E-statistics and successful refinement of the structures, the space group was assigned. The structures were solved by direct methods with the aid of successive difference Fourier maps, and were refined against all data using APEX4 software with SHELXL in conjunction with SHELXLE.[12-14] Full-matrix least-squares refinements were carried out by minimizing $\Sigma w(F_o^2 - F_c^2)^2$ with the SHELXL weighting scheme.[12] All non-hydrogen atoms were refined using anisotropic displacement parameters and hydrogen atoms were calculated in ideal positions with $U_{iso}(H) = 1.2\ U_{eq}(C)$. Neutral atom scattering factors for all atoms and anomalous dispersion corrections for the non-hydrogen atoms were taken from *International Tables for Crystallography*.[15] Structural illustrations were generated with Mercury and Platon.21 for Windows.[16, 17] CCDC 2253558-2253561 contain the supplementary crystallographic data for this paper. These data are provided free of charge by The Cambridge Crystallographic Data Centre.

Single Crystal X-Ray Structure Determination of Compound 1 (CCDC 2253559).

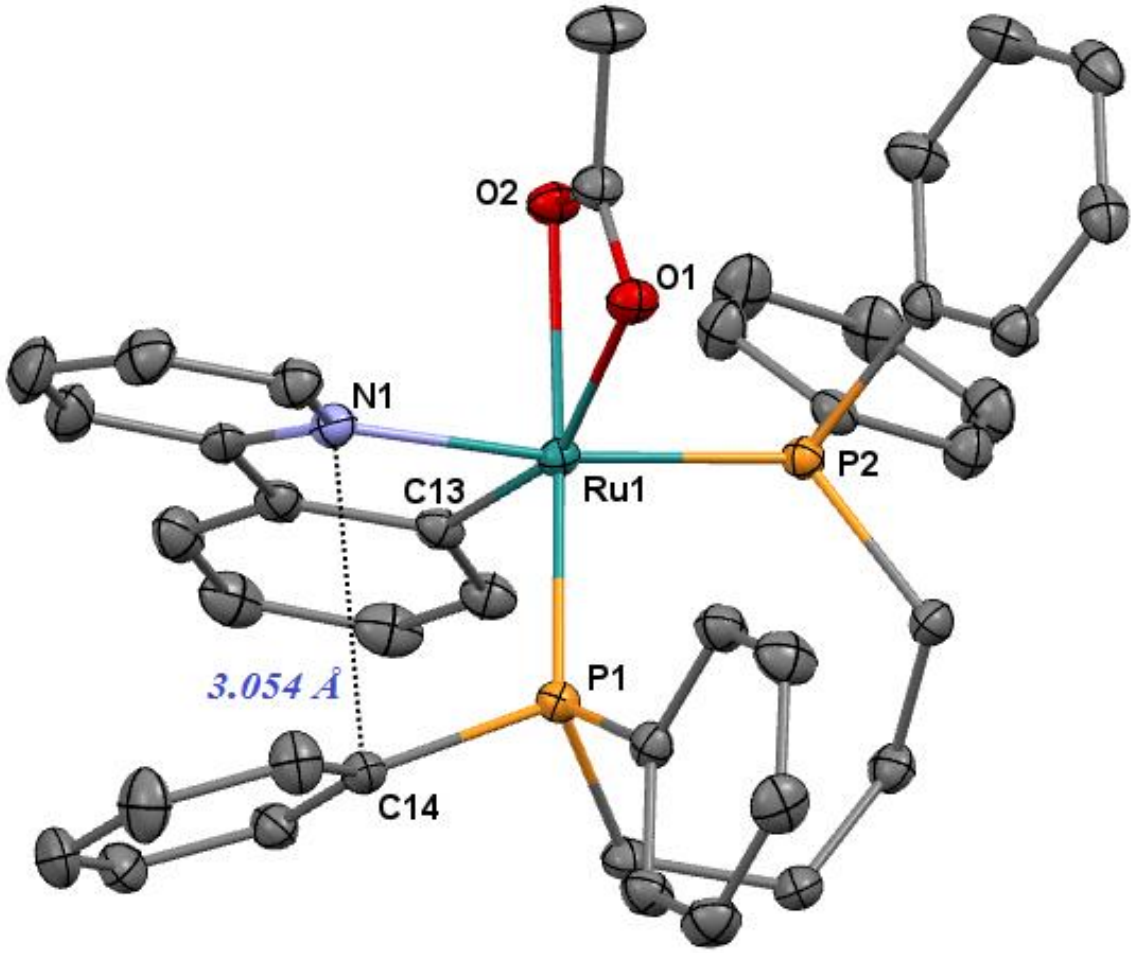

Figure S70. ORTEP style plot of compound **1** in the solid state (CCDC 2253559). Ellipsoids are drawn at the 50% probability level. Hydrogen atoms are omitted for clarity. Selected bond lengths [Å] and angles [°]: Ru1–N1 2.1030(16), Ru1-C13 2.0342(18), Ru1-O2 2.2242(13), Ru1-P1 2.2292(5), Ru1-O1 2.2582(13), Ru1-P2 2.2814(5), C13-Ru1-N1 79.89(7), C13-Ru1-O2 102.61(6), N1-Ru1-O2 83.18(5), C13-Ru1-P1 86.15(5), N1-Ru1-P1 91.65(4), O2-Ru1-P1 168.81(4), C13-Ru1-O1 158.30(6), N1-Ru1-O1 86.67(6), O2-Ru1-O1 58.57(5), P1-Ru1-O1 111.37(4), C13-Ru1-P2 101.34(5), N1-Ru1-P2 172.56(4), O2-Ru1-P2 89.40(4), P1-Ru1-P2 95.747(18), O1-Ru1-P2 89.90(4).

Single Crystal X-Ray Structure Determination of Compound 1 (CCDC 2253559).

Detailed Crystallographic Data.

Diffractometer operator:	A. A. Heidecker
Scanspeed	1-3 s per frame
dx	40 mm
Frames:	2109 measured in 8 XYZ data sets
phi-scans with delta phi	0.5/1.0
omega-scans with delta omega	0.5

Crystal Data:

Chemical formula [$C_{41}H_{39}NO_2P_2Ru$]		Density (calculated) = 1.467 g/cm^3
Formula weight 740.74		Absorption coefficient = 0.601 mm^{-1}
monoclinic, *P* 21/n		Mo *K*α radiation, λ = 0.71073 Å
a = 9.8638(10) Å	α = 90°	Cell parameters from 106782 reflections
b = 17.891(2) Å	β = 90.761(4)°	θ = 2.28–27.48°
c = 19.013(2) Å	γ = 90°	*T* = 100(2) K
V = 3355.0(6) Å^3		clear orange fragment
Z = 4		0.050 x 0.164 x 0.222 mm
F(000) = 1528		

Data collection:

Bruker D8 Venture Duo IMS diffractometer	7691 independent reflections
Radiation source: TXS rotating anode	6956 reflections with $I > 2\sigma(F^2)$
Helios optic monochromator	R_{int} = 0.0769
Theta range for data collection	θ_{max} = 27.48°, θ_{min} = 2.28°
Index ranges	-12<=h<=12, -23<=k<=23, -24<=l<=24
Absorption correction	Multi-Scan, *SADABS* 2016/2, Bruker

Max. and min. transmission:	0.7043 and 0.6692
106782 measured reflections	Coverage of independent reflections = 99.9%

Data refinement:

Refinement method	Full-matrix least-squares on F^2
Refinement program	SHELXL-2018/3 (Sheldrick, 2018)
Structure solution technique	direct methods
Structure solution program	SHELXT 2018/2 (Sheldrick, 2018)
Function minimized	$\Sigma\ w(Fo^2 - Fc^2)^2$
Data / restraints / parameters	7691 / 0 / 425
Final R indices	6956 data; $I > 2\sigma(I)$ R1 = 0.0273, wR2 = 0.0676
	all data R1 = 0.0320, wR2 = 0.0704
Weighting scheme	$w = 1/[\sigma^2(Fo^2) + (0.0262P)^2 + 3.6827P]$
	where $P = (Fo^2 + 2Fc^2)/3$
$\Delta/\boldsymbol{\sigma}_{max}$	0.001
Goodness-of-fit on F^2	1.041
Largest diff. peak and hole	0.449 and -0.464 $eÅ^{-3}$
R.M.S. deviation from mean	0.069 $eÅ^{-3}$

Single Crystal X-Ray Structure Determination of Compound 2 (CCDC 2253561).

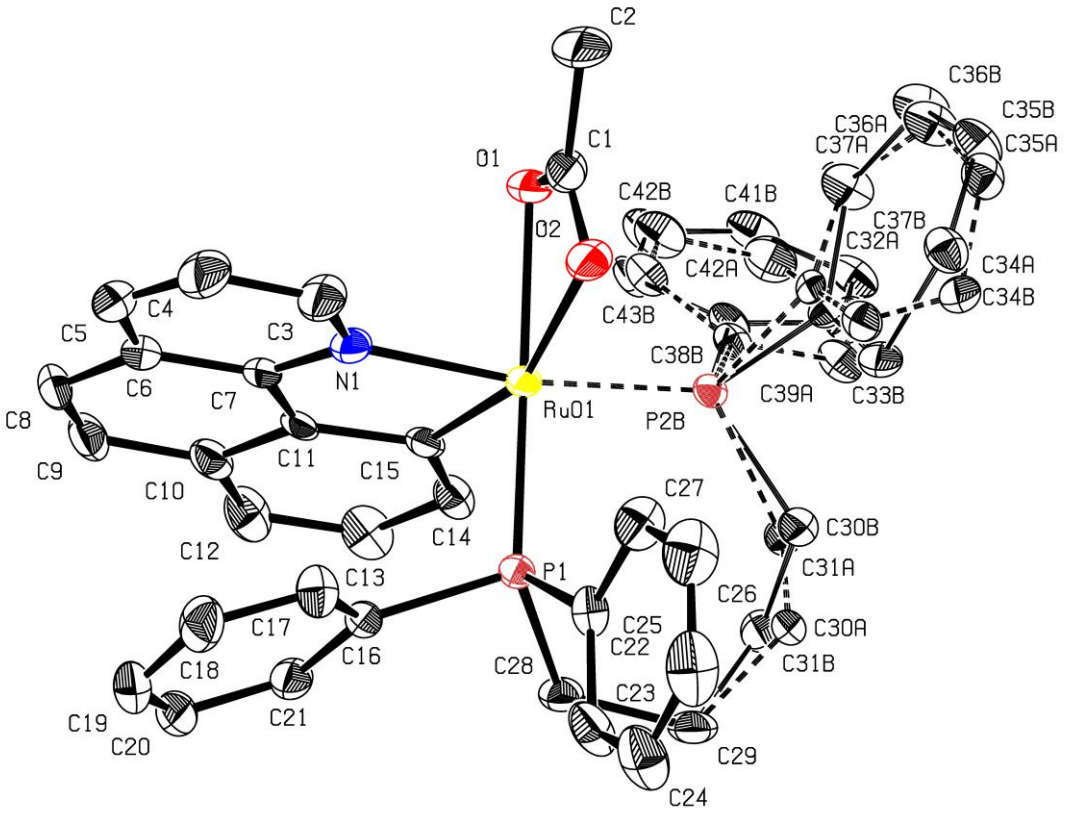

Figure S71. ORTEP style plot of compound **2** in the solid state (CCDC 2253561). Ellipsoids are drawn at the 50% probability level. Hydrogen atoms are omitted for clarity. Selected bond lengths [Å] and angles [°]: Ru1-C15 2.040(3), Ru1-N1 2.115(3), Ru1-P2A 2.201(3), Ru1-O1 2.209(2), Ru1-P1 2.2338(8), Ru1-O2 2.237(2), Ru1-P2B 2.348(3), C15-Ru1-N1 80.84(12), C15-Ru1-P2A 105.26(13), N1-Ru1-P2A 171.13(10), C15-Ru1-O1 104.13(11), N1-Ru1-O1 83.62(10), P2A-Ru1-O1 88.59(10), C15-Ru1-P1 83.76(8), N1-Ru1-P1 92.51(8), P2A-Ru1-P1 94.53(8), O1-Ru1-P1 170.46(8), C15-Ru1-O2 159.86(10), N1-Ru1-O2 85.91(10), P2A-Ru1-O2 86.46(11), O1-Ru1-O2 59.07(10), P1-Ru1-O2 112.06(8), C15-Ru1-P2B 96.00(12), N1-Ru1-P2B 169.52(11), O1-Ru1-P2B 87.51(10), P1-Ru1-P2B 97.09(7), O2-Ru1-P2B 94.32(10).

Single Crystal X-Ray Structure Determination of Compound 2 (CCDC 2253561)

Detailed Crystallographic Data.

Diffractometer operator:	A. A. Heidecker
Scanspeed	1-8 s per frame
dx	40 mm
Frames:	3689 measured in 12 XYZ data sets
phi-scans with delta phi	0.5/1.0
omega-scans with delta omega	0.5

Crystal Data:

Chemical formula [$C_{43}H_{39}NO_2P_2Ru$]		Density (calculated) = 1.457 g/cm^3
Formula weight 764.76		Absorption coefficient = 0.581 mm^{-1}
monoclinic, *C* 2/c		Mo *K*α radiation, λ = 0.71073 Å
a = 29.656(5) Å	α = 90°	Cell parameters from 188606 reflections
b = 9.7750(17) Å	β = 106.902(5)°	θ = 1.88-27.48°
c = 25.141(4) Å	γ = 90°	*T* = 100(2) K
V = 6973.2(19) Å^3		clear light yellow-orange plate
Z = 8		0.030 x 0.132 x 0.398 mm
F(000) = 3152		

Data collection:

Bruker D8 Venture Duo IMS diffractometer	8003 independent reflections
Radiation source: TXS rotating anode	7248 reflections with $I > 2\sigma(F^2)$
Helios optic monochromator	R_{int} = 0.0966
Theta range for data collection	θ_{max} = 27.48°, θ_{min} = 1.88°
Index ranges	-38<=h<=38, -12<=k<=12, -32<=l<=32

Absorption correction	Multi-Scan, *SADABS* 2016/2, Bruker
Max. and min. transmission:	0.9830 and 0.8020
188606 measured reflections	Coverage of independent reflections = 100.0%

Data refinement:

Refinement method	Full-matrix least-squares on F^2
Refinement program	SHELXL-2018/3 (Sheldrick, 2018)
Structure solution technique	direct methods
Structure solution program	SHELXT 2018/2 (Sheldrick, 2018)
Function minimized	$\Sigma\ w(Fo^2 - Fc^2)^2$
Data / restraints / parameters	8003 / 277 / 587
Final R indices	7248 data; $I > 2\sigma(I)$ R1 = 0.0501, wR2 = 0.0926
	all data R1 = 0.0571, wR2 = 0.0955
Weighting scheme	$w = 1/[\sigma^2(Fo^2) + 39.9662P]$
	where $P = (Fo^2 + 2Fc^2)/3$
$\Delta/\boldsymbol{\sigma}_{max}$	0.001
Goodness-of-fit on F^2	1.214
Largest diff. peak and hole	0.436 and -1.068 eÅ^{-3}
R.M.S. deviation from mean	0.087 eÅ^{-3}

Single Crystal X-Ray Structure Determination of Compound 3 (CCDC 2253560)

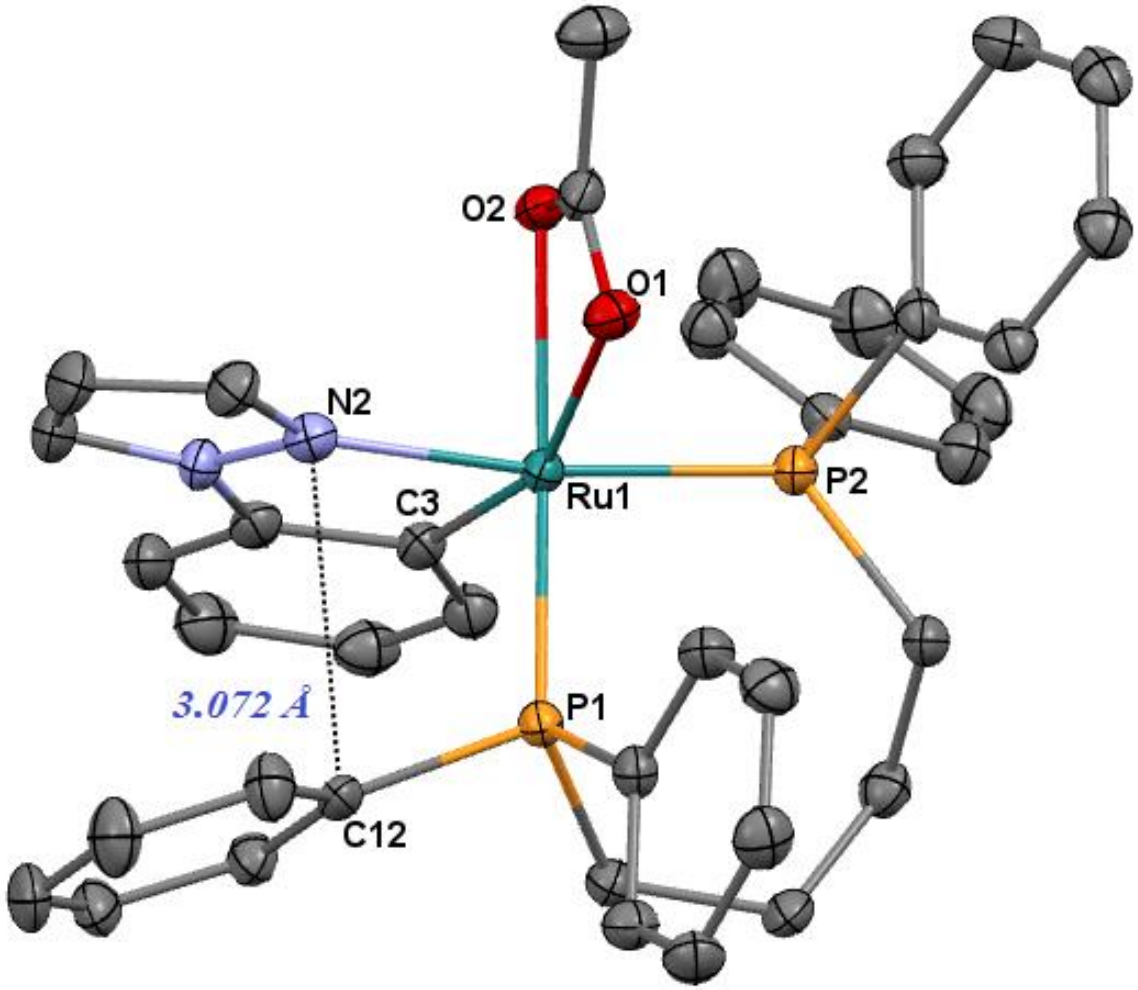

Figure S72. ORTEP style plot of compound **3** in the solid state (CCDC 2253560). Ellipsoids are drawn at the 50% probability level. Hydrogen atoms are omitted for clarity. Selected bond lengths [Å] and angles [°]: Ru1-C3 2.054(4), Ru1-N2 2.084(3), Ru1-P1 2.2282(10), Ru1-O2 2.233(2), Ru1-O1 2.247(2), Ru1-P2 2.2756(10), Ru1-C1 2.581(4), P1-C12 1.834(3), C3-Ru1-N2 79.56(13), C3-Ru1-P1 85.38(10), N2-Ru1-P1 92.22(8), C3-Ru1-O2 103.57(11), N2-Ru1-O2 83.44(10), P1-Ru1-O2 169.09(7), C3-Ru1-O1 158.67(11), N2-Ru1-O1 86.02(10), P1-Ru1-O1 110.99(7), O2-Ru1-O1 58.84(9), C3-Ru1-P2 101.12(10), N2-Ru1-P2 171.92(8), P1-Ru1-P2 95.85(3), O2-Ru1-P2 88.59(7), O1-Ru1-P2 91.01(7).

Single Crystal X-Ray Structure Determination of Compound 3 (CCDC 2253560)

Detailed Crystallographic Data.

Diffractometer operator:	A. A. Heidecker
Scanspeed	1-10 s per frame
dx	40 mm
Frames:	1673 measured in 8 XYZ data sets
phi-scans with delta phi	0.5/1.0
omega-scans with delta omega	-0.5/0.5

Crystal Data:

Chemical formula [$C_{39}H_{38}N_2O_2P_2Ru$]		Density (calculated) = 1.459 g/cm^3
Formula weight 729.72		Absorption coefficient = 0.606 mm^{-1}
Monoclinic, *P* 21/n		Mo *K*α radiation, λ = 0.71073 Å
a = 9.845(2) Å	α = 90°	Cell parameters from 58152 reflections
b = 17.644(4) Å	β = 90.757(7)°	θ = 2.13-25.36°
c = 19.132(4) Å	γ = 90°	*T* = 100(2) K
V = 3323.0(12) Å^3		clear green rectangle
Z = 4		0.081 x 0.089 x 0.105 mm
F(000) = 1504		

Data collection:

Bruker D8 Venture Duo IMS diffractometer	6080 independent reflections
Radiation source: TXS rotating anode	5164 reflections with $I > 2\sigma(F^2)$
Helios optic monochromator	R_{int} = 0.0920
Theta range for data collection	θ_{max} = 25.36°, θ_{min} = 2.13°
Index ranges	-11<=h<=11, -21<=k<=21, -21<=l<=23
Absorption correction	Multi-Scan, *SADABS* 2016/2, Bruker

58152 measured reflections | Coverage of independent reflections = 99.9%

Data refinement:

Refinement method	Full-matrix least-squares on F^2
Refinement program	SHELXL-2018/3 (Sheldrick, 2018)
Structure solution technique	direct methods
Structure solution program	SHELXT 2018/2 (Sheldrick, 2018)
Function minimized	$\Sigma\, w(Fo^2 - Fc^2)^2$
Data / restraints / parameters	6080 / 0 / 416
Final R indices	5164 data; $I > 2\sigma(I)$ R1 = 0.0402, wR2 = 0.0942
	all data R1 = 0.0514, wR2 = 0.1008
Weighting scheme	$w = 1/[\sigma^2(Fo^2) + (0.0400P)^2 + 7.1188P]$
	where $P = (Fo^2 + 2Fc^2)/3$
$\Delta/\boldsymbol{\sigma}_{max}$	0.001
Goodness-of-fit on F^2	1.060
Largest diff. peak and hole	1.125 and -0.687 eÅ^{-3}
R.M.S. deviation from mean	0.094 eÅ^{-3}

Single Crystal X-Ray Structure Determination of Compound 4 (CCDC 2253558).

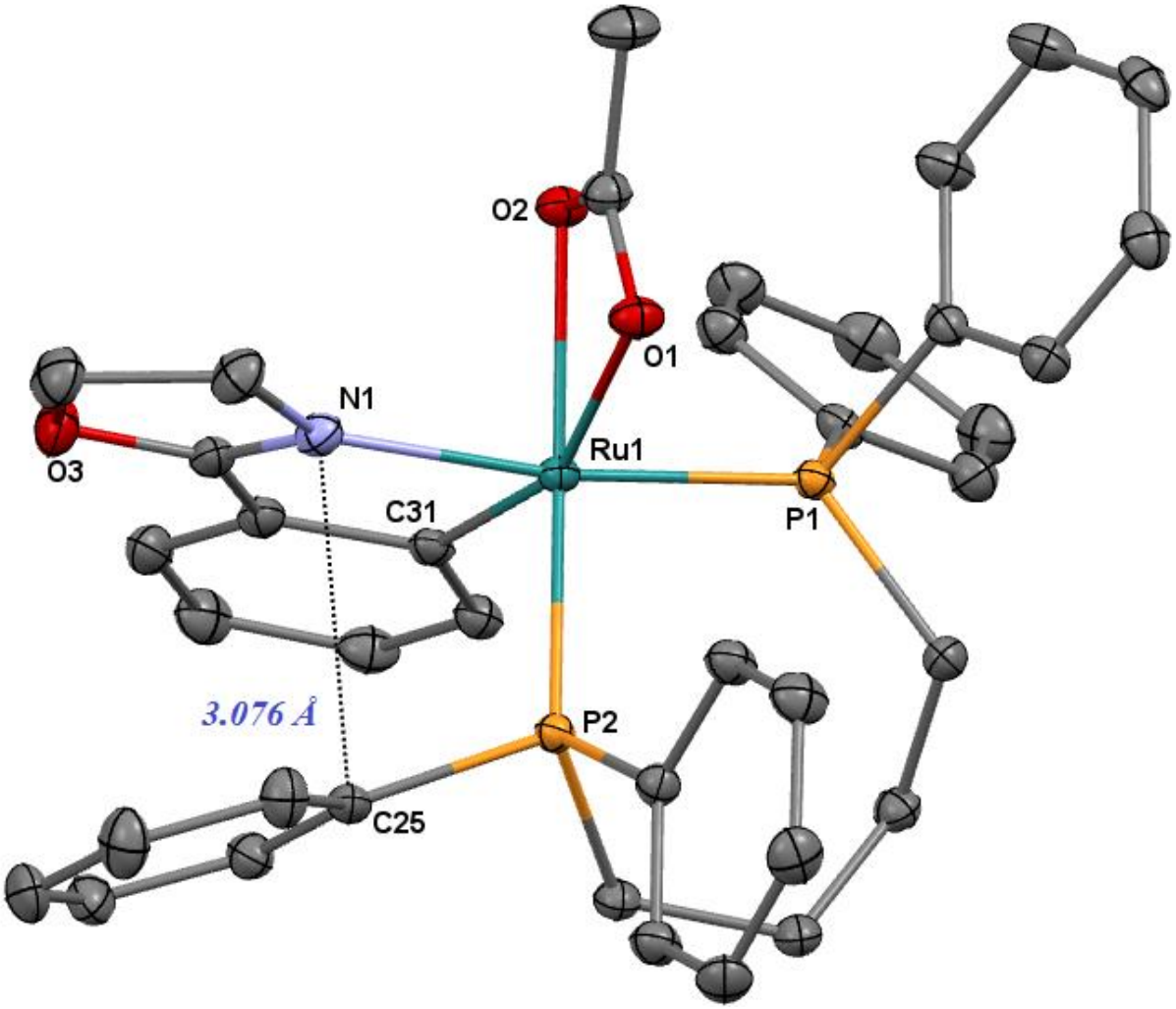

Figure S73. ORTEP style plot of compound **4** in the solid state (CCDC 2253558). Ellipsoids are drawn at the 50% probability level. Hydrogen atoms are omitted for clarity. Selected bond lengths [Å] and angles [°]: Ru1-C31 2.0514(13), Ru1-N1 2.1104(11), Ru1-O2 2.2160(9), Ru1-P2 2.2271(4), Ru1-O1 2.2453(10), Ru1-P1 2.2635(4), C31-Ru1-N1 79.34(5), C31-Ru1-O2 103.49(4), N1-Ru1-O2 83.25(4), C31-Ru1-P2 86.49(4), N1-Ru1-P2 92.80(3), O2-Ru1-P2 168.31(3), C31-Ru1-O1 158.95(4), N1-Ru1-O1 86.57(4), O2-Ru1-O1 58.97(3), P2-Ru1-O1 109.94(3), C31-Ru1-P1 100.24(4), N1-Ru1-P1 171.64(3), O2-Ru1-P1 88.77(3), P2-Ru1-P1 95.510(13), O1-Ru1-P1 91.44(3).

Single Crystal X-Ray Structure Determination of Compound 4 (CCDC 2253558)

Detailed Crystallographic Data.

Diffractometer operator:	A. A. Heidecker
Scanspeed	1-4 s per frame
dx	40 mm
Frames:	3904 measured in 13 XYZ data sets
phi-scans with delta phi	-0.5/1.0
omega-scans with delta omega	-0.5/0.5

Crystal Data:

Chemical formula [$C_{39}H_{39}NO_3P_2Ru$]		Density (calculated) = 1.478 g/cm^3
Formula weight 732.72		Absorption coefficient = 0.613 mm^{-1}
monoclinic, *P* 21/n		Mo *K*α radiation, λ = 0.71073 Å
a = 9.8933(6) Å	α = 90°	Cell parameters from 209391 reflections
b = 17.5880(9) Å	β = 91.121(2)°	θ = 2.15-27.88°
c = 18.9275(12) Å	γ = 90°	*T* = 100(2) K
V = 3292.8(3) Å^3		clear yellow fragment
Z = 4		0.190 x 0.202 x 0.377 mm
F(000) = 1512		

Data collection:

Bruker D8 Venture Duo IMS diffractometer	7838 independent reflections
Radiation source: TXS rotating anode	7478 reflections with $I > 2\sigma(F^2)$
Helios optic monochromator	R_{int} = 0.0340
Theta range for data collection	θ_{max} = 27.88°, θ_{min} = 2.15°
Index ranges	-13<=h<=13, -23<=k<=23, -24<=l<=24
Absorption correction	Multi-Scan, *SADABS* 2016/2, Bruker

209391 measured reflections | Coverage of independent reflections = 100.0%

Data refinement:

Refinement method	Full-matrix least-squares on F^2
Refinement program	SHELXL-2018/3 (Sheldrick, 2018)
Structure solution technique	direct methods
Structure solution program	SHELXT 2018/2 (Sheldrick, 2018)
Function minimized	$\Sigma\ w(Fo^2 - Fc^2)^2$
Data / restraints / parameters	7838 / 0 / 416
Final R indices	7478 data; $I > 2\sigma(I)$ R1 = 0.0204, wR2 = 0.0509
	all data R1 = 0.0218, wR2 = 0.0519
Weighting scheme	$w = 1/[\sigma^2(Fo^2) + (0.0213P)^2 + 2.8079P]$
	where $P = (Fo^2 + 2Fc^2)/3$
$\Delta/\boldsymbol{\sigma}_{max}$	0.001
Goodness-of-fit on F^2	1.050
Largest diff. peak and hole	0.369 and -0.466 eÅ^{-3}
R.M.S. deviation from mean	0.053 eÅ^{-3}

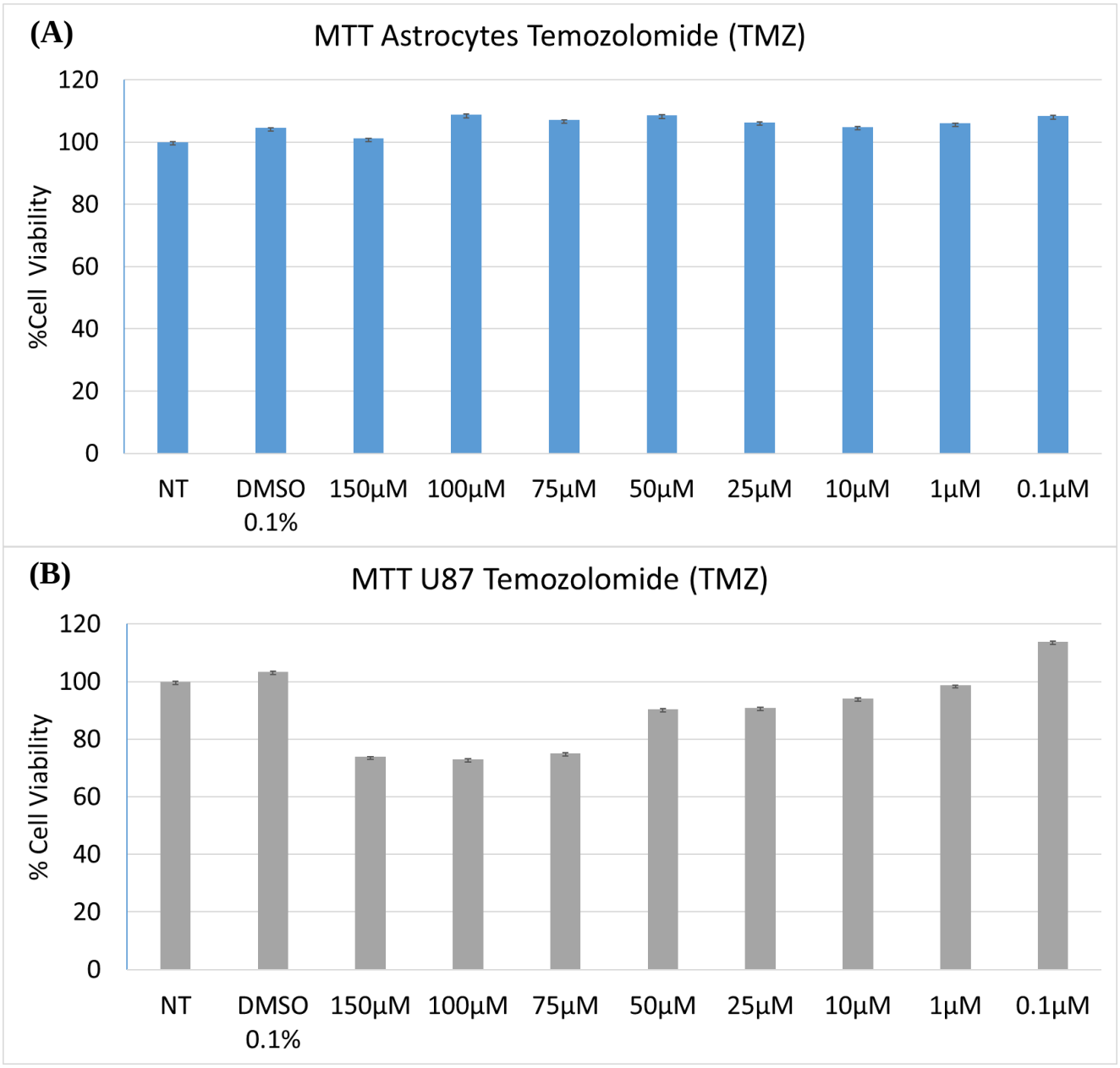

Figure S74. Cell viability measured by MTT assay of Astrocytes (**A**) and U87 MG cells (**B**) treated with Temozolomide (TMZ) for 72 h.

References

1) (a) K. Gatto, J. D. Reinheimer, K. Shafer, J. T. Gerig, *Org. Magn. Reson*, **1974**, *6*, 577-579. (b) Y. Sarrafi, M. Tajbakhsh, R. Hosseinzadeh, M. Sadatshahabi, K. Alimohammadi, *Synth. Commun.*, **2012**, *42*, 678-685.

2) R. Lin, F. Chen, N. Jiao, *Org. Lett.*, **2012**, *14*, 4158-4161.

3) (a) G. A. Olah, O. Farooq, S. M. F. Farnia, J. A. Olah, *J. Am. Chem. Soc.*, **1988**, *110*, 2560-2565. (b) H-J. Cristau, A. Bazbouz, P. Morand, E. Torreilles, *Tetrahedron Lett.*, **1986**, *27*, 2965-2966. (c) B. Skillinghaug, C. Skold, J. Rydfjord, F. Svensson, M. Behrends, J. Savmarker, P. J. R. Sjoberg, M. Larhed, *J. Org. Chem.*, **2014**, *79*, 12018-12032.

4) D. E. Alonso, S. E. Warren, *J. Chem. Educ.*, **2005**, *82*, 1385-1386.

5) A. K. Mishraa, J. N. Moorthy, *Org. Chem. Front.*, **2017**, 4, 343-349.

6) (a) M. Li, B. Li, H.-F. Xia, D. Ye, J. Wu, Y. Shi, *Green Chem.*, **2014**, *16*, 2680-2688. (b) T. Ohkuma, M. Koizumi, H. Doucet, T. Pham, M. Kozawa, K. Murata, E. Katayama, T. Yokozawa, T. Ikariya, R. Noyori, *J. Am. Chem. Soc.*, **1998**, *120*, 13529–13530. (c) T. Vielhaber, C. Topf, *Appl. Catal. A: Gen.*, **2021**, *623*, 118280.

7) S. Yadav, R. Gupta, *ACS Sustain. Chem. Eng.*, **2023**, *11*, 8533-8543.

8) H. Shimizu, D. Igarashi, W. Kuriyama., Y. Yusa, N. Sayo and T. Saito, *Org. Lett*., **2007**, 9, 1655-1657.

9) H. Yu, Y. Luo, K. Beverly, J. F. Stoddart, H.-R. Tseng, J. R. Heath, *Angew. Chem. Int. Ed.* **2003**, *42*, 5706-5711.

10) *APEX suite of crystallographic software*, APEX4 Version 2021-10-0, Bruker AXS Inc., Madison, Wisconsin, USA, **2021**.

11) *SAINT*, Version 8.40A and *SADABS*, Version 2016/2, Bruker AXS Inc., Madison, Wisconsin, USA, **2016/2019**.

12) G. M. Sheldrick, *Acta Crystallogr. Sect. A* **2015**, *71*, 3-8.

13) G. M. Sheldrick, *Acta Crystallogr. Sect. C* **2015**, *71*, 3-8.

14) C. B. Hübschle, G. M. Sheldrick, B. Dittrich, *J. Appl. Cryst.* **2011**, *44*, 1281-1284

15) *International Tables for Crystallography, Vol. C* (Ed.: A. J. Wilson), Kluwer Academic Publishers, Dordrecht, The Netherlands, **1992**, Tables 6.1.1.4 (pp. 500-502), 4.2.6.8 (pp. 219-222), and 4.2.4.2 (pp. 193-199).

16) C. F. Macrae, I. J. Bruno, J. A. Chisholm, P. R. Edgington, P. McCabe, E. Pidcock, L. Rodriguez-Monge, R. Taylor, J. van de Streek, P. A. Wood, *J. Appl. Cryst.* **2008**, *41*, 466-470.

17) A. L. Spek, *Acta Crystallogr. Sect. D* **2009**, *65*, 148-155.